

HIGH-SPEED BICMOS MEMORIES

Drew Eric Wingard

Technical Report No. CSL-TR-95-659

January 1995

This research has been supported by ARPA contract N00039-91-C-0138.
The author also acknowledges support from a National Science Foundation Graduate Fellowship.

HIGH-SPEED BICMOS MEMORIES

Drew Eric Wingard

Technical Report: CSL-TR-95-659

January 1995

Computer Systems Laboratory
Departments of Electrical Engineering and Computer Science
Stanford University
Stanford, California 94305-4055

Abstract

Existing BiCMOS static memories do not simultaneously combine the speed of bipolar memories with the low power and density of CMOS memories. Beginning with fundamentally fast low-swing bipolar circuits and zero-power CMOS storage latches, we introduce CMOS devices into the bipolar circuits to reduce the power dissipation without compromising speed and insert bipolar transistors into CMOS storage arrays to improve the speed without power nor density penalties.

Replacing passive load resistors with switched PMOS transistors reduces the amount of power required to keep bipolar decoder outputs low. The access delay need not increase because the load resistance is quickly reduced via a low-swing signal when the decoder could switch. For ECL NOR decoders, we apply a variable BiCMOS current source that is simplified by carefully regulating the negative supply. We also develop techniques that improve the reading and writing characteristics of the CMOS-storage, emitter-access memory cell.

A 16K-word 4-bit asynchronous CSEA memory was fabricated in a 0.8- μm BiCMOS technology and accesses in 3.7ns while using 1.75W. An improved 64Kx4 design is simulated to run at 3.4ns and 2.3W. Finally, a synchronous 4Kx64 CSEA memory is estimated to operate at 2.5ns and 2.4W in the same process technology.

Key Words and Phrases: static memories (SRAM), BiCMOS circuit techniques, low-swing signalling, CSEA memory cell, pulsed circuits

Copyright © 1994

by

Drew Eric Wingard

Acknowledgments

I must start off by thanking my advisor, Prof. Mark Horowitz. He sets seemingly impossibly high standards by example, and challenges his students to accomplish more than they thought possible. I will never forget our meetings, where he would often point out the shortcomings in my ideas before I was halfway through revealing them — of course I will especially remember the few (but increasingly more frequent) times when I was actually right. On top of the delight of intellectual challenge, he is a truly nice person who encourages his students (again by example) to expand their horizons at Stanford by pitching in and helping other researchers in areas where our group is strong.

I would also like to thank my associate advisor, Prof. Bruce Wooley, who provided so many interesting research attractions and distractions. The best examples of each were the sigma-delta chip, with Brian Brandt and the kind folks at TI, and my “endless” Cadence purgatory. At least Bruce had to read this thesis! I am greatly indebted to Prof. John Gill, who had the unenviable task of chairing my orals committee and reading a thesis outside his field. Thanks also to Prof. Greg Kovacs, who sat on my orals committee.

A number of people and organizations helped with this research. Don Stark was distracted from his own thesis for long enough to do some substantial layout, and essentially all of the verification, of the fabricated SRAM. Mark Horowitz spent more long nights helping than any of us care to remember. The staff of Texas Instrument’s Semiconductor Process and VLSI Design Laboratories built and helped test that memory. In particular, I would like to thank Harvey Davis, Lisa Dyson, Eng Born, and Bob Garcia for mask generation, die assembly, and testing assistance and Tom Holloway for fabrication. Ashwin Shah, David Scott, Bob Hughes, and Pallab Chatterjee supported this project within TI. Furthermore, Jay Glanville (then at Seiko Instruments), the Integrated Systems Laboratory at USC/ISI, and Jim McVittie and Steven Taylor at Stanford’s IC Lab helped debug and modify the design errors. This research was also supported by a National Science Foundation Graduate Fellowship, and by Advanced Research Projects Agency Contract No. N00039-91-C-0138.

Eight years is a long time to work on anything. For me, it felt more like working on everything. Faces and projects that I’ll remember include Brian and the sigma-delta, John Shott

et al. and the Stanford BiCMOS project, Mike Smith, John Manentis, Don Ramsey, Tom Chanak, Phil Lacroute, *et al.* and TORCH, and Marc Loinaz, Peter Lim, and the OaCIS stockers.

I've also been fortunate to run into a bunch of people to have fun with: the CIS softball team, the `basketball@blaze` group, the birthday club (Brian & Jan, Greg & Joan, Paul, Dave, Brian L., Walter, and Pete), and the “boys” of the Oak Grove Hotel — Ajay, Chris, Erich, Ike, Joost, Larry, and Wolf.

My family deserves recognition for supporting me both emotionally and financially, and especially for never getting tired of hearing, “I’ll be done in another <year|month|week>.” My best friend, Eric Freeman, put forth virtually all of the effort to keep in touch while I convinced myself that I was too busy to call. I’d also like to thank Tracey Sealer for convincing me to go to graduate school in the first place.

My most memorable experience that I’ll take away from Stanford began when I volunteered (once again) to work on something other than my thesis. And ended up getting much more involved than I would have ever dreamed — but not with the project. Instead, I fell in love. Laura Schragar has shown me more patience and support than I could have ever hoped, and so I must thank her most of all. Forever.

Table of Contents

Acknowledgments	iii
Table of Contents	v
List of Tables	ix
List of Figures.....	xi
Chapter 1 Introduction	1
Chapter 2 High Speed Static Memory Subsystems	5
2.1 Static Memory Basics	5
2.1.1 Fast SRAM Organization and Conventions.....	7
2.1.2 Decoders	9
2.1.3 Column Read/Write Circuits	11
2.1.4 Banks	11
2.2 CMOS Static Memories.....	13
2.2.1 CMOS Static Memory Cells.....	14
2.2.2 Complete CMOS SRAMs.....	16
2.2.3 Reducing CMOS SRAM Delay	18
2.3 Bipolar Static Memories	20
2.3.1 Bipolar Static Memory Cells	22
2.3.2 Complete Bipolar SRAMs	24
2.4 BiCMOS Static Memories	28
2.4.1 BiCMOS Design Styles	28
2.4.2 Complete BiCMOS SRAMs.....	29
2.5 Summary	31
Chapter 3 Low-swing BiCMOS Decoders.....	35
3.1 Bipolar Decoder Power Dissipation	36
3.2 Pre-decoding for Diode Decoders.....	37
3.3 Diode Decoder with Switched PMOS Load Resistor	39
3.3.1 Basic Operation.....	40
3.3.2 Switched PMOS Load Design Considerations	41
3.3.3 Reference Generation	44
3.3.4 Address Line Sharing.....	46

3.3.5 Results.....	47
3.4 Pulsed Diode Decoders.....	49
3.4.1 Basic Operation.....	50
3.4.2 Capacitively-pulsed Diode Decoders.....	52
3.4.3 NMOS Capacitor Diode Decoders.....	54
3.4.4 Summary.....	56
3.5 Pulsed <i>NOR</i> Decoders.....	58
3.5.1 Basic Operation.....	59
3.5.2 Pulsed Current Source.....	60
3.5.3 Pulsed Address Buffers and Address Line Drivers.....	62
3.5.4 Bank Selection.....	66
3.5.5 Reference Generation.....	68
3.5.6 Summary.....	70
3.6 Word Line ECL-CMOS Converter.....	71
3.6.1 Low-Power Word Line Level Converter.....	72
3.6.2 Use in Pulsed Word Line Discharge.....	73
3.7 Summary.....	75
Chapter 4 Sense and Write Techniques for CSEA Memories.....	77
4.1 CSEA Basics.....	78
4.2 Single-ended Bit Line Sensing.....	81
4.2.1 Simplified Sensing.....	82
4.2.2 Effects of Emitter and Bit Line Resistance.....	84
4.2.3 Data-dependent Supply Noise.....	86
4.2.4 Bit Line Reference Design.....	91
4.3 Two-level Cascode Sense Amplifier.....	91
4.3.1 Sense Reference Design.....	92
4.3.2 Two-level Cascode Network.....	94
4.3.3 Cascode Reference Design.....	95
4.3.4 Results.....	97
4.4 Pulsed Sensing.....	98
4.4.1 Theory of Operation.....	99
4.4.2 Pulsed Bit Line Circuitry.....	101
4.4.3 Peripheral and Reference Circuits.....	103
4.4.4 Results.....	107
4.5 CSEA Writing Techniques.....	108
4.5.1 Single-ended Versus Differential Cell Writing Issues.....	108
4.5.2 Local Word Line Qualification.....	110
4.6 Summary.....	111

Chapter 5 Results	113
5.1 An Experimental 64K CSEA SRAM	114
5.1.1 Cell Design	114
5.1.2 Organization.....	115
5.1.3 Measured Results.....	118
5.2 Proposed 256K CSEA SRAM	121
5.2.1 Results.....	123
5.3 A Synchronous 256K CSEA SRAM	125
5.4 Summary	127
 Chapter 6 Conclusion	 129
6.1 Future Work.....	130
 Chapter 7 Bibliography	 133

List of Tables

Table 1-1	Process Characteristics	3
Table 5-1	4K×64 SRAM Power Variation	127
Table 5-2	SRAM Performance Comparison	128

List of Figures

Figure 2-1	External SRAM Interface	7
Figure 2-2	Internal SRAM Organization.....	9
Figure 2-3	Basic Decoder Structure	10
Figure 2-4	Banked SRAM Organization	13
Figure 2-5	A CMOS <i>NAND</i> Gate	14
Figure 2-6	A 6T CMOS Memory Cell	15
Figure 2-7	Simplified CMOS SRAM Read Access Path	17
Figure 2-8	An ECL <i>NOR</i> Gate	21
Figure 2-9	Schottky Barrier Diode Load Memory Cell	22
Figure 2-10	Bipolar Decoders	25
Figure 2-11	Bipolar SRAM Read Access Path	27
Figure 2-12	BiCMOS SRAM Read Access Path	32
Figure 3-1	Simplified Word Line Driver.....	36
Figure 3-2	A Push-pull Address Buffer.....	38
Figure 3-3	A Pre-decoding Address Buffer.....	39
Figure 3-4	A PMOS Load Diode Decoder	40
Figure 3-5	PMOS Load Characteristics.....	43
Figure 3-6	PMOS Load Gate Swing Over Process and Temperature	44
Figure 3-7	Gate Switching Waveforms for PMOS Loads.....	45
Figure 3-8	PMOS Load Reference Generator	46
Figure 3-9	Address Buffer with Segmented Address Lines	47
Figure 3-10	Advantages of Pulsed Signalling for Diode Decoders.....	51
Figure 3-11	A Capacitively-Pulsed Diode Decoder	52
Figure 3-12	A NMOS Capacitor Pulsed Diode Decoder	54
Figure 3-13	An Adjustable V_{BE} Multiplier	55
Figure 3-14	Power/Delay Comparison of Pulsed Diode Decoders	57
Figure 3-15	A Pulsed <i>NOR</i> Gate	59
Figure 3-16	Variable Level Shift for Pulsed Current Sources.....	61
Figure 3-17	A Pulsed Current Source.....	61
Figure 3-18	Pulsed Current Source Reference	63
Figure 3-19	Pulsed Address Line Routing	65
Figure 3-20	A Pulsed Address Buffer with Pulsed Address Lines.....	65
Figure 3-21	A Pulsed Bank Selection Decoder	67
Figure 3-22	A V_{SS} Generator	69

Figure 3-23	A Word Line Level Converter	73
Figure 3-24	A Level Converter-Based Pulsed Word Line Discharge System	74
Figure 4-1	CMOS-Storage, Emitter-Access Memory Cell	78
Figure 4-2	CSEA Memory Read Access Path.....	80
Figure 4-3	CSEA Cell Bit Line Sensing Model	83
Figure 4-4	Model for Worst-Case Reading Zero.....	84
Figure 4-5	Read Word Line Swing Variation	87
Figure 4-6	V_{Drop} Dependence on R_{P1}	90
Figure 4-7	Sense Amplifier Reference Circuit.....	93
Figure 4-8	A Two-Level Cascode Sense Amplifier	95
Figure 4-9	Clamp1 Reference Generator	97
Figure 4-10	Sense Path Performance with Supply Noise.....	98
Figure 4-11	Oversimplified Bit Line Sense Model	99
Figure 4-12	Comparison of Switching Waveforms.....	100
Figure 4-13	A Pulsed CSEA Bit Line	102
Figure 4-14	Simulated Pulsed Bit Line Waveforms.....	103
Figure 4-15	Pulsed Bit Line Reference	105
Figure 4-16	Pulsed Bit Line Control Circuits.....	105
Figure 4-17	Pulsed Bit Line Reset Reference	106
Figure 4-18	Write Qualification Circuit	110
Figure 5-1	Fabricated CSEA Memory Cell.....	115
Figure 5-2	CSEA Cell Layout	116
Figure 5-3	16K×4 SRAM Organization.....	117
Figure 5-4	Critical Access Path for 16K×4 SRAM	119
Figure 5-5	Chip Photomicrograph of 16K×4 CSEA SRAM	120
Figure 5-6	Oscillograph of Bank-switching Read Access.....	121
Figure 5-7	Simulated Switching Waveforms for 16K×4 SRAM.....	122
Figure 5-8	64K×4 SRAM Organization.....	123
Figure 5-9	Simulated Switching Waveforms for 64K×4 SRAM.....	124
Figure 5-10	Pulsed Address Line Routing	126

Chapter 1

Introduction

Changes in integrated circuit processing technology provide new challenges, and sometimes new opportunities, for SRAM designers. A case in point is BiCMOS. This relatively new technology, which integrates components from both bipolar and CMOS processes, offers the opportunity to design systems with the high switching speed of ECL bipolar circuits or the low power dissipation and high density of CMOS circuits. The challenge of BiCMOS circuit design is to achieve high speed, high density, and low power, simultaneously. The field of fast SRAMs provides an excellent arena in which to compare BiCMOS circuit designs, since SRAMs are simple to design, perform a useful function, and are very easy to compare. At the lower power end of the spectrum, a number of BiCMOS SRAMs achieve faster access than CMOS designs at nearly equivalent power and density [1 2 3]. However, at the other end, the BiCMOS memories with nearly-bipolar access times dissipate much more power than their CMOS counterparts [4 5]. This dissertation explores the use of BiCMOS technology to build very high-speed SRAMs at power and density levels appropriate for integration onto single-chip computers.

This thesis comprises six chapters. Since SRAM design is a highly developed field, this thesis builds upon many ideas from previous work. Chapter 2 provides background material for understanding the content and context of this work. After discussing SRAM organizational issues that affect performance, the chapter focuses on the performance characteristics of static memories fabricated in the major silicon-based integrated circuit technologies. In particular, the chapter zeroes in on the advantages and disadvantages of CMOS, bipolar, and BiCMOS memories in terms of speed, power, and capacity.

A major speed advantage of bipolar memories arises from the fast switching offered by low-swing bipolar decoders. Unfortunately, the power dissipation of bipolar decoders is prohibitive for many high-capacity applications. Chapter 3 introduces new techniques that reduce the power of low-swing decoders without substantially increasing the delay. By

replacing the standard decoder load resistor with a switched PMOS transistor, gate currents and load resistances may be simultaneously varied so that a decoder gate dissipates much less current when it is unselected. If decoder selection is sufficiently rapid, then active transitions are not delayed. The chapter demonstrates this approach for improving the power dissipation of diode *AND* and ECL *NOR* decoders. For ECL *NOR* decoders, the switched PMOS load is combined with a new pulsed current source to reduce the average power of the decoder *NOR* gate. The pulsed signalling needed by such a gate has speed as well as power advantages, but places stringent requirements on the pulsed current sources and their supplies. To address this issue the chapter proposes a new on-chip supply generator that uses the capacitance of the memory arrays to supply the transient charge required by the current pulses. Finally, the chapter introduces a low-power ECL-CMOS level converter that is appropriate for providing pulsed word line discharge currents that improve both memory access time and power.

Another significant component of the access time in most BiCMOS memories results from the delay in amplifying the low-swing decoded address into sufficiently large voltages to access a CMOS memory cell. The CMOS-storage emitter-access (CSEA) memory cell, which has been previously integrated [6], is accessed with a low-swing word line, and thus has the potential for faster access. However, the CSEA cell requires careful design to overcome the limitations of its single-ended read port and full-swing write port. Chapter 4 describes techniques that provide fast and robust CSEA sensing and writing. A primary concern of low-swing single-ended reads is the effects of transient supply variation on the bit lines. The chapter opens with an analysis of the noise margin of CSEA bit line sensing in the presence of array parasitics and supply noise; the analysis shows that CSEA sensing can be robust due to the high read current supplied by the CSEA memory cell. However, the bit lines are only part of the problem, since the large amount of multiplexing required for large SRAMs leads to the use of very low-swing signalling elsewhere in the sense path. The chapter introduces a new two-level cascode sense amplifier that improves access time by reducing the capacitance on long global wires while maintaining excellent signal integrity in the presence of supply noise. For pulsed CSEA memories, a better solution is proposed that improves the delay by effectively beginning each access with the bit line close to its switching point. This method is especially applicable for wide access widths, where the column overhead of the pulsed sensing is reduced. Finally, the chapter attacks the write performance issues, by applying the word line ECL-CMOS level converter of Chapter 3 and a modified divided word line technique to provide fast writes with large noise margin and small cell area.

Chapter 5 puts together the work of Chapters 3 and 4 by exploring the design of several different CSEA SRAMs. It reports experimental results of a 16K×4 CSEA memory that delivers 3.7-ns read access time in a 0.8- μm BiCMOS process technology [7–8]. This technology provides 0.8- μm NMOS and PMOS channel lengths with silicided polysilicon and diffused regions, a 7-GHz f_T NPN bipolar transistor, and 3 levels of tungsten metallization. Important process characteristics are summarized in Table 1-1. Because this was the fabrication technology for the experimental memory, it is also used throughout this thesis as the process for circuit exploration and simulation; in this way fair comparisons are possible between fabricated and simulation-based designs. While the 16K×4 memory utilizes several of the design techniques of this thesis, the 64K×4 simulation-based design of Section 5.2 provides faster (3.4ns) and more robust reads due to the incorporation of improved circuits from Chapters 3 and 4. This performance level is achieved at much lower power than has been reported for bipolar memories. The pulsed circuit techniques of this thesis offer additional speed and power advantages for synchronous static memories. Chapter 5 describes a complete pulsed BiCMOS memory that offers 2.5-ns access time at a power dissipation of less than 3W. These designs show the performance advantages that can be achieved by combining CMOS transistors into low-swing ECL-style logic gates.

Table 1-1 Process Characteristics

Parameter	Value
Minimum NPN Emitter	1.6 μm × 0.8 μm
NPN β	100
NPN f_T	7GHz
NMOS/PMOS Minimum Gate Length	0.8 μm
NMOS/PMOS t_{ox}	20nm
Contacted First Metal Pitch	2.8 μm
Contacted Second Metal Pitch	2.8 μm
Contacted Third Metal Pitch	3.2 μm

The final chapter summarizes the contributions of this thesis. It also suggests a few areas where additional research could advance these results.

Chapter 2

High Speed Static Memory Subsystems

This thesis focuses on circuit design techniques for high performance BiCMOS static memories. In order to provide a framework for understanding the techniques and the issues behind them, this chapter provides an overview of high-speed SRAM design. The chapter discusses basic SRAM structures and terminology, and provides historical perspective on the circuits used in SRAMs. In particular, the design of SRAMs in CMOS, bipolar, and BiCMOS technologies is described, because the techniques of Chapters 3 and 4 borrow and expand upon circuits and concepts from each of the three technologies.

The chapter's organization reflects these goals. Section 2.1 introduces the architectural structure and function of a typical SRAM as well as the SRAM terminology used in this thesis. Section 2.2 discusses high-speed memories built exclusively from CMOS transistors. While its extremely low static current memory cell and high packing density once provided its principal advantages, new circuit techniques and faster devices have rapidly closed the access time penalty versus bipolar and BiCMOS designs. Section 2.3 describes the fastest silicon memories currently built — those constructed from high-speed bipolar technology. While density and power considerations prevent the use of bipolar memories in most systems, low-swing access techniques developed for these SRAMs are widely and increasingly being applied to other technologies. SRAMs built using the hybrid technology BiCMOS are the topic of Section 2.4. The additional design flexibility inherent in BiCMOS has produced a wide variety of performance tradeoffs, including some SRAMs with nearly-bipolar speed and nearly-CMOS power and density.

2.1 Static Memory Basics

All computer memories have a mechanism for storing their data, but *static* memories are unique because they utilize active devices that are connected in a positive feedback loop to retain their data. The active feedback allows static memories to hold their data as long as

power is applied. In contrast, *dynamic* memories typically store their data as charge on a capacitor, and since the charge may leak away, the data can be lost unless it is *refreshed* (i.e. re-stored). All of the memories of this thesis are *random-access memories* (RAMs), which says that external circuitry may access the stored data in an arbitrary order. Some other types of static memories, such as queues, do not allow random access. Furthermore, a RAM supports both *writing* (i.e. updating) and *reading* (i.e. interrogating) the stored data at roughly equal speeds and in an arbitrary ordering. The memories described in this thesis are thus all termed static RAMs, or SRAMs.

RAMs are typically compared on the basis of four performance metrics:

- Capacity — how many bits of data the memory may store at once
- Power — how much power the memory requires to operate
- Read Access Time — how much delay exists between the time when the system presents an address to the memory and the time when the memory presents the read data back to the system
- Write Cycle Time — how much delay exists between the time when the system presents both data to be written and the address at which to write and the time when the memory is prepared to accept further read or write requests from the system

SRAMs have performance advantages over other memories which make them suitable for certain applications. First, SRAMs that are fabricated in CMOS technologies can have very low standby power, so CMOS SRAMs are very attractive for low-power applications such as battery-powered systems; dynamic memories suffer the disadvantage of power-consuming refresh cycles. Second, SRAMs usually offer significantly faster access and cycle times than other memories. This advantage makes SRAMs popular for high-speed buffer memories and cache memories. A final advantage is that SRAMs are readily built in the same technologies used for building large digital circuits such as microprocessors, so SRAMs are increasingly used as fast on-board memories for high-integration digital integrated circuits. These advantages outweigh the principal disadvantage of SRAMs: they tend to have lower capacity than dynamic memories, due to the larger number of active devices in an SRAM memory cell and the wires required to connect them.

2.1.1 Fast SRAM Organization and Conventions

An SRAM presents a simple interface to the system designer. A simplified view of this interface appears in Figure 2-1. An SRAM appears to implement a linear array of $N_{Locations}$ storage locations, each of which can contain a single W -bit quantity of data (i.e. a *word*). The word is the fundamental unit of data communication between the system and the SRAM, since all bits in a word are read or written simultaneously. This memory is said to be *organized* as $N_{Locations}$ words by W bits, and has a total memory capacity of N_{Bits} bits, where N_{Bits} is simply:

$$N_{Bits} = N_{Locations} W \quad (2-1)$$

The interface features three types of inputs and one type of output. The N_{Addrs} -bit wide input address field specifies which one of the $2^{N_{Addrs}}$ (i.e. $N_{Locations}$) memory locations is being accessed. The single-bit command field determines whether the current access reads or writes the selected location. The W -bit write data field supplies the new data that is to be written into the selected location if the command field specifies writing. Finally, the W -bit read data field outputs the contents of the selected memory location during read commands.

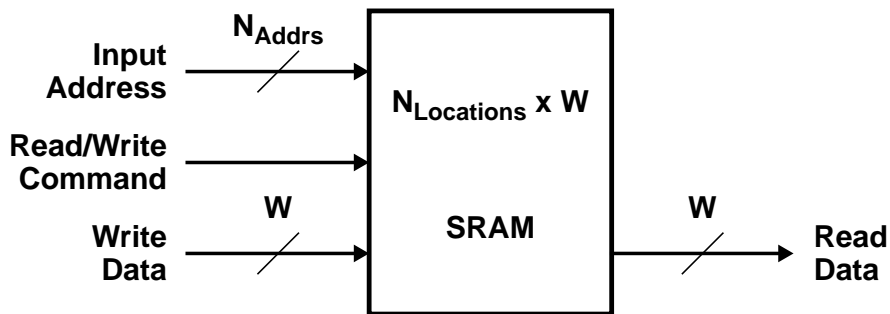


Figure 2-1 External SRAM Interface

The internal structure of a static memory is composed largely of memory cells, which each hold one bit of data and thus form the fundamental unit of storage. One can view an SRAM memory cell as a black box with three classes of connections to the outside world, or *ports*:

- **Power Ports** — These terminals supply constant voltage potentials that the cell uses to maintain its stored value and source and/or sink current when the cell

communicates through its other ports. These ports usually are omitted from block diagrams and schematics because they convey no signalling information and connect every cell together. There are typically two such ports per cell.

- Selection Ports — These ports select a given cell to be read and/or written, usually via a change in voltage potential. This thesis consistently draws the physical wires that connect the selection ports of memory cells as horizontal lines and terms them *word lines*; a word line is a wire that selects (at least) one word's width of bits. There is usually one such port per cell.
- Communication Ports — Values read from or written to the memory cell pass through the communication ports. This thesis consistently terms the wires that connect these memory cell ports as *bit lines* because they allow the transmission of the stored single-bit values into and out of the cell; bit lines appear as vertical lines in SRAM diagrams. There is typically one communication port per cell, but it often involves a pair of differential bit lines that communicate complementary data values.

The memory cells are designed to tile into two-dimensional arrays, with the word lines connected to each cell in a row, and the bit lines connected to each cell in a column. While the external organization would suggest a memory array $N_{Locations}$ words tall by one word wide, physical constraints that arise from the fact that $N_{Locations}$ is typically many thousand times larger than W require an internal organization with an aspect ratio much closer to unity. As depicted in Figure 2-2, the tall thin logical array may be folded into a nearly square physical array such that a single word line selects multiple words simultaneously.

The blocks outside the memory array convert the address, command, and data values presented by the controlling system into the appropriate word line and bit line signalling required to access the array. In particular, the *row decoder* selects the word line that contains the desired word, while the *column decoder* selects the requested word from among those selected by the word line. By constraining the number of rows per array (N_{Rows}) and the number of words per column (N_{Cols}) to each be powers of two, the addresses for the row and column decoders are trivially generated by simply routing $\log_2 N_{Rows}$ bits of the input address to the row decoder, and the remaining $\log_2 N_{Cols}$ bits to the column decoder. Meanwhile, the command and write data inputs direct the *column read/write* circuitry to either sense the read data from, or write the input data to, the bit lines of the selected word. Both the decode and column read/write circuitry deserve additional mention, since they greatly affect the overall SRAM performance.

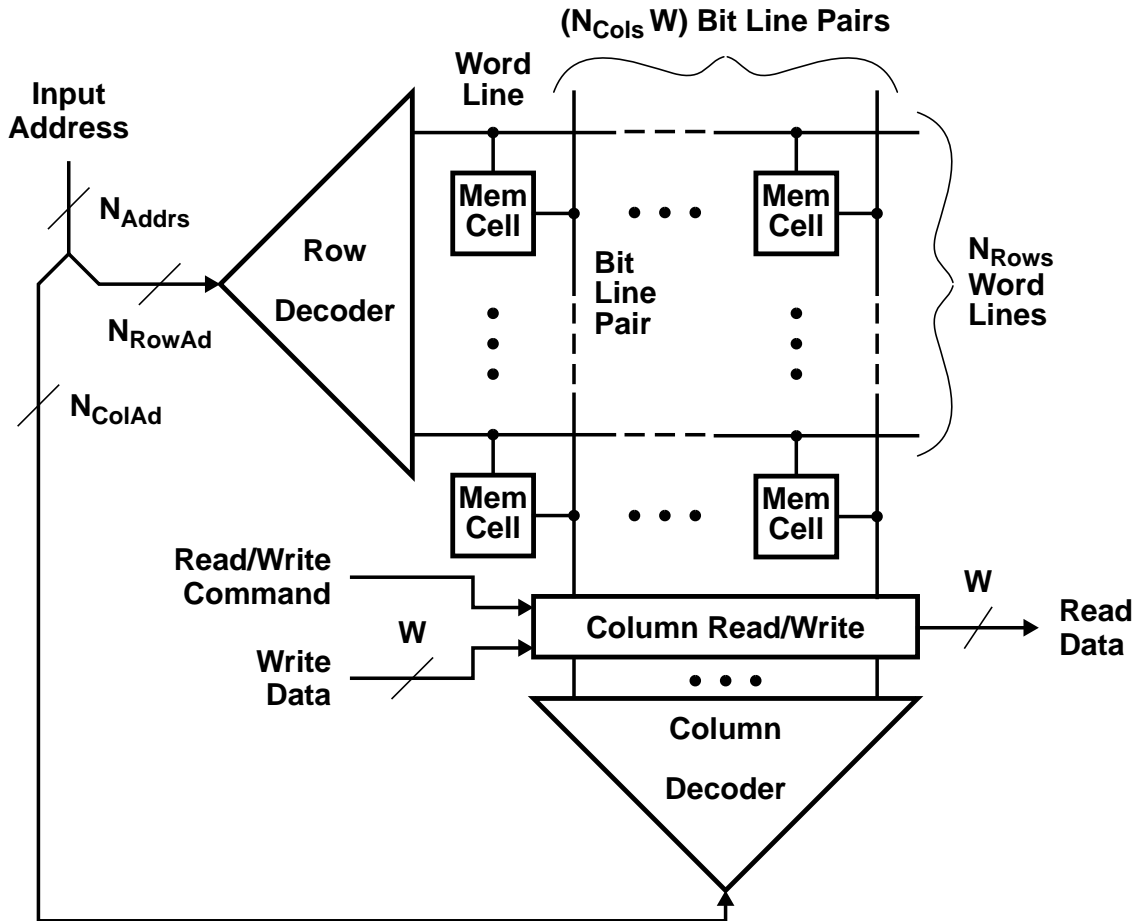


Figure 2-2 Internal SRAM Organization

2.1.2 Decoders

Decoders perform a logically simple function that turns out to be fairly complicated to implement in a high-performance way. The goal is quite straightforward: given an N -bit input address, select whichever of the 2^N output lines is identified by the address. Given true and complemented versions of each address bit, decoding reduces to simply a N -input *AND* gate for each output line; the correspondence between output lines and addresses is programmed by choosing which version of each input bit (i.e. true or complemented) to connect to the inputs of each *AND* gate. High-speed decoder design is more complex because as the memory capacity increases, the number of address bits rise so the number of inputs per *AND* gate (i.e. the gate *fan-in*) increases. Since increased *fan-in* gates have higher delay, most large SRAM decoders use multiple stages of *AND* logic that each have lower delay due to reduced *fan-in*. In addition, increasing capacity also increases the number of memory cells affected by each decoder output, which is to say that the gate *fan-out* goes up. Increasing *fan-out* further complicates the design, since the delay of logic gates

increases with *fan-out*. Many SRAMs add additional gain stages to their decoders to quickly drive large loads.

While the decoding structures described later in this chapter, and in Chapter 3, have many differences, they all follow the basic structure of Figure 2-3. The *input buffers* increase the signal strength of the N input addresses to drive the capacitance of the decoder gates, while generating (at least) true and complemented versions of each input on the *address line* outputs. For multi-stage decoders, the input buffers typically include the first decoding stage and thus produce *pre-decoded* address lines, where each line represents a logical conjunction of two or more inputs.¹ The address lines select the desired decoder *AND* gate, which in turns selects a *driver* that increases the signal strength to handle the large *fan-out* of the array (for row drivers), or generates control signals for the column read/write circuitry.

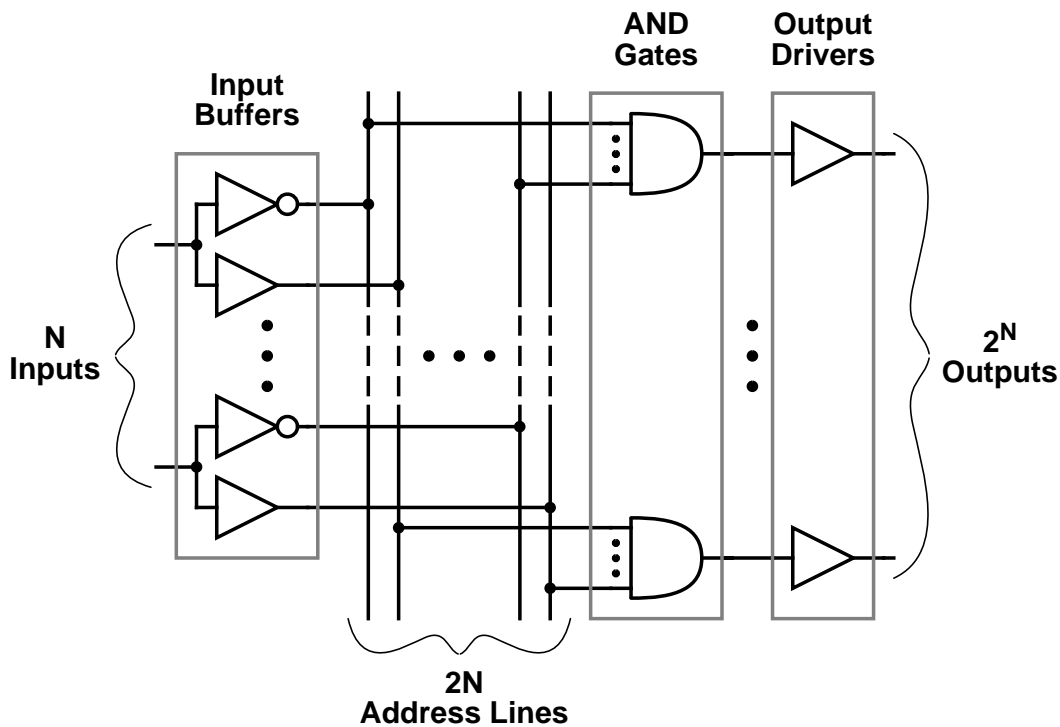


Figure 2-3 Basic Decoder Structure

¹The number of bits pre-decoded by each input buffer is often two, because the four wires needed to communicate the four possible states of two bits is no more than what is required to send both true and complement versions of two addresses; beyond three bits of pre-decoding the number of required wires grows rapidly, increasing both the required routing area and the total decoder wiring capacitance.

2.1.3 Column Read/Write Circuits

The column read/write circuits also have a simple logical description that is substantially more difficult to implement for large, high-speed SRAMs. On a read access, the column decoder directs the read/write circuits to steer the bit line data from the selected word to the *output buffer*, which drives the read data to the system. The logic that steers one of many inputs to the output is known as a *multiplexer*. As the memory capacity increases, both the number of inputs to each multiplexer and the number of cells on each bit line rise. The increased capacitance is especially difficult on the bit lines, since the read current from a memory cell is typically not high enough to rapidly charge the parasitic capacitance from hundreds or thousands of other memory cells on the same bit line. As a result, fast SRAMs often use low-swing signalling for reading their bit lines; the basic idea is to begin each read with the differential bit lines at the same potential, and then to amplify the difference between the bit lines that develops once the word line selects the memory cell. Unfortunately, the *sense amplifier* typically requires too much power and physical space to implement with each bit line pair. Thus, the sense amplifiers typically operate on the outputs of the multiplexers. However, this arrangement adds the large capacitance of the multiplexer onto the bit line capacitance, which slows the access. Instead of paying this access penalty, many memories break the multiplexer into stages with reduced capacitance and insert a sense amplifier between the first and second stages; for very large memories the intermediate multiplexer capacitance is often high enough that adopting low-swing signalling between multiplexers (with additional sense amplifiers) provides higher performance.

On a write access, the input write data must be steered to the bit lines of the selected word; because this logic steers one value to one of many places, it is known as *demultiplexing*. While most CMOS SRAMs once used the same bidirectional pass transistors to accomplish both multiplexing and demultiplexing, many fast SRAMs now have parallel paths so that the read path may use smaller swings than the write path and so the memory may begin a write access as soon as a previous read has cleared the bit lines. The write circuits typically get little benefit from low-swing signalling, since the devices that drive the demultiplexer and the bit lines can be much larger than the devices attached to the bit lines, so traditional buffering works quite well.

2.1.4 Banks

While both decoders and read/write circuits may be modified to maintain certain performance parameters as memory capacity increases, intrinsic problems with the memory

array itself eventually begin to reduce the performance. This performance degradation arises from several factors. All the memory cells on the selected word line attempt to charge their bit line capacitance, independent of whether the bit lines are part of the selected word. Thus, very long word lines waste lots of power in charging unselected bit lines. A second factor is the intrinsic delay of the wires that form the word and bit lines; as the arrays grow, so does both the resistance of these wires and the capacitance that loads them. As a result, the distributed wire RC delay grows as the square of the array dimensions, which slows the access time. Finally, the number of cells on a bit line begins to slow the access, since there are practical limits to how small a bit line swing may be reliably sensed.

Rather than tolerate the performance limitations of large arrays, SRAM designers avoid these problems by using several smaller arrays (often termed *banks*). For example, Figure 2-4 depicts a large memory array which is then broken into four smaller arrays. The smaller arrays have higher performance because they feature fewer cells per word line and bit line. However, there is a penalty to this approach: the required amount of decoding increases. In the figure, the number of decoder gates doubles, since the number of both word and bit lines doubled when the arrays were split apart. Furthermore, the *fan-in* of the decoders increases. Considering the row decoders in the example, the individual decoder blocks control half as many word lines as those in the large array, which requires one less bit of decoding. However, these decoders also must select between the four banks, since only one word line should be selected at once to reduce the power in unselected cells; this extra decoding requires two additional bits of decoding, so the decoder AND gates in the four-bank case each have one more input than those of the single array.

The increased decoding that results from banked SRAM designs limits the memory performance in several ways. The increased decoder *fan-in* slows the access. The increased die area devoted to decoding reduces the memory capacity. Finally, for technologies such as ECL where the basic decoder dissipates static power, the decoding power increases in proportion to the number of decoders. As a result, designing large and fast SRAMs requires complex analysis to determine the appropriate array sizing and organization to maximize performance. The next sections look at these tradeoffs for CMOS, bipolar, and BiCMOS SRAMs.

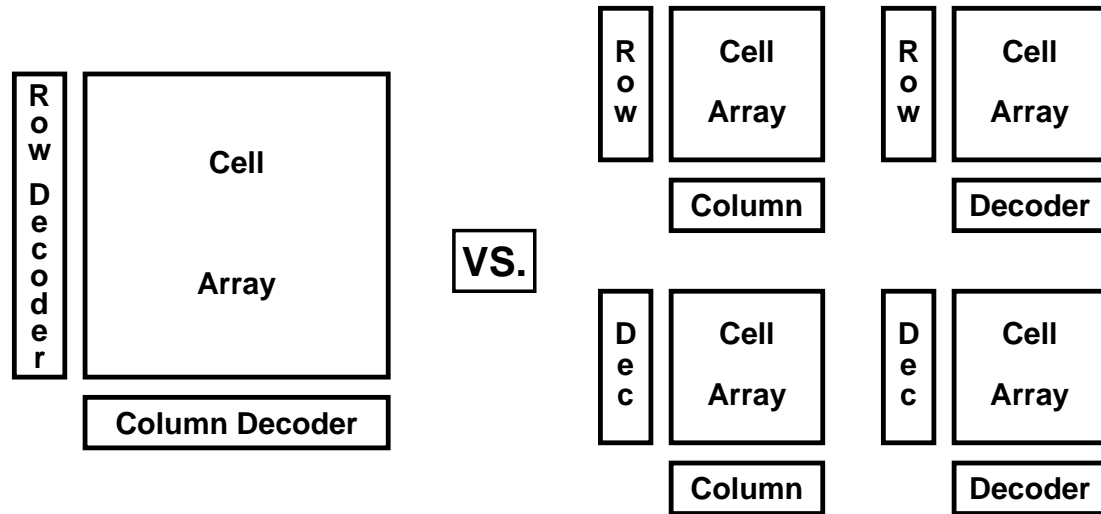


Figure 2-4 Banked SRAM Organization

2.2 CMOS Static Memories

SRAMs implemented in CMOS technologies dominate the marketplace, because CMOS memories offer low power and high capacity solutions. Traditionally, CMOS SRAMs were much slower than the bipolar alternatives, but rapid improvement in CMOS device performance due to technology scaling and innovative circuit design technique have greatly narrowed the gap. This section describes the design of fast CMOS SRAMs, with an emphasis on understanding the advantages of CMOS technology that will be exploited by the circuits of this thesis.

Complementary MOS (CMOS) circuit technology takes advantage of the insulating gate terminal and near-zero “off” current of the Metal-Oxide-Semiconductor Field-Effect Transistor (MOSFET) to implement logic gates that dissipate nearly-zero static power. By utilizing n-channel and p-channel MOSFETs (i.e. NMOS and PMOS transistors), which have opposite threshold voltages, classic CMOS circuits implement switch networks that guarantee that no current paths exist between the power supplies once the inputs transition; the action of the switches connects the output to one of the supplies while isolating the output from the other supply. For example, in the CMOS *NAND* gate of Figure 2-5, the output is high (V_{DD}) if either input is high, since one or both of PMOS transistors P1 and P2 are conducting and the output is isolated from the low supply (V_{SS}) by at least one of the series-connected NMOS devices. The output is low only if both inputs are low, where the only conducting path is to V_{SS} via N1 and N2.

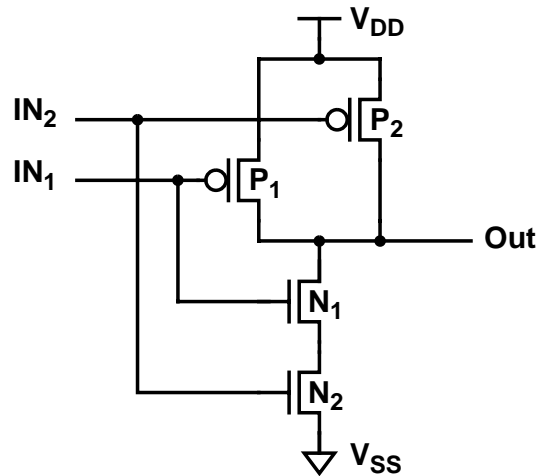


Figure 2-5 A CMOS NAND Gate

The output levels of CMOS gates are the two supply voltages V_{SS} and V_{DD} , so switching outputs swing the entire supply range. Such large signal swings are the primary source of the increased delay in CMOS circuits versus bipolar ones, since for a fixed device current it requires twice as long to charge a capacitor twice as much voltage. However, the large swings also guarantee that the next stage of logic sees inputs that are close enough to the supplies to turn off one device type, so idle CMOS circuits use no power.

The density advantages of CMOS result in part from its low power dissipation. While competing technologies may also implement millions of components per die, their power consumption levels are too high for the heat-removal capabilities of standard packaging. This is not to say that all CMOS dies are low-power. The advantage of CMOS is that gates only require power when they switch, which is to say when they are accomplishing useful work. Competing technologies where the basic gates require static power are at a disadvantage because in most digital systems, and certainly all SRAMs, most of the circuitry is idle at any given moment. The next subsection introduces the simple circuit that occupies most of the space, while requiring little of the power, of many CMOS and BiCMOS SRAMs: the 6T CMOS memory cell.

2.2.1 CMOS Static Memory Cells

The fastest CMOS SRAMs use six-transistor (6T) CMOS static memory cells because the other alternatives have slower cell rise times and thus longer write times. The cell area penalty for the 6T cell is substantial, roughly 50% over the competing cell types, but is still only about $76\mu\text{m}^2$ in a $0.8\text{-}\mu\text{m}$ technology, which permits enough capacity for many

applications. Furthermore, because the 6T cell requires only bulk PMOS and NMOS devices, 6T cell-based SRAMs are often implemented on the same integrated circuit as other parts of the system that uses the SRAM, which improves system integration.

The 6T cell itself is quite simple. Two CMOS inverters with each inverter's output connected to the other inverter's input (*cross-coupled*) create a very stable, nearly zero power latch that is the basis for the memory cell shown in Figure 2-6. The latching operation is very simple: if node **D** is higher than the switching threshold of the N2-P2 inverter then NMOS device N2 pulls down node \bar{D} , in turn causing P1 to pull node **D** higher. This positive feedback action forces $D = V_{DD}$ and $\bar{D} = V_{SS}$, (neglecting any effects of N3 and N4). We say that the memory cell stores one when node **D** is high and \bar{D} low. Similarly, if the cell stores zero then **D** is low and the positive feedback forces \bar{D} high. The leakage current in such a latch is very small. In common bipolar memories the storage current per memory cell is less than 10^{-15} Amps (1 femtoAmp), so the idle current of a megabit memory array is less than 1 nA. Thus CMOS memory arrays require very little standby power.

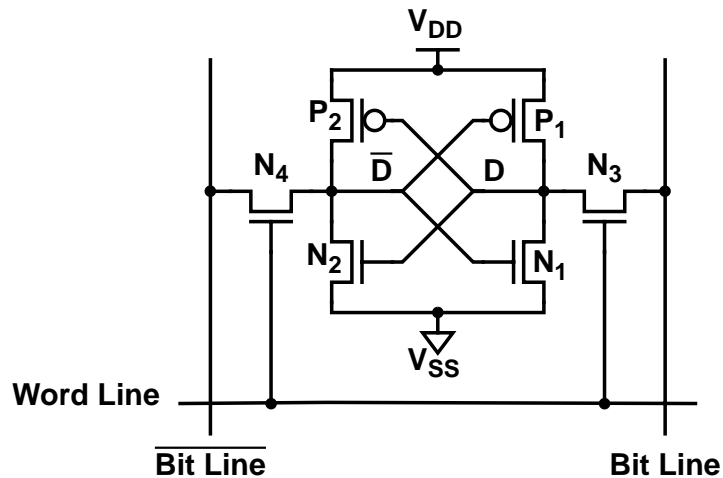


Figure 2-6 A 6T CMOS Memory Cell

The latched value is both altered and read through the NMOS access devices N3 and N4. Because PMOS transistors have higher on resistances than NMOS devices of the same size, it is simplest to flip the cell state by overpowering a PMOS device by pulling down its drain with the NMOS access device on the same side. This memory cell is written by raising the word line, often to V_{DD} , and pulling the bit line down to V_{SS} on the cell side that needs to be low. For instance, if a cell storing one is to be flipped then node **D** needs to drop so the bit line driver pulls BitLine to V_{SS} which causes access transistor N3 to fight

P2. N3 easily drops D low enough for P2 to begin turning on and then the latching action will rapidly finish flipping the internal cell nodes.

External circuitry can read the cell by raising the word line without driving either bit line. The cell access transistors then discharge one bit line towards V_{SS} and charges the other towards $V_{DD} - V_{Th}$. The high capacitance of the bit line presents a problem in reading the cell: when the word line first rises, the bit lines do not immediately change so they appear like voltage sources. If a read access begins with a bit line voltage that is too low, the access device will fight its PMOS device and may inadvertently flip the cell on a read access. Since NMOS transistors pull down more strongly than up, it is difficult to overpower an NMOS inverter device with the NMOS access transistor. Thus, higher bit line potentials are much less likely to unintentionally write a cell. The situation is often improved by making N1-N2 have higher drive strength (i.e. larger W/L) than N3-N4, which makes it impossible to disturb the cell value with a high bit line potential. Thus, the column read/write circuits must ensure that the bit lines are at safe (i.e. relatively high) levels before the word line rises to begin a read access.

A 6T CMOS cell can provide very fast read access, since the cell begins pulling on the bit line as soon as the word line rises past V_{Th} . The issues in making CMOS SRAMs go fast have much more to do with quickly raising the word line, and rapidly sensing the bit lines.

2.2.2 Complete CMOS SRAMs

The read access path of current megabit-class CMOS SRAMs have many (twenty or more) address pins and therefore require lots of decoding. As a result, CMOS decoders often utilize three or more stages of decoding to avoid the delay associated with ten-input series MOS transistor gating. For the sake of clarity Figure 2-7 presents a simplified view of a CMOS read path that retains the major circuit types present in fast CMOS SRAMs.

The input buffer generates true and complemented versions of each address bit, which are used to drive pre-decoded address lines. This pre-decoding is typically performed in two or three bit groups by a CMOS *NAND* gate followed by an inverter, with the inverter providing load-driving capability (using large device width) as well as the required logical inversion to implement the pre-decode *AND* function. The pre-decoded address lines are typically heavily loaded because they run the entire height of the row decoder and therefore have substantial wire capacitance along with the loading from the gate capacitance of the row decoders.

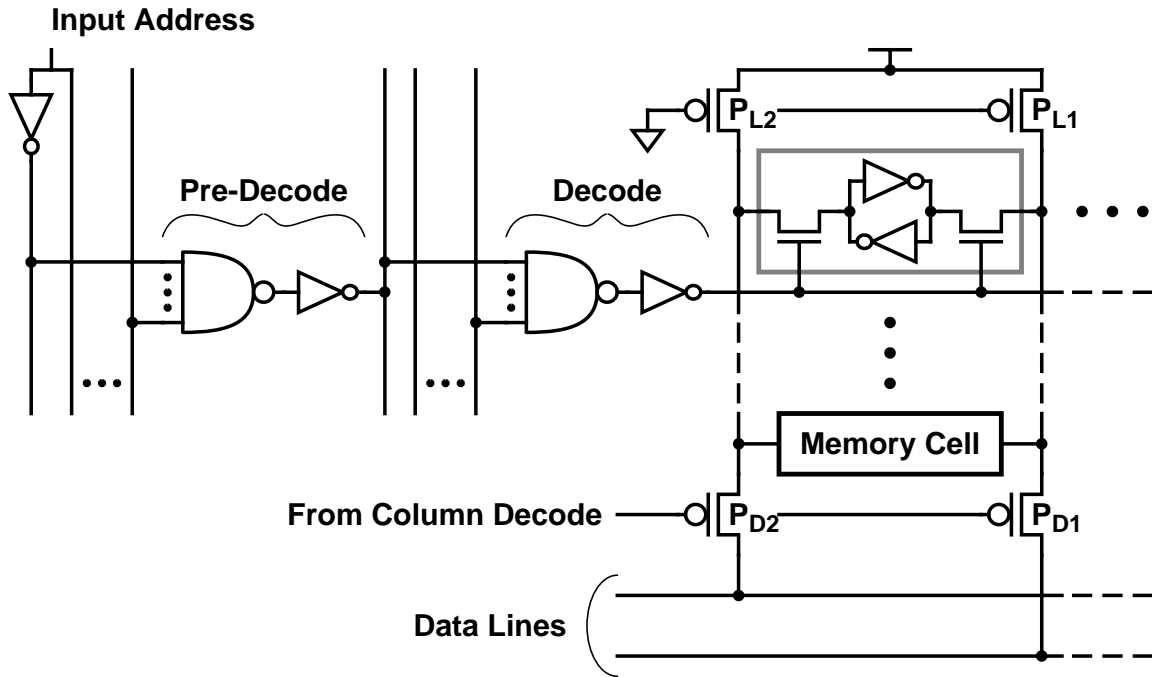


Figure 2-7 Simplified CMOS SRAM Read Access Path

Multi-input *NAND* gates also form the row decoder, often using small devices to minimize the loading on the address lines. The row decoder output is complemented and increased in drive capability by one or more inverters to control the heavily-loaded word line and thus access the memory cell.

The column decoder is implemented like the row decoder, and controls the column multiplexer to select which pair of bit lines are connected to the shared *data lines* via PMOS transistors P_{D1} and P_{D2} . The bit line load transistors P_{L1} and P_{L2} are weak PMOS devices that prevent the bit lines from dropping to unsafe levels (where newly-selected cells might be accidentally written) during reads; they are weak enough to be easily overpowered during intentional cell writes. A memory cell on a selected word line and selected bit lines pulls a current I_{Read} from the bit line on the low side of the cell. This current discharges the bit line capacitance, as well as the connected data line capacitance, until the bit line voltage drops enough that the bit line load will source I_{Read} . Meanwhile, the bit line load on the complementary bit line charges its data line towards $V_{DD} - V_{Th}$. The voltage difference between the data lines is detected by the sense amplifier. The output of the sense amplifier goes to the output buffer, which increases the drive strength of the signal and completes the access.

2.2.3 Reducing CMOS SRAM Delay

The *critical path* through a large SRAM would normally pass through the row decoder, word line driver and then the sense amp; the column decoder has a little more time to accomplish its task, so it normally does not delay the read access. A fast SRAM therefore requires rapid word line decoding and driving, as well as quick bit line sensing.

Minimizing the word line delays requires effectively integrating the logical decode function with the large *fan-out* requirements. Since each row address bit can select every word line, each address bit has a total *fan-out* of the number of word lines times the loading on each word line C_{WL} divided by the input buffer's input loading C_{IB} , i.e.

$$fan-out = 2^{N_{Rows}} \frac{C_{WL}}{C_{IB}} \quad (2-2)$$

The actual *fan-out* is higher because the decode gates utilize series gating, which provides lower output drive per unit of input capacitance than do inverters. CMOS inverter chains provide minimum load driving delays when the number of stages is set so that the *fan-out* per stage is approximately e [9]. This explains why large row decoders for fast SRAMs often use ten or more inverting gates to turn a row address into a word line transition. With so many gates to work with, such decoders typically further reduce delay by distributing the decode function among multiple gates beyond one level of pre-decoding.

A common method to improve the speed of CMOS logic chains is to use synchronous (i.e. *clocked*) design styles, which begin each access in a fixed *reset* state and then conditionally transition to the active state. For fast SRAMs, only one decoder output should ever be selected so the number of transitions in a clocked decoder is fairly small and thus power dissipation does not change much. More importantly, the transistors in the clocked gates may be sized to minimize the delay of the active-going transition, since the reset transition is generated via the clock and is thus independent. For instance, if the NMOS devices in the row decoder's *NAND* gates are increased in width versus the PMOS' width, the *NAND* output will begin falling at a lower input value (and hence earlier in the input's rising transition) and will supply more current and thus discharge its load more rapidly. If the NMOS/PMOS width ratio is increased such that the total input load is constant, then the PMOS width must decrease and thus the rising delay will increase. If a PMOS device is added in parallel with the other PMOS transistors with its gate activated by the reset clock, the rising delay is improved without sacrificing the fast falling delay.

CMOS logic gates with extra reset transistors form the basis for designs using *post-charge* logic [10–11] or the similar *self-resetting* circuits [12–13]. In order to let the selection devices be as wide as possible for a given input capacitance, these techniques make the deselection devices too weak to meet the required deselection delay. Instead, additional reset devices are added in parallel to the weak transistor and are activated by a delayed version of the selection signal output from the same gate; in other words, after the gate fires (i.e. switches to a selected state), its own output is fed back to reset the gate after a fixed delay (usually a few inverter delays), or *post-charged*.

The *RC* delay of the word lines is very significant for large CMOS SRAMs, which often have several thousand cells per row. The *divided word line* technique [14] reduces this delay by allocating two word lines for each row. The higher-resistance *global* word line runs the entire length of a row, and connects only to a set of buffers distributed along the row. The buffers drive much shorter *local* word lines that connect to the access transistors of the memory cells. This technique minimizes delay by reducing the capacitance of the long wires. The local word line buffers typically provide an additional level of decoding that ensures that only one local word line is high, and thus that only a subset of the cells on a row are selected.

Decoding the address inputs and driving the word lines takes about half the access time. The remaining delay is spent sensing the stored data and driving the output pins. The primary techniques used to reduce CMOS sensing delays involve extensive use of low voltage swing circuits to minimize the time required to charge the large capacitances present on the shared bit and data lines. The load problem is greatest on the bit lines, where one NMOS access device must move a wire connected to the drain terminal of every other access device on that bit line, as mentioned in Section 2.1.1. In order to minimize the delay, the bit line load devices become much stronger *clamp* devices, only active during reads, that guarantee that the bit lines begin an access at very nearly the same potential. The clamp transistors also limit the bit line read swings to minimize the bit line recovery time while ensuring that the sense amplifier has enough differential swing to resolve. Fast SRAMs minimize the delay by minimizing the required swing; as long as the bit lines start off at the same potential, delay will reduce as the sense amplifier sensitivity increases. Clocks are often used to activate the clamp devices to rapidly restore the bit line voltages following write cycles.

Because there are often thousands of columns in a SRAM, there is also a delay problem due to the high level of multiplexing required on the shared data lines. In order to reduce

this delay, many SRAMs utilize several levels of data lines (and hence multiplexing) with sense amplifiers connecting each level to the next, which allows the SRAM to improve the delay both by reducing the total capacitance in the access path and by reducing the voltage swings along each stage in the path.

The resulting CMOS SRAMs deliver access times that are much closer to those of bipolar SRAMs than is possible using traditional full-swing CMOS circuits [15]. The penalty of low-swing signalling is increased power dissipation, since the increased-sensitivity sense amplifiers use substantially more power than the full-swing circuits that they replace. However, as the next section shows, fast CMOS SRAMs use substantially less power than their bipolar counterparts, primarily due to the lack of static current in the memory cells.

2.3 Bipolar Static Memories

This section describes the design of bipolar SRAMs, which have delivered the fastest access and cycle times of any silicon-based technology [16 17 18 19 20]. Bipolar decoding and sense techniques used in these memories are the basis for some of the new techniques presented in this thesis.

The low-swing ECL bipolar logic circuits that implement the decoders are particularly interesting because they offer much faster switching speeds than CMOS circuits, although they use static current sources that substantially increase their power dissipation. In order to better understand the speed advantage of bipolar circuits, consider the ECL *NOR* gate of Figure 2-8. Bipolar junction transistors (BJTs) transistors Q1, Q2, and Q3 form a simple current switch that performs the desired logical function: the shared current (I_{Gate}) is switched into the load resistor (R_{Gate}) if either input is higher than the reference (V_{Ref}), and I_{Gate} thus flows through Q3 only if both inputs are below V_{Ref} . The *emitter follower* formed by Q4 and I_{EF} isolates R_{Gate} from the output capacitance (C_{Load}), and so the gate delay is dominated by the *RC* term arising from R_{Gate} times the capacitance at the shared collector node (A). For a fixed I_{Gate} (i.e. fixed gate power), the *RC* delay is proportional to the gate swing (V_{Swing}), since

$$V_{Swing} = I_{Gate} R_{Gate} \quad (2-3)$$

Thus, ECL circuits switch faster as V_{Swing} is reduced. Practical considerations limit the minimum swing to be about 700mV in most ECL systems, which is much smaller than the

3-V to 5-V swings common in CMOS systems. This speed advantage comes at the expense of power dissipation, since I_{Gate} and I_{EF} flow continuously, rather than only when the gate is switching.

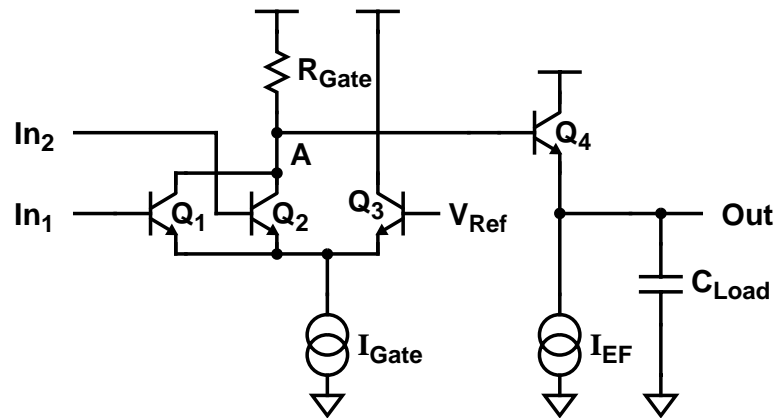


Figure 2-8 An ECL NOR Gate

The emitter follower supplies a lesser portion of the bipolar speed advantage. The high forward current gain (β) of the BJT makes the emitter follower an excellent buffer for driving large *fan-out*. While output ringing considerations under high-gain conditions typically limit the I_{EF}/I_{Gate} ratio at traditional ECL logic swings to around five, this signal strength improvement is achieved without using a level-restoring gate, so the delay is reduced. The emitter follower delay is typically one third that of a level-restoring gate, so emitter followers greatly improve the delay of high *fan-out* structures like decoders.

Besides its use for rapidly driving large loads from relatively low power gates, the emitter follower also provides a key ECL logical function: the outputs of several ECL gates (with emitter follower outputs) may be connected together, resulting in a shared output that is high if any of the gate outputs are high. This interconnection of emitter follower circuits thus performs the logical *OR* function and is called a *wired-or* because the function is performed simply by *wiring* the gate outputs together. The wired-or is better than an *OR* function built with current-switching stages because it is faster (runs at emitter follower rather than current switch speeds) and requires fewer devices.

Because the output of an emitter follower is one V_{BE} below its input, emitter followers implement a level shift that enables the use of stacked ECL current switches that do not saturate. This thesis labels signals that have been through $N V_{BE}$ drops as LN . Thus, node A in the Figure 2-8 is $L0$, while the gate output is $L1$. A two-level stack of current switches

with $L1$ inputs on the top level would thus require $L2$ inputs on the bottom level to avoid saturating the BJTs in the bottom stack.

With this background in place, the speed advantages of the bipolar memory cell, with its low-swing word line and high read current will be clear. Unfortunately, the static power dissipation of the cell makes it unsuitable for most high-capacity SRAMs.

2.3.1 Bipolar Static Memory Cells

The fastest bipolar SRAMs use the *Schottky Barrier Diode (SBD) load* memory cell [16], which is depicted in Figure 2-9. The SBD load cell stores its data in a latch formed by the multi-emitter transistors $Q1$ and $Q2$, and the load resistors R_{H1} and R_{H2} . Assuming that both bit line-connected cell emitters conduct no current and that node D is higher than \bar{D} , most of the current I_{Stby} flows through $Q2$, causing a $I_{Stby}R_{H2}$ drop from the word line, WordLine1, to \bar{D} . Since $Q1$ conducts almost no current, R_{H1} supplies only the base current for $Q2$ and hence D is at about the same potential as WordLine1. Thus the cell latches into a state with a voltage difference between internal cell nodes of about $I_{Stby}R_H$, assuming this value is less than the turn-on voltage of the SBD.

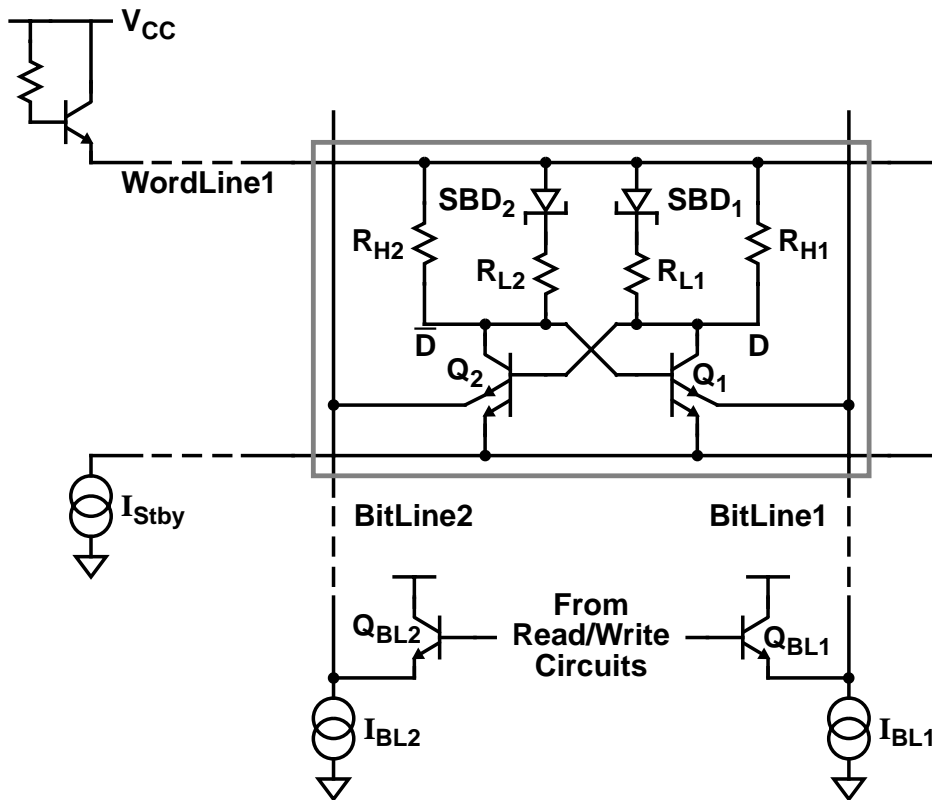


Figure 2-9 Schottky Barrier Diode Load Memory Cell

In order to read the cell, the word line driver raises **WordLine1** by about 0.8V, which would tend to raise both **D** and $\overline{\text{D}}$ by the same amount in the absence of the bit line circuits. The external bit line circuits consist of pull-down current sources I_{BL1} and I_{BL2} , and common emitter BJTs **QBL1** and **QBL2** that prevent the off-side cell transistor from turning on during reads. Because the bases of **QBL1** and **QBL2** are set at roughly the midpoint of the **WordLine1** swing, the cell transistor whose base voltage is higher (**Q2** in this case) conducts most of I_{BL} while, on the other bit line, $\overline{\text{D}}$ is lower than the reference and thus **QBL1** steers most of the current. In this way **BitLine2** charges to one V_{BE} below **WordLine1**, while **BitLine1** is clamped by **QBL1**; the bit line voltage difference is readily sensed using a differential pair to finish the read access.

The preceding assumes that the I_{BL} running through **Q2** does not greatly affect **D** and $\overline{\text{D}}$; the purpose of the SBDs is to make this true. In order to minimize the power required to keep the cells latched, I_{Stdby} should be set as low as the following restrictions allow; I_{Stdby} is typically around $10\mu\text{A}$. A small I_{Stdby} implies a large value for R_H (tens of $k\Omega$), and if the cell read current I_{BL} had to flow through R_H this would limit I_{BL} to be a small multiple of I_{Stdby} in order to prevent bipolar saturation in the cell. Because a large value of I_{BL} (roughly 1 mA) is desired to rapidly move the heavily-loaded bit lines, SBDs are added to the cell in parallel with R_H to supply the cell read current without much added voltage drop. In other words, the SBDs allow a much larger ratio of I_{BL} to I_{Stdby} than would otherwise be possible. SBDs are chosen over junction diodes because they have a lower turn-on voltage than the BJT's V_{BE} , which prevents the transistor supplying the read current from becoming saturated, and because SBDs require less cell area than junction diodes.

For read to standby current ratios approaching β the base current of **Q2** during a cell read is large enough to cause significant drops across its base resistor R_{H1} . This tends to decrease the voltage difference between **D** and $\overline{\text{D}}$. R_{L1} and R_{L2} add a resistive component to the SBD load curves that somewhat limits the reduction in voltage margin, but poor matching of component values limit the usefulness of this approach. This decrease in the high cell voltage during reads therefore limits the practically achievable active to standby current ratios, and leads to significant standby power in large bipolar memory arrays.

Peripheral circuits write the cell by raising the word line to its selected value, and pulling current from the cell transistor whose collector node should be low. If that side of the cell already happens to be low then the cell state does not change. However, flipping the cell requires pulling current from the transistor with the low cell potential on its base, so the base of that bit line's clamp device must be lowered so the bit line is free to drop enough to

turn on the cell transistor. Meanwhile, the other clamp device should raise the other bit line so no read current flows through the other cell transistor. For example, to write a cell that stores one to zero, QBL2 raises BitLine2 so Q2 does not supply I_{BL} , while QBL1 lets BitLine1 drop until Q1 turns on. Once Q1 turns on, I_{BL} discharges \bar{D} until it drops below \bar{D} , at which point I_{Stdby} switches to Q1 and thus \bar{D} rises to complete the write.

The read current supported by the SBD load cell is much larger than that of a 6T CMOS cell, and hence provides faster bit line sensing, especially with the excellent voltage sensitivity of bipolar differential amplifiers. Furthermore, rapid cell reads and writes require only low-swing signals, which makes the cell a good match for extremely-fast ECL bipolar decoders.

2.3.2 Complete Bipolar SRAMs

The peripheral circuits of a bipolar SRAM require careful design to deliver the fast access permitted by the memory cell. After detailing two options for the decoding function, this section discusses an example implementation of a bipolar SRAM access path.

Traditional bipolar decoders fall into two categories based upon the basic decoding gate. Because the logical *AND* function implemented by a decoder would require many-level series stacking to construct from standard ECL structures, bipolar decoders are typically built either from ECL *NOR* gates with complemented inputs or *AND* gates built using diode logic.

The diode *AND* gate that implements the *diode decoder* [21] is shown in Figure 2-10; it implements the *AND* function because the output is low if any of the inputs are low. Like ECL gates, the diode decoder uses a resistor to passively pull the output to the high state and therefore requires static current to keep its output low. Unlike an ECL gate, however, this static current is supplied through the input diodes so the output of a diode decoder begins to change as its inputs change, rather than once the inputs cross a threshold. The diode decoder therefore offers the potential of lower delay than the (ECL gate-based) *NOR* decoder, assuming equivalent input transition times. However, the decoder output swing is determined by the input swing since there is no level-restoring gate.

The figure also shows the ECL *NOR* gate that is the basis of a *NOR* decoder. While it normally requires extra inverters on the inputs of a *NOR* gate to implement the *AND* function, the address lines of a decoder usually have both true and complemented versions of each address, so the input inversion reduces to simple rewiring. Since the *NOR* inputs are active

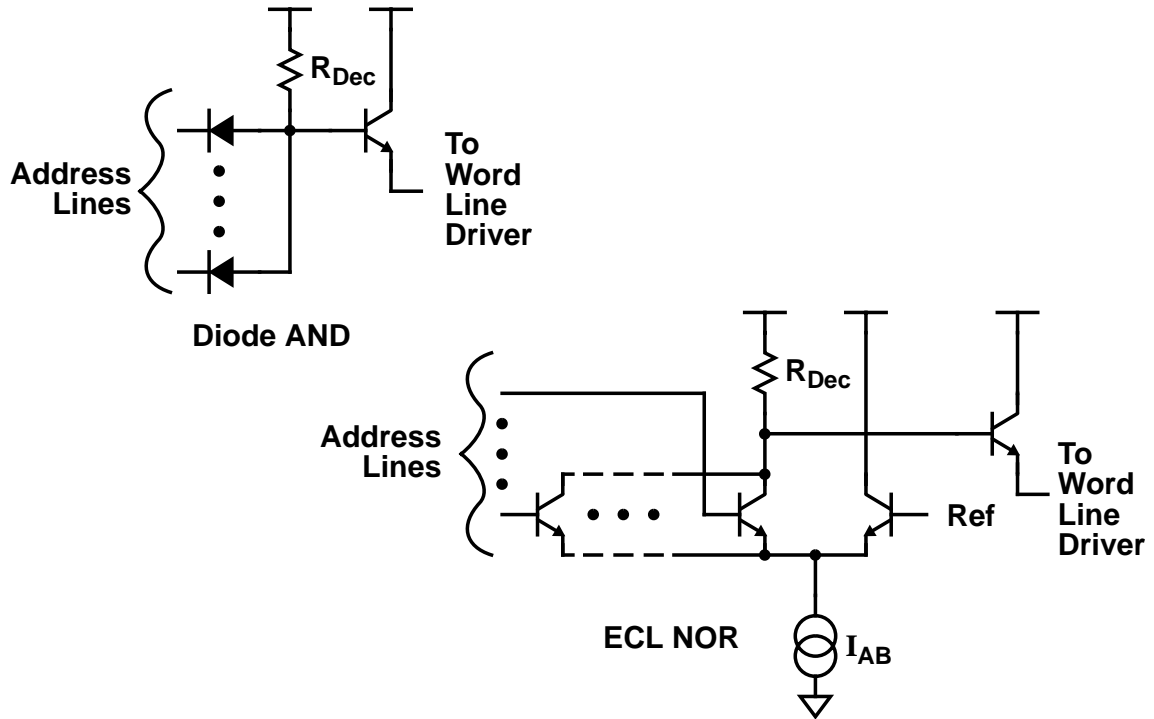


Figure 2-10 Bipolar Decoders

low (i.e. a decoder is selected only if all of its inputs are low), pre-decoding the address lines can be performed by a simple wired-or structure; for instance, the four wired-or conjunctions of two addresses generate only one low (i.e. selected) address line. Simple pre-decoding is the main advantage of *NOR* decoders, although its level-restoring gate structure also allows smaller swings on the heavily-loaded address lines than on the gate outputs. These advantages are balanced by potentially increased delay due to the two level-restoring gain stages of the *NOR* decoder (one each in the input buffer and the *NOR* gate) versus only one for the diode decoder. Furthermore, the *NOR* decoder needs increased power dissipation because it requires separate current to pull down both the address lines and the decoder internal node, while the diode decoder uses the same current for both.

Both decoders provide fast, low-swing outputs, but do this at the expense of substantial power dissipation. Since nearly all decoder outputs must be low, the total decoder gate current (I_{Dec}) is roughly

$$I_{Dec} = \frac{N_{Rows} V_{Swing}}{R_{Dec}} \quad (2-4)$$

for each decoder type, where V_{Swing} is the decoder output swing and R_{Dec} is the load resistance. R_{Dec} must be fairly low for fast access, so the decoding power is often the second largest component of bipolar SRAM power dissipation after the memory cells. Chapter 3 introduces techniques that greatly improve the power dissipation of low-swing decoders.

Figure 2-11 depicts the read access path of a typical high-speed bipolar SRAM, consisting of input buffers with pre-decoded outputs, *NOR* decoders, Darlington word line drivers, SBD load memory cells, bit line decoders and pre-amplifiers, cascode sense amplifiers, and output buffers. A brief description of each circuit follows.

Each input buffer consists of an ECL inverter with complementary outputs connected to pre-decoded wired-or address lines. This wired-or structure produces very fast pre-decoded outputs, since the delay is increased only by the extra parasitic capacitance of the second emitter of each emitter follower on the inverter. Many technologies allow sharing of the collector and base regions of the followers to minimize this capacitance.

The pre-decoded address lines drive the ECL *NOR* decoder gates. Pre-decoding makes these decoders faster because of reduced base-collector and collector-substrate capacitance on the decoder output node. A decoder output controls a pair of cascaded emitter followers that drives a word line across the memory cell array. Such a connection of emitter followers is often called a *Darlington* pair and is capable of rapidly driving large capacitances because the effective current gains of each stage are multiplied. The pull-down current source in the middle of the Darlington helps speed the falling transition, which is otherwise discharged only by the base current of the second BJT.

The stored data values for memory cells on the selected word line are sampled only if the cell is also connected to a selected bit line pair. The column decoder selects a pair of bit lines by steering I_{BLCs} into both bit lines and I_{Pre} into their differential pair. Meanwhile, both bit line clamp devices are set to a base potential midway in the word line swing. As described in Section 2.3.1, a voltage difference develops on the bit lines due to the cell state; this difference causes the *pre-amplifier*, (i.e. the differential pair), to pull different currents from the data lines, which are shared with the other unselected columns. The sensed currents may be turned back into voltages with a resistor, but the large loading on the data lines (due to potentially very many unselected pre-amplifiers) would give a large delay if the resistors were attached directly to the data lines.

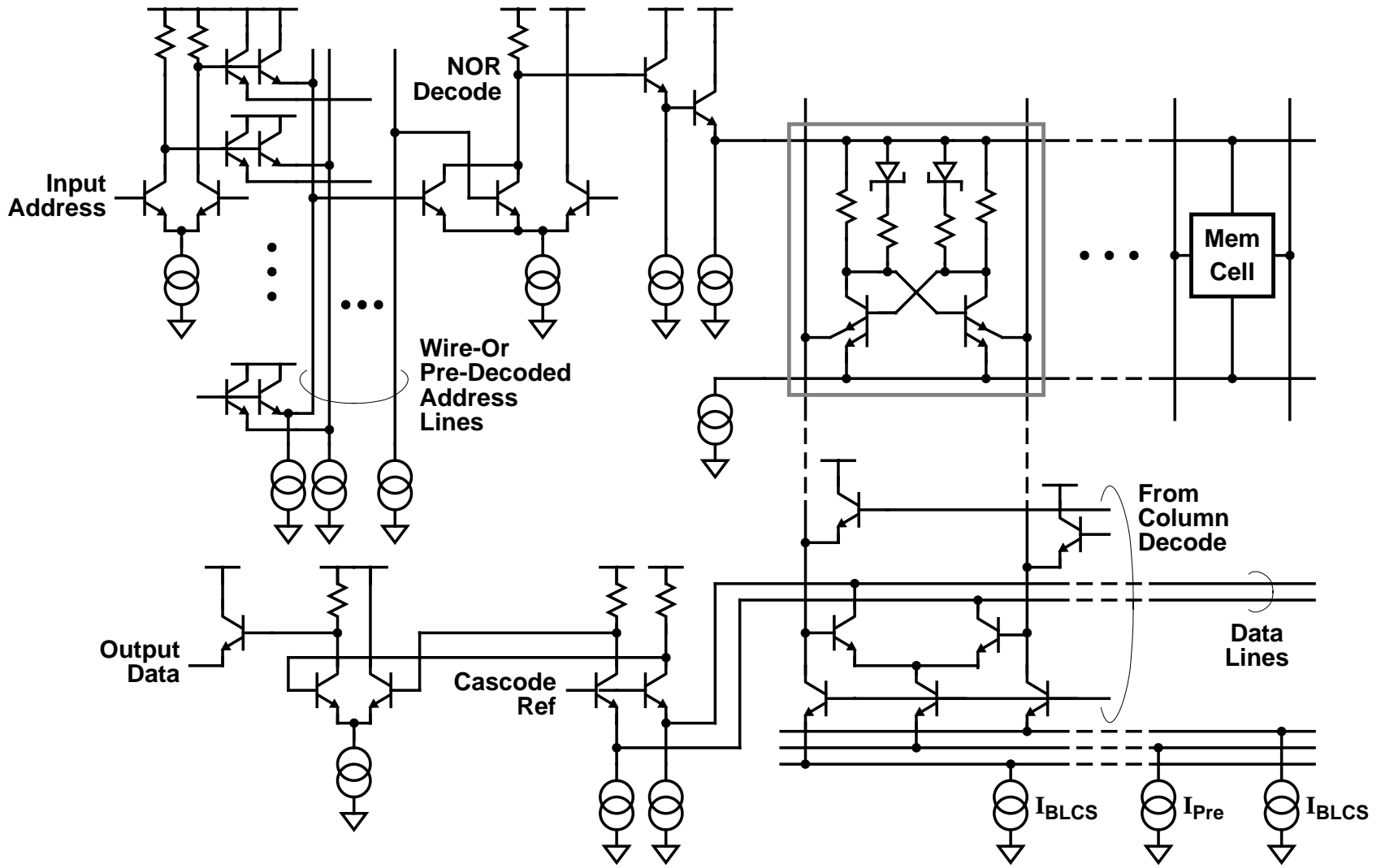


Figure 2-11 Bipolar SRAM Read Access Path

BJTs with reference voltages on their bases and inputs at their emitters, in what is known as a *cascode* configuration [22], provide large output current differences with very low input swings (60mV per decade of current). Since the data line delay is roughly $C_{DL} V_{Swing}/I_{Pre}$, the cascode sense amplifier greatly reduces the data line voltage swings and thereby minimizes the data line delay, while providing a lower-capacitance output node that has greatly-reduced RC delay. The differential output of the sense amplifier then goes through emitter followers to a final ECL output buffer, which restores the read data to normal ECL voltage levels and, when the data must be driven off-chip, increases the drive strength of the signal to rapidly drive a 50- Ω transmission line.

Bipolar SRAMs deliver very fast access due to their low-swing signalling and the excellent voltage sensitivity and current drive capabilities of bipolar transistors. However, the static power dissipated by the memory cell and the peripheral circuits prevents the use of this technology for most large memories. BiCMOS SRAMs, which are the subject of the next section, offer the opportunity to combine the best of CMOS and bipolar SRAMs to come up with superior solutions.

2.4 BiCMOS Static Memories

By incorporating NMOS, PMOS and NPN BJT devices on the same integrated circuit, BiCMOS process technology offers the promise of hybrid SRAM solutions that combine the low power and high capacity characteristics of CMOS with the fast access and cycle times of bipolar memories. While existing BiCMOS SRAMs achieve speed/power/capacity combinations that neither CMOS nor bipolar designs can match, BiCMOS designs do not deliver bipolar speeds at CMOS power levels. Existing BiCMOS memories bridge the gap between CMOS and bipolar to deliver intermediate speed at intermediate power [3 23 24 25 26 27 28 29 30 31 32 33 34 35 36]. After describing two basic BiCMOS design styles, as well as the interfacing problem, the section details the brief history of fast BiCMOS static memories.

2.4.1 BiCMOS Design Styles

The two main BiCMOS design styles differ based on the circuit families they imitate. The first style uses large signal swings and CMOS-derived logic gates, often with bipolar output stages. The canonical example of a large-swing BiCMOS circuit is the *BiCMOS buffer* [37], which exists in many flavors. The main advantages of this style over CMOS structures are improved gate delay versus *fan-out* characteristics, due to the BJTs, coupled with

zero static power dissipation due to the CMOS logic. Furthermore, large-swing BiCMOS is similar enough to CMOS that many design programs can be simply modified to handle the new structures. Unfortunately, the large-swing BiCMOS is so similar to CMOS that it does not provide greatly-enhanced speed.

The competing design style starts with small-swing ECL circuits, which have superior speed characteristics, and adds MOS transistors to improve power dissipation. The MOS devices, generally speaking, save power by allowing current-switching ECL logic gates to be powered down when their outputs cannot change. As long as the critical paths through such circuits pass mostly through bipolar transistors, the resulting delay is comparable to ECL bipolar circuits. This thesis is intended as an example of the benefits of low-swing BiCMOS.

Many BiCMOS systems use both design styles, which requires *level conversion* between the two signalling domains. The delay and power required to amplify a low-swing signal to full CMOS levels is often outweighed by the benefits provided by the separate domains. For instance, a BiCMOS SRAM could use ECL circuits to implement very fast decoders and CMOS memory arrays to save static power; while the resulting design is somewhat slower than a bipolar memory, it uses much less power.

2.4.2 Complete BiCMOS SRAMs

The original BiCMOS SRAMs were essentially CMOS SRAMs with a few BJTs added in the periphery to improve the access time. The improvements were largely due to three replacements:

- ECL Input/Output (I/O) interface instead of TTL
- BiCMOS buffers instead of CMOS inverter for load drivers
- Bipolar small-swing sensing instead of MOS

The ECL I/O interface helps because the required ECL output swings are readily generated by a simple ECL inverter with an emitter follower output that drives a well-specified, terminated transmission line. The electrical environment permits much faster signal transitions than does TTL, and the driver circuit has fewer stages than a TTL output driver does, so the output delay is substantially reduced. For most BiCMOS SRAMs, the penalty for an ECL interface is at the input, where small input signals must be converted to full CMOS levels to drive the memory array. However, the delay penalty for this conversion is offset by the complexity, and hence delay, of the TTL input buffer, which has amplification

requirements of its own. The delay reduction provided by the ECL interface is very significant: a recent design that can support both interfaces (with a simple mask change) has a 6-ns access time through the ECL interface, but requires 8-ns through the TTL interface [36].

In order to maintain an access path that looked very much like the well-understood CMOS SRAM, these early designs converted their ECL inputs to CMOS levels at the input buffers. The converted inputs controlled decoder and driver circuits that were essentially just the normal CMOS logic gates with BiCMOS buffer-style outputs. The BiCMOS buffers, having superior load-driving ability, allowed these decoders to drive their word lines with fewer level-restoring buffer stages and thus less delay.

Replacing the CMOS sense path with bipolar sensing circuits was particularly simple, especially since the CMOS designs were already copying some of the low swing techniques popular in bipolar SRAMs. In fact, except for the MOS bit line switches, which allow one bipolar differential pair to be shared among multiple bit line pairs, the sense path of some BiCMOS SRAMs looks just like a bipolar SRAM, with column-selected differential pairs connected to shared data lines whose swing is limited by a cascoded sense amplifier that feeds a bipolar output buffer.

Nearly all BiCMOS SRAMs reported to date utilize the same memory cells found in CMOS SRAMs and thereby compete with CMOS for memory density while providing faster access times. In order to minimize the sense delay of 6T CMOS memory cells, the cell read current should be maximized, which requires large word line swings. Thus, most BiCMOS SRAMs require a time-consuming level conversion somewhere between their inputs and the memory arrays. As was just mentioned, the early designs converted their inputs at the input buffers. Later designs have gradually moved the level conversion closer to the word line driver, exchanging fast, high-power ECL decoding structures for slower but lower power CMOS gates with BiCMOS buffer outputs.

Once the level converter has been moved to the word line driver, the access path of a BiCMOS SRAM looks very similar, both in decoding and sensing, to that of a bipolar SRAM and so it is not surprising that the access times are similar. Continued process scaling has reduced the maximum permitted terminal voltages of MOS transistors to around 3V from 5V; this change reduces the supply voltages for CMOS circuits and allows ECL circuits operating at 5-V supplies to provide CMOS-like swings with simpler level

converters. An example of this appears in the decoding path of the BiCMOS memory shown in Figure 2-12, which is modelled after [4].

As the figure shows, the access path is virtually identical to the bipolar path of Figure 2-11, except for the memory cell itself. The 6T CMOS cell array connects to a negative supply V_{SS} that is generated by an on-chip voltage regulator [38] to be about 3V below V_{CC} and therefore the maximum voltage constraints on the MOSFETs is satisfied. The bipolar devices, on the other hand, run off a negative supply of 5.2V and can thereby directly drive the word line from the *NOR* decoder with CMOS-like $3V_{BE}$ swings simply by increasing the resistance R_{Dec} . The *NOR* decoder BJTs do not saturate as long as their bases get no higher than $3V_{BE}$ below V_{CC} , which is guaranteed by the wired-or pre-decoder. The resulting word line levels, i.e. unselected at $4V_{BE}$ ($\sim V_{SS}$) and selected at one V_{BE} below V_{CC} , provide a large enough swing to achieve good read current with reasonable cell device sizes and therefore provides substantially improved access times at moderate density penalties. The main reason bipolar memories are faster than a BiCMOS SRAM such as Figure 2-12 is simply that the BJTs in a bipolar process have higher performance than those in a BiCMOS process. However, along with bipolar-class access times comes bipolar-class power dissipation, since although the CMOS memory cell array dissipates very little power, the bipolar peripheral circuits have high power dissipation, especially for large memory capacities with multiple banks of decoders [5].

2.5 Summary

Designers have spent an enormous amount of effort to improve the speed of static memories as the capacity increases. Larger memories need more decoding and have larger interconnect loading, so gate *fan-in* and *fan-out* are constant issues. The increasing delay and power consumption of large memory arrays leads to the use of smaller memory banks, which require more decoders with higher *fan-in*. Furthermore, the large amount of multiplexing in the sense path often leads to multiple low-swing stages for fast access.

SRAMs fabricated in different technologies adapt to these challenges in different ways. Fast CMOS SRAMs derive substantial power advantage from zero static power memory cells and large-swing logic. However, the large-swing logic has higher delay than small-swing logic, so CMOS SRAMs often use complex clocking schemes and low-swing bipolar-derived sense circuits to speed their access. Meanwhile, bipolar SRAMs are typically much simpler and faster, because basic ECL circuits switch very rapidly and can drive

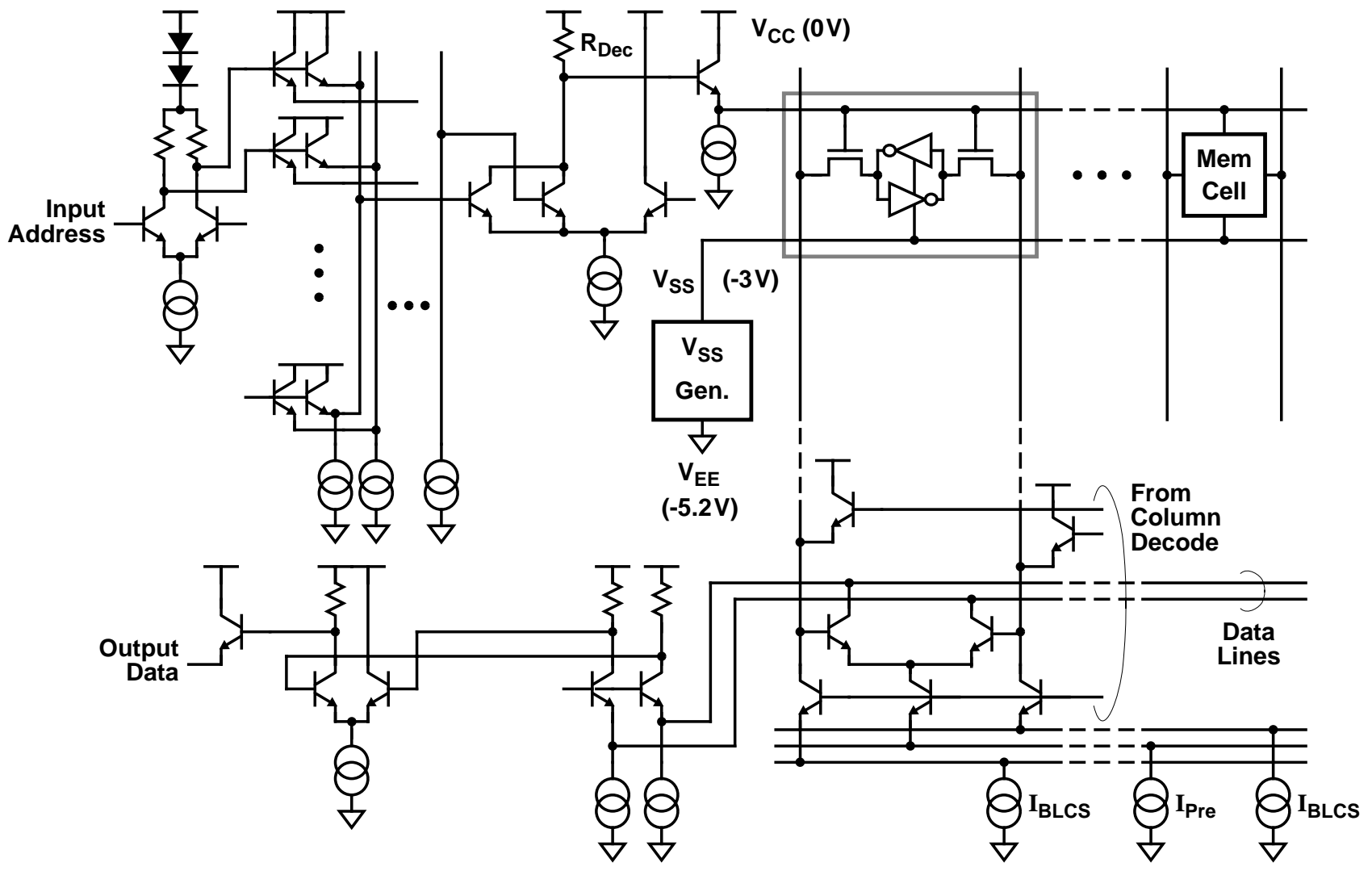


Figure 2-12 BiCMOS SRAM Read Access Path

large *fan-out*. Unfortunately, the static power dissipation of both the memory cells and the peripheral circuits give bipolar memories much higher power dissipation, and effectively limit their capacity.

The hybrid technology BiCMOS promises to deliver the best of both worlds, but has traditionally fallen somewhat short of that goal. The original BiCMOS SRAMs had mostly CMOS-derived circuits and therefore delivered somewhat faster performance than CMOS at nearly-equivalent power. In order to improve the delay, faster peripheral circuits are required, but merging low-swing bipolar peripheral circuits with full-swing CMOS memory arrays requires time-consuming level conversion and increases the power consumption by using constant-current logic. The power dissipation gets substantially worse as capacity increases, since more banks require more constant-current decoders.

This thesis shows that introducing some MOS transistors into these ECL peripheral circuits can deliver nearly equivalent speed at substantially lower power levels. Chapter 3 uses the unique characteristics of MOSFETs to create bipolar decoders whose power is dynamically varied, while Chapter 4 focus on improving the sense and write characteristics of CSEA memories, which do not require level conversion for read accesses.

Chapter 3

Low-swing BiCMOS Decoders

Decoding structures play a crucial role in determining the performance of fast SRAMs. In many SRAMs the row decoding process, which begins when the address is presented to the memory and ends when a word line selects the desired cells, consumes roughly half of the read access time. As the previous chapter notes, bipolar decoders are traditionally fastest due to their low signal swings and their ability to quickly drive large capacitances with emitter followers. However as the memory capacity increases, the number of decoders rises, and since a bipolar decoder dissipates static power, the decoding power increases. For high capacity BiCMOS memories the power of bipolar decoders can be prohibitive.

This chapter discusses hybrid BiCMOS circuits that reduce the power dissipation of low-swing bipolar-style decoders while preserving their high-speed operation. The chapter focuses on row decoders, because they are usually in the critical access path of a fast SRAM. After Section 3.1 quantifies the magnitude of the power problem, the next few sections describe techniques that improve primarily the power dissipation of diode decoders. While the improvement in overall performance is quite good, decoder delay and power can be further improved by using pulsed ECL circuit techniques. A key aspect of decoders that makes them amenable to pulsed techniques is the nearly identical logical and physical paths seen by each of their inputs, so all inputs tend to arrive at any given point in the decoding tree at the same time, assuming they entered the decoder simultaneously (typically gated by a clock signal). Section 3.4 explores the impact of pulsed techniques on diode decoders, while Section 3.5 applies pulses to *NOR* decoders.

Pulsed circuit techniques can also be applied to the word line driver. Section 3.6 describes a circuit to implement pulsed word line signalling that uses large-swing outputs to reduce the power required to discharge the word lines. This chapter shows several methods by which MOS transistors may improve the power dissipation, and hence the overall performance, of low-swing ECL-style circuits.

3.1 Bipolar Decoder Power Dissipation

A fundamental restriction in SRAM design is that no more than one word line should ever be simultaneously active in any bank; since most SRAM cells are selected by a high level on their word line, this implies that all but one of the word lines must be low at any given time. In ECL-style signalling, the word line driver is often similar to Figure 3-1, and as in other ECL circuits, the decoder must pull current from the load resistor R_{Dec} to keep its output low. R_{Dec} is usually part of the decoder gate itself, and since all but one of a decoder's outputs are zero, the amount of current required for the decoders themselves is simply:

$$I_{Dec} = \frac{(N_{Rows} - 1) V_{Swing}}{R_{Dec}} \quad (3-1)$$

where N_{Rows} is the number of rows in the decoder and V_{Swing} is the decoder (and thus nearly the word line) voltage swing.

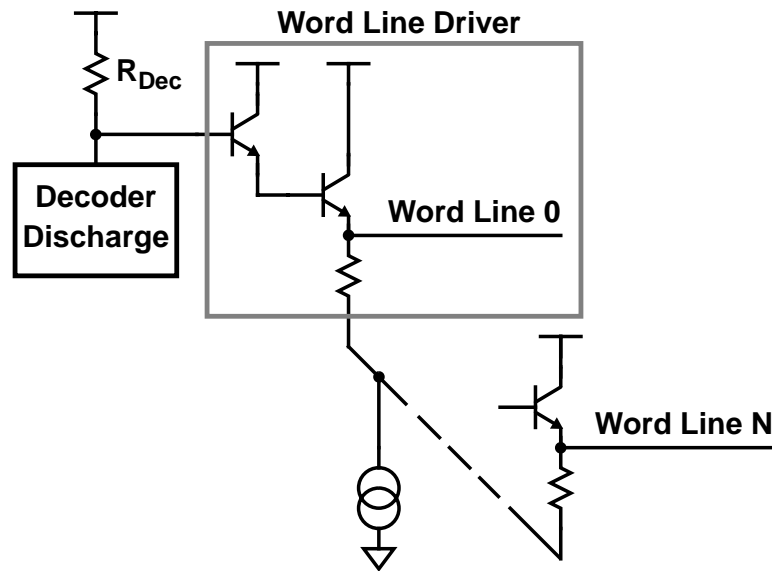


Figure 3-1 Simplified Word Line Driver

For single-array designs, the number of decoders therefore scales with N_{Rows} and thus as the square root of the memory size. The power of low-swing bipolar decoders increases more rapidly than the number of decoders, because *fan-in* and *fan-out* considerations both require increasing power dissipation per decoder. Since the decoder rise time is the pull-up resistance times the node capacitance, which is dependent on the $\log_2 N_{Rows}$ input devices in each decoder, R_{Dec} must decrease as the gate *fan-in* increases to maintain a

given delay. In order to maintain constant decoder swings, the current per decoder must therefore rise. Also, as the number of cells per word line increases, the pull-down current on this line also needs to increase to maintain the delay. Unless R_{Dec} is decreased by the same proportion, the current gain of the Darlington-connected word line drivers will need to increase, which can lead to ringing in their transient response. Thus, increasing the decoder *fan-out* may necessitate increased decoding power as well.

For banked designs that maintain constant bank sizes as the memory size increases, the power scaling is much worse. Since doubling the memory capacity implies doubling the number of banks, the total number of decoders increases linearly with the memory capacity. While this is not a problem for CMOS decoders, which dissipate very little power when inactive, doubling the number of bipolar decoders doubles the power dissipation. Because power dissipation and sensing considerations often dictate that only one word line should be high in the entire memory, all of the bits that determine the active bank must also affect the row decoder. The row decoder therefore has $\log_2(N_{\text{Rows}}N_{\text{Banks}})$ input bits, which is more than a single square array; for instance, for a quadrupling of the memory size, the banked decoders each get two more inputs while the row and column decoders of a square array each get a single extra input. The reason for this is simple: the banked design must perform more decoding to select among the shorter word and bit lines. Thus, the *fan-in* of the bank decoders increases more rapidly than that of the square decoders, and thus the power per decoder for equal delay rises more quickly as well. The decoding power of a banked design therefore increases super-linearly with the memory capacity.

Many banked designs improve the situation somewhat by increasing both the bank size and the number of banks as the memory capacity increases. While this technique might limit the super-linear increase in power, even a linear increase is unacceptable. The following sections attack this problem. By reducing the *fan-in* of the final decoder gate, the decoder power need not increase as rapidly with increasing memory size. By dynamically varying the decoder resistance, unselected decoder banks need not spend as much power as the selected bank. And by pulsing the word line discharge current, the Darlington does not need to fight the discharge current, so the decoder may have a higher driving resistance.

3.2 Pre-decoding for Diode Decoders

Most CMOS memories use pre-decoding to reduce the *fan-in* (and thus improve the speed) of their decoders, and a similar technique can be used in bipolar diode decoders. In

a conventional diode decoder each address line is driven by a push-pull buffer (Figure 3-2) that steers a current I_{AdBuf} into each unselected address line via Q1 and Q2 [18]. The inverter formed by Q3, Q4 and the emitter followers serves primarily to rapidly charge the rising address line. Pre-decoding the address lines is readily accomplished by increasing the complexity of the pull-up gate and removing the current switches in the pull-down path.

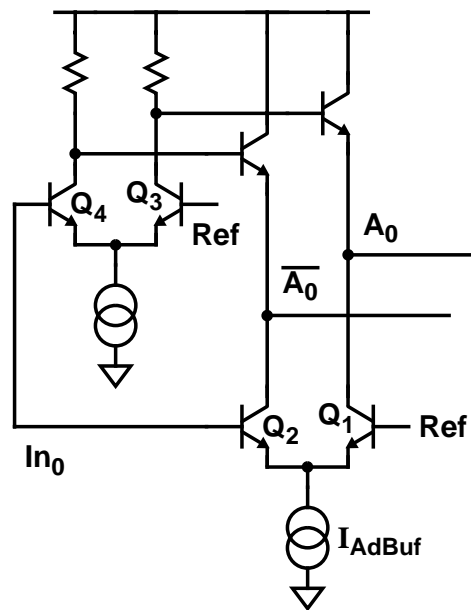


Figure 3-2 A Push-pull Address Buffer

A pre-decoding address buffer is shown in Figure 3-3. In this buffer, one of the two inputs is level-shifted and then these two inputs are used to feed four different two-level series stacks, which generate the four possible *AND* combinations of two inputs: A_0A_1 , $\overline{A_0}A_1$, $A_0\overline{A_1}$, and $\overline{A_0}\overline{A_1}$. This pre-decoding reduces the number of diodes in each decoder by a factor of two, since each address line represents a two-bit *AND*. Each gate output has a discharge current of $2I_{AdBuf}/3$, so that the three low address lines together pull the same $2I_{AdBuf}$ from the decoder array as do two bits' worth of the traditional address buffers. These outputs have a somewhat faster fall time than the traditional ones, since each line uses two thirds as much pull-down current to drive half as many diodes and two thirds as much wire width (since the currents are much too high for minimum-width wires).

Pre-decoding improves the overall decoding speed at the expense of some stacked gates (with an associated access penalty that is smaller than the improvement from reducing the number of diodes in each decoder) and about a third more current, since the high output now wastes pull-down current that was previously steered away. However, this lack of

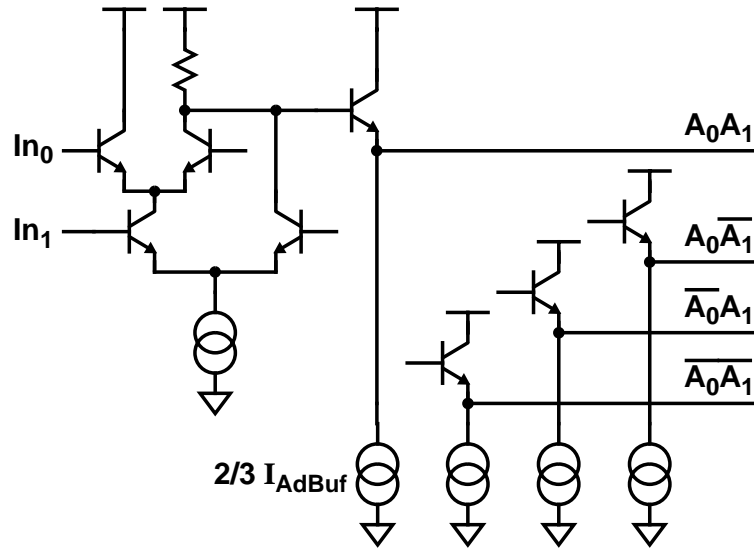


Figure 3-3 A Pre-decoding Address Buffer

current steering in the pull-down current provides an opportunity for further performance enhancements, which are described in the next few sections.

3.3 Diode Decoder with Switched PMOS Load Resistor

In a memory incorporating multiple banks of row decoders, current could conceivably be steered into only the decoders of the selected array, saving the power that would otherwise go into unselected arrays. This would make the decoder more CMOS-like, since unselected banks would dissipate little power. Unfortunately, the unselected diode decoders would then all float high because the current required to keep them low was removed. All the associated word lines would therefore float high as well, which is not allowed. Even if this was acceptable, the current required to rapidly discharge these heavily-loaded lines upon re-selection of the array would dwarf the power savings of partial array activation. Thus, for such a scheme to be effective requires a diode decoder that can be powered down without letting its output float high. One method of accomplishing this function is to replace R_{Dec} with a variable load formed by a PMOS device.

With a variable PMOS load element, such a decoder has two distinct states. In the unselected state, the decoder control circuits set the PMOS gate potential so the equivalent resistance of the PMOS device is relatively high, which minimizes the current required to keep the decoder output low. In the selected state, the PMOS load approximates the resistance of R_{Dec} , so the modified decoder switches as rapidly as the original decoder.

Achieving rapid bank selection without vulnerability to process and temperature variation requires careful PMOS device sizing and reference level design. Furthermore, the reduced decoder current provided by the switched PMOS loads exposes address line parasitics that can slow the access. This section discusses these matters in detail, and shows that after addressing them large power savings are possible.

3.3.1 Basic Operation

Figure 3-4 depicts a diode decoder with a power-down input. The standard resistor load in the diode decoder is replaced by a PMOS transistor P1, allowing the resistance of the load to be adjusted. In the selected (powered up) state, each decoder in the bank will have a high level on $\overline{\text{BankSelQ}}$ and a low level on $\overline{\text{BankSelP}}$. The low level of $\overline{\text{BankSelP}}$ is set by Q3 and makes the resistance of P1 the desired (low) value for normal decoder operation.

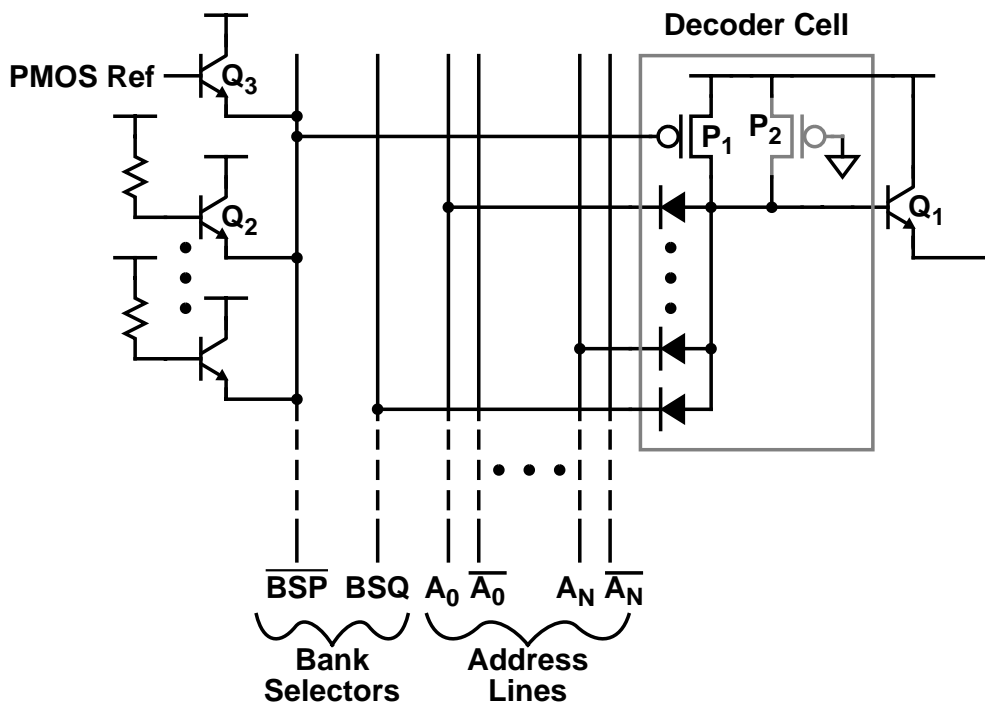


Figure 3-4 A PMOS Load Diode Decoder

A decoder is deselected by pulling $\overline{\text{BankSelP}}$ high via Q2 to $V_{CC} - V_{BE}$, which greatly increases the resistance of P1. Very little current is then required to keep the decoder outputs low; this is readily provided by $\overline{\text{BankSelQ}}$, which transitions downward upon deselection. $\overline{\text{BankSelQ}}$ also guarantees that no word lines are high in unselected banks and provides some safety margin during selection transitions (i.e. in case P1 turns on slightly

before the decoder inputs begin pulling current). Transistor P2 is a very weak device to provide a path to V_{CC} in case $\overline{\text{BankSelP}}$ ever turns P1 completely off. P1 is sized to minimize the required gate voltage swing for selection without greatly increasing the decoder's parasitic capacitance, so as to minimize any delay penalty for the switched load device.

3.3.2 Switched PMOS Load Design Considerations

The switched PMOS load, if it is to be a useful replacement for a simple resistor, must have similar performance characteristics in the “on” (low resistance) state. These characteristics are demonstrated by first describing the PMOS device sizing versus selection swing tradeoffs and then comparing the switching performance of the PMOS load with a resistor.

If the PMOS load is operated entirely in the *linear* region, where its drain current I_{Drain} is more dependent on V_{DS} , then its load characteristic over its operating region will more closely approximate the resistor it is designed to mimic. This is readily demonstrated by considering the load characteristic of the resistor (using Ohm's Law):

$$I_{\text{Load}} = \frac{V_{\text{Load}}}{R_{\text{Dec}}} \quad (3-2)$$

and of the PMOS device in the linear region of operation ($|V_{GS} - V_{Th}| > |V_{DS}|$) [39]:

$$I_{\text{Load}} = I_{\text{Drain}} = K_p \frac{W}{L} \left[(V_{GS} - V_{Th}) V_{DS} - \frac{V_{DS}^2}{2} \right] \quad (3-3)$$

Since both equations specify zero current when the output is high (i.e. $V_{\text{Load}} = V_{DS} = 0$), the selection voltage and device ratio are set such that the PMOS device supplies the same current as would the resistor when the output is low (i.e. $V_{\text{Load}} = V_{DS} = V_{\text{Swing}}$). Combining the above equations:

$$|V_{GS} - V_{Th}| = \frac{1}{K_p \frac{W}{L} R_{\text{Dec}}} + \frac{V_{\text{Swing}}}{2} \quad (3-4)$$

which is valid provided the PMOS device is linear, i.e.

$$|V_{GS} - V_{Th}| > V_{Swing} \quad (3-5)$$

or equivalently

$$\frac{1}{K_p \frac{W}{L} R_{Dec}} > \frac{V_{Swing}}{2} \quad (3-6)$$

Assuming that the PMOS load deselection is accomplished as in Figure 3-4, node BankSelP will be unselected at $V_{CC} - V_{BE}$ and selected at $V_{CC} - |V_{GS}|$. This selection swing V_{Sel} should be minimized for low selection delay, but reducing V_{Sel} implies increasing W/L , which increases PMOS device parasitic capacitances and thus lengthens the load rise and fall times. Also, reducing the selection swing to small values can push the PMOS device into saturation. Figure 3-5 depicts simulated load lines for three different PMOS sizes and the selection swings required to make each mimic a $2\text{-K}\Omega$ R_{Dec} with V_{Swing} of 0.8V .

Saturation greatly increases the differential resistance of the load at $V_{CC} - V_{Swing}$, and thus makes the low output voltage very sensitive to the load current, and therefore more sensitive to device mismatch. Furthermore, the increasing load resistance can lengthen the tail of the RC -dominated falling output voltage transition. These two factors make saturated loads undesirable for traditional ECL-style gates, where the current into the load is fixed. However, these factors do not substantially degrade a diode decoder load, since the exponential current-voltage relationship of the input diodes rapidly increases the pull-down current into the load such that the output voltage follows the input voltage; similarly, the diode gate is relatively insensitive to device mismatch because the low output voltage is determined as the low input voltage plus the diode V_{BE} . In fact, the input diodes so completely dominate the falling transition that one might consider intentionally choosing a saturated PMOS load for diode decoders, since the saturated load pulls up more quickly than a linear PMOS load. However, increasing the PMOS W/L to reach saturation can increase the device parasitics (on the decoder node) enough to erase the speed advantages of a reduced BankSelP swing, as well as increasing the current required to rapidly discharge BankSelP. The PMOS loads in this thesis are designed to have V_{Sel} nearly equal to standard ECL logic swings (i.e. about 0.8V). With V_{Swing} , V_{BE} , and $|V_{Th}|$ all nearly the

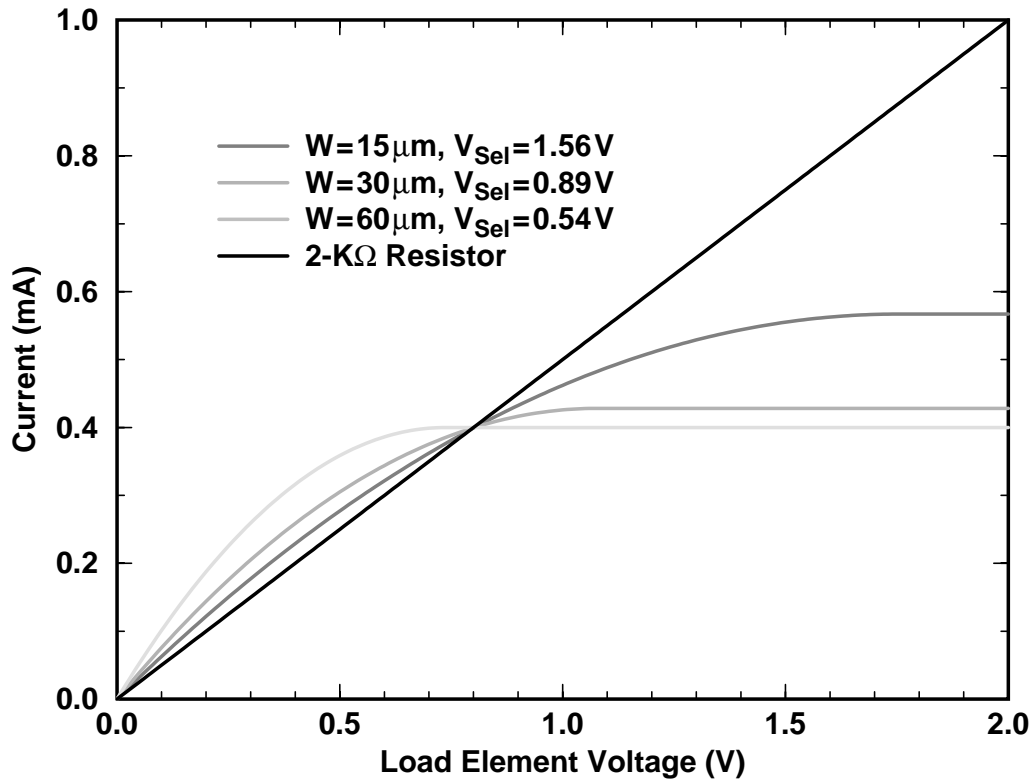


Figure 3-5 PMOS Load Characteristics

same level, this implies that the switched PMOS load is designed to be on the edge of saturation.

The selection swing should not increase substantially with variation in manufacturing process parameters or operating temperatures, in order to avoid losing the speed advantages of low-swing signalling. Circuit simulations indicate that a 1.1-V V_{Sel} is achievable even under worst-case processing conditions at room temperature. V_{Sel} must increase with temperature, but its increase is no worse than that of the other ECL signals in such a design, which are typically proportional to absolute temperature (*PTAT*). The variation of the required selection swing over process and temperature variation appears as Figure 3-6. Since the worst-case swing is only 220mV greater than the nominal swing, the PMOS load selection swing always stays fairly small (and thus quick).

The transient behavior of the switched PMOS load closely matches that of the simple resistor, especially for diode decoders. Figure 3-7 shows circuit simulation of 0.4-mA 4-input diode decoders and ECL inverters with resistor or PMOS loads, each driving a 1.6-mA emitter follower; the PMOS loads are the 30- μm devices from Figure 3-5, with nominal V_{Sel} of 0.89V. The diode decoders begin their transitions early because they do

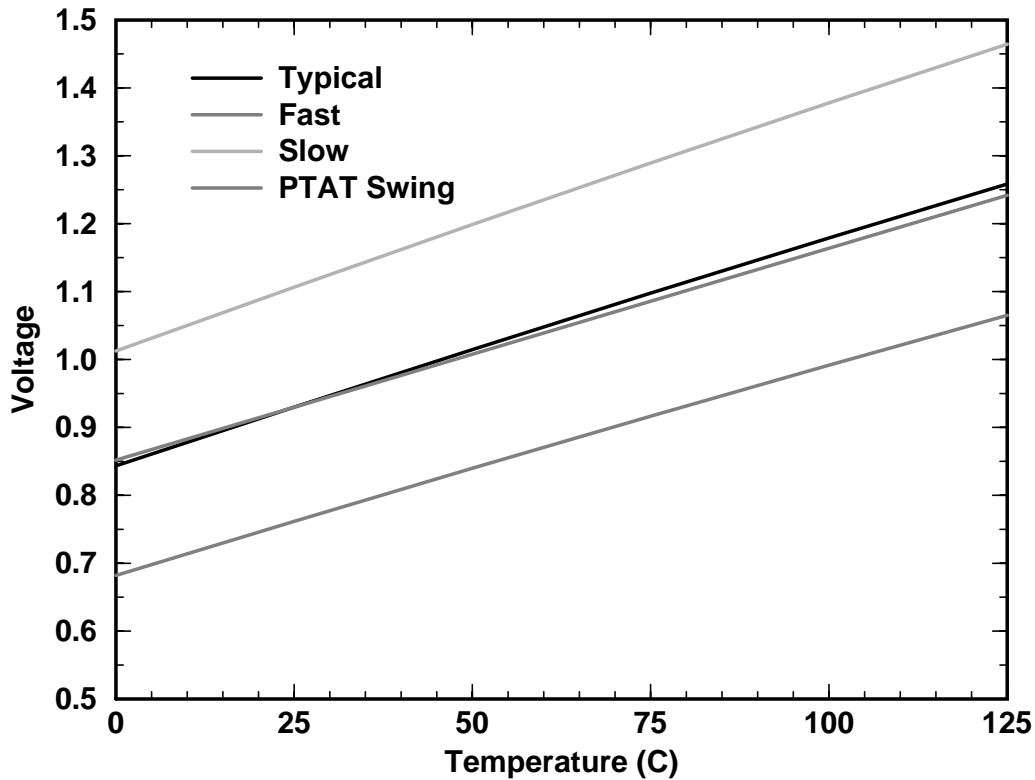


Figure 3-6 PMOS Load Gate Swing Over Process and Temperature

not wait for their inputs to cross a threshold as do the inverters, and they deliver less than 0.8-V swings because they are driven with the same voltage input as the inverters (for purposes of comparison only) and so diode V_{BE} variations between high and low currents decrease the swing. The rising transitions are very comparable for both load devices, regardless of gate type, while the falling transitions for the diode decoders are similar because the diode's exponential current forces these transitions to closely follow their input. The falling PMOS load inverter transition requires about 70ps longer to reach the swing midpoint than does the resistor load due to both larger parasitics and larger device currents at intermediate voltages, as was noted above. Section 3.5 discusses ECL *NOR* gate circuits using switched PMOS loads that are tolerant of this added delay.

3.3.3 Reference Generation

The power savings potential offered by the switched PMOS load is realized only if the selection node swings are rapidly delivered. Because switching a node between two arbitrary and well-controlled voltages is difficult, the PMOS load switches between a reference-controlled active (low) level and an inactive (high) level of one V_{BE} below V_{CC} . Using a reference allows the use of simple wired-or selection drivers, which simply need

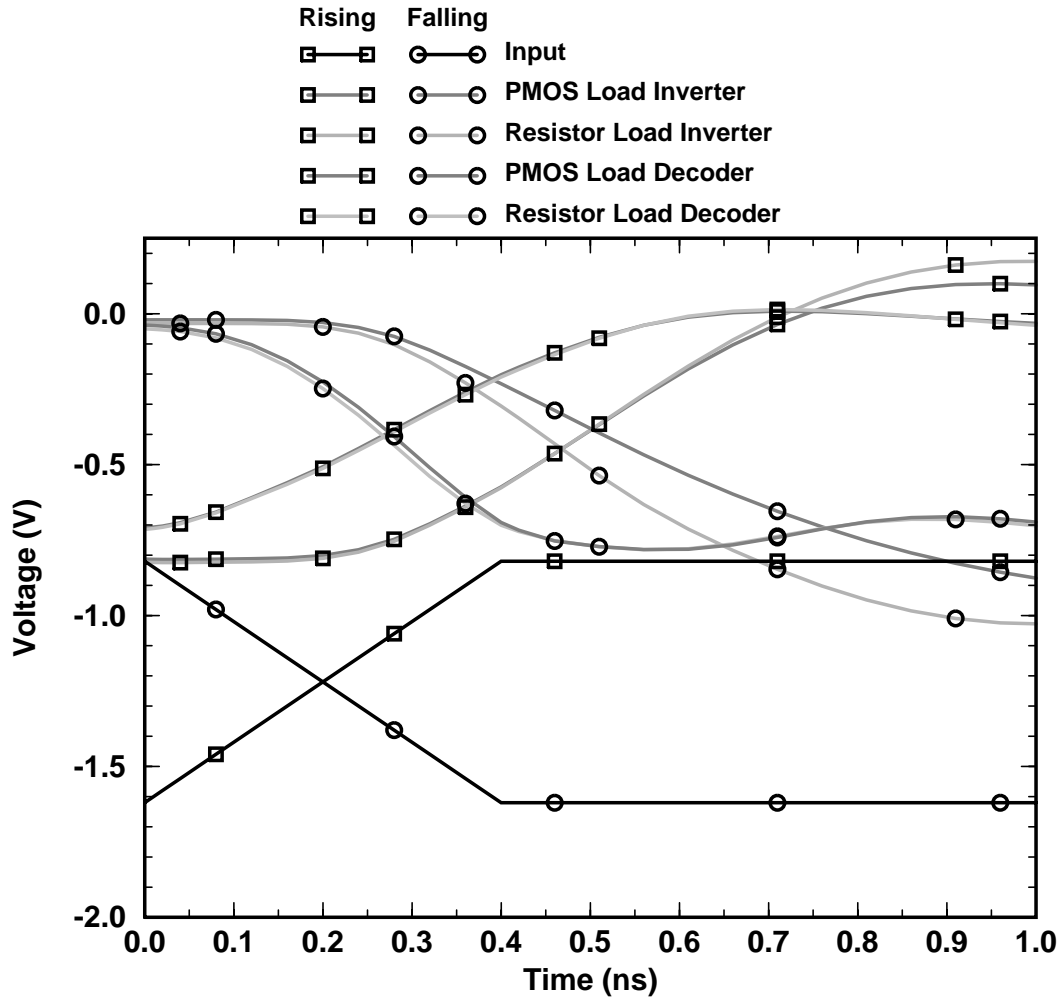


Figure 3-7 Gate Switching Waveforms for PMOS Loads

to guarantee that their swing is larger than the selection swing, so that their low value is below the reference and thus the reference will set the overall selected voltage.

A circuit to generate a reference one V_{BE} above the desired selection level is depicted in Figure 3-8. Identical current sources pull the active decoder current I_{Dec} from both a replica of the PMOS load element (selectable P1 in parallel with weak P2) and a resistor R_{Dec} with the desired load resistance. The drops across each load are shifted down by D1 and D2 (to prevent saturation of Q1 and Q2) and are compared by the feedback amplifier formed by Q1, Q2, P3, and P4 to generate a voltage PMOSRef that is one V_{BE} (via Q3) above the gate voltage required to make the load drops equal. PMOS current-mirror loads are used in the amplifier both to increase the gain and to make the load characteristics track those of P1 and thus reduce the offset of the amplifier. The second amplifier is connected as a unity-gain buffer and serves to isolate the internal reference nodes from switching transients occurring from the use of the buffered reference PMOSRefBuf. The

3.3.4 Address Line Sharing

second amplifier uses a bipolar current switch and PMOS current-mirror loads, like the first amplifier. Circuit simulations indicate that the reference generator has excellent stability in response to both transient supply variation and varying load current on PMOSRefBuf, if compensation capacitance is added to node PMOSRef.

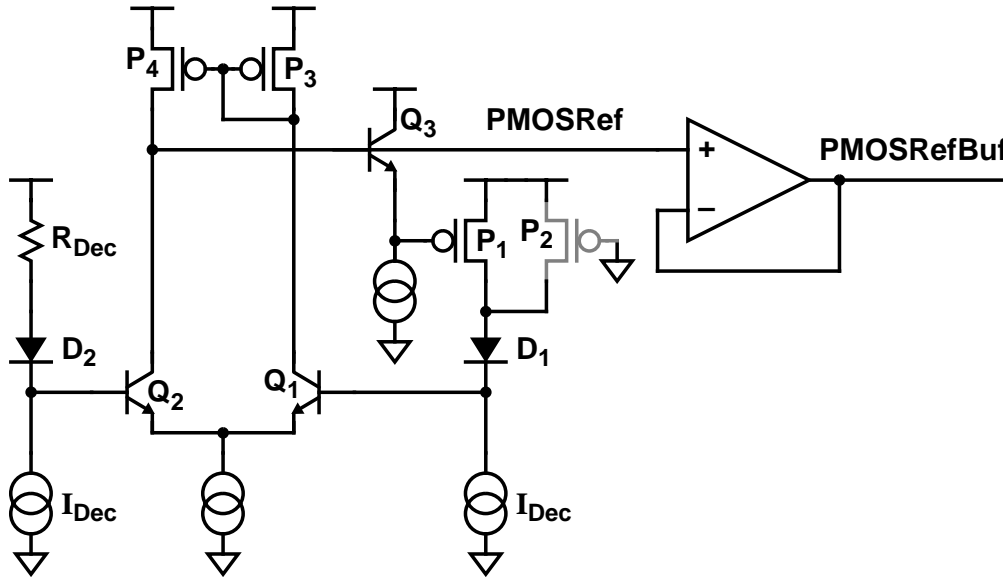


Figure 3-8 PMOS Load Reference Generator

3.3.4 Address Line Sharing

Reducing the power required by the diode decoder creates the new problem of driving the high-capacitance address lines. In a conventional diode decoder the current that keeps the decoders low is proportional to the number of decoder gates. Thus, the current to capacitance ratio is constant. However, by powering down most of the decoders only the current is reduced — the total capacitance is still proportional to the number of decoders.

To reduce this problem, each bank can have its own set of address lines, and therefore minimize the loading on the (segmented) address lines. To continue to save power, only one set of address lines should be powered at a time, so the bank selection circuitry should steer the pull-down current into the selected bank's address lines. Since the pre-decoding address buffers do not themselves use any current steering in the pull-down path, there is room for at least one level of steering here. However, if the current is steered among N_{Banks} banks, there may not be enough room for a stacked (i.e. $\log_2 N_{Banks}$ tall) current tree so one stage of bank address decoding gates may be needed to provide select signals for a one-level (i.e. 1-of- N_{Banks}) current-steering gate; this additional level of gates delays the access.

In practice a combination of these approaches usually produces the best results, since the address line current is high enough to rapidly discharge the capacitance of a few banks. For instance, a memory with sixteen banks could be subdivided into quadrants of four banks each. One set of address lines could then serve each quadrant, so the address line current would be shared by four sets of address lines. This steering is readily accomplished by two-level current switching trees, and the four decoder banks loading each set would not significantly slow the address lines. A modified pre-decoding address buffer for such a configuration appears as Figure 3-9.

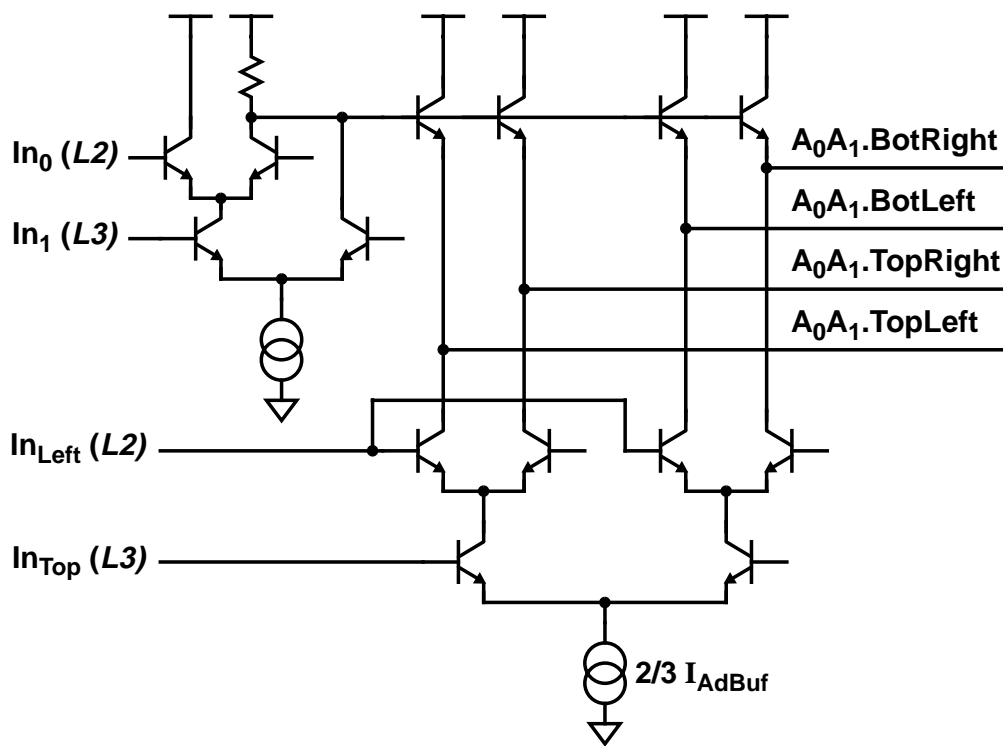


Figure 3-9 Address Buffer with Segmented Address Lines

3.3.5 Results

The combination of pre-decoding address buffers with segmented address lines and switched PMOS load diode decoders provides fast access at reduced power. Ideally, only the selected bank of decoders draws current, so the decoding power may be reduced to $1/N_{Banks}$ of that required by resistive-load decoders. Unfortunately, the current required by unselected decoders and the switched PMOS loads increases the power dissipation beyond this limit. Unselected decoders must each pull a fraction of the selected decoder current

I_{Dec} from their PMOS load to maintain a low output; the current required is simply

$$I_{Unsel} = I_{Dec} \frac{R_{Dec}}{R_{Off}} \quad (3-7)$$

where R_{Off} is the equivalent resistance of the unselected decoder load. For systems with a large number of banks, the unselected decoder power is often comparable to the selected decoder power, because there are many more unselected decoders and R_{Off}/R_{On} ratios much larger than ten require large selection swings.

The high capacitance on the bank selection node $\overline{\text{BankSelP}}$ also increases the decoder power. Because the transition of $\overline{\text{BankSelP}}$ needs to be quick for low decoding delay, the capacitance of the PMOS gate terminals require a large discharge current. This discharge current must equal about a quarter of the load current supplied by the PMOS transistor (i.e. I_{Dec}) for fast selection, so if simple static sources supply the discharge currents then a substantial amount of the power saved by switching the decoders will be lost. A single discharge source may be steered to the selected bank, since only one $\overline{\text{BankSelP}}$ drops per access. However, as described in Section 3.3.4, this requires an *AND* of the bank addresses, which may either require too many levels of series gating to avoid saturation or an extra stage of ECL gates (and thus extra delay) to generate select signals. Like the segmented address line drivers, a two-level current switch provides a hybrid solution that reduces the power by a factor of four. Even with reduced discharge current each follower on the wired-or selection lines needs the ability to charge that $\overline{\text{BankSelP}}$ by itself and therefore the gates need sufficiently low load resistance to avoid emitter follower oscillation problems. Therefore, the current in the ECL gates that drive these followers is about one quarter of the $\overline{\text{BankSelP}}$ discharge current.

An example shows the impact of the standby and control current on the power dissipation. In a sixteen-bank design, the ideal power dissipation is 1/16 (6.25%) that of traditional resistive decoders. If the PMOS loads change resistance by a factor of ten, then the fifteen unselected banks draw 9.4% additional power. For the $\overline{\text{BankSelP}}$ nodes, with one quarter of I_{Dec} per load and two levels of current steering, an additional 6.25% is required in discharge current sources; with a factor of four between discharge currents and the gates that drive the wired-or followers, 6.25% more current is needed. In this example, the ideal power ratio of 6.25% increases to 28.15% once the non-idealities are considered. While this is less than one-third of the original power, it is about five times the ideal value.

In conclusion, the switched PMOS load offers enticing power savings for diode decoders by allowing unselected banks of decoders to keep their outputs low with much less static current while providing fast access in the selected bank. However, the substantial power required by the controlling circuitry reduces the savings significantly. A new approach is therefore desired that minimizes the control power without sacrificing access time. The next two sections describe techniques that can achieve this goal.

3.4 Pulsed Diode Decoders

Many fast CMOS SRAMs use synchronization signals (i.e. *clocks*), that allow designers to minimize access delay and power. Starting from a low-power reset state, synchronous SRAMs selectively enable power-consuming circuits, based upon the requested address. Once the access is complete, the SRAM resets its internal signals to their inactive state, thus preparing for the next access. The power savings come both from activating circuits for only part of the access cycle (i.e. when they need to be active) and from only enabling the circuits that may possibly switch; for example, a multi-bank design would only enable the decoder bank that is selected by the bank address. The delay reduction results primarily from separating the selection and reset circuitry, so each path can be tuned for optimum speed, as was discussed in Section 2.2.2.

Bipolar SRAMs, as well as those BiCMOS SRAMs with mostly-bipolar access paths, tend not to have clocks because of the basic ECL gate structure, which uses passive load resistors to pull up gate outputs, and thus requires substantial static current to keep an output low. A low-power ECL reset state would thus have all outputs high, which is unacceptable for signals such as word lines that are active high. This thesis describes new techniques that utilize clocks with active loads to reduce both delay and power dissipation of BiCMOS SRAMs. These techniques succeed, in much the same way as CMOS circuit techniques, by reducing power dissipation in a reset state, quickly selecting power-consuming circuits to accomplish the access, restricting signal transitions to speed logic gates, and building separate reset paths to speed both selection and reset transitions.

While there are many ways to use clocks in SRAMs, this thesis is concerned with techniques that use a single input clock (which guarantees that all input transitions occur simultaneously) and from this signal generate controlled pulses that select specific circuits for activity, remain active long enough for these circuits to select the following stage of circuits, and then cause their circuits to reset when they go inactive. At each stage of the

3.4.1 Basic Operation

access, new pulses are generated from the immediately previous stage, with timing skew equal to the stage delay. In order to minimize the overhead associated with controlling these pulses, the pulses are typically part of the data stream; in other words, since all internal signals begin in an inactive (i.e. reset) state, stage N is activated by the active transitions of signals from stage $N - 1$ and stage N activates stage $N + 1$ in turn.

This section applies pulsed techniques to diode decoders, while later sections extend these techniques to both *NOR* decoders and other stages of a BiCMOS SRAM. Pulsing a diode decoder improves its performance primarily because all inputs to the selected decoder rise simultaneously, and therefore the junction capacitance of the diode provide charge that speeds the rising transition. The next subsection discusses adding explicit capacitance to further speed the decoder; the effects of the injected charge on unselected decoders lead to the use of an MOS capacitor to reduce the unwanted charge. This section closes with a summary that questions the usefulness of the capacitively-assisted decoders, given the power of the extra circuitry needed to control them.

3.4.1 Basic Operation

A pulsed diode decoder may be built just like the traditional diode decoder of Figure 2-10. The differences are in the address buffer that drives the decoder, and the word line driver that capacitively loads it. The decoder begins its access with all its input lines low, so all the word lines in the system start low and thus no memory cells are selected. The address buffers pulse (i.e. raise) the selected address lines to begin the access; the selected decoder therefore sees all of its inputs rise at once, which forces the decoder to charge more quickly than when only one input transitions. The base-emitter diode capacitances supply charge to hasten the transition, whereas in the traditional decoder only one input might rise and thus the capacitance of the other inputs' diodes would hinder the rising transition. The access is further improved by removing the large static currents from the Darlington word line drivers. This change helps by reducing the total amount of base charge required to make the Darlington charge the word line, thus further reducing the current required through the load resistor to charge the decoder. The word line driver employs a separate reset path to discharge its output, which is discussed in a later section.

Circuit simulations of the selection delay through the diode decoder and word line driver circuitry versus decoder current appear as Figure 3-10. Delays are compared for three

circuit configurations:

- Traditional decoders with static word line discharge
- Pulsed decoders with static word line discharge
- Pulsed decoders with pulsed word line discharge

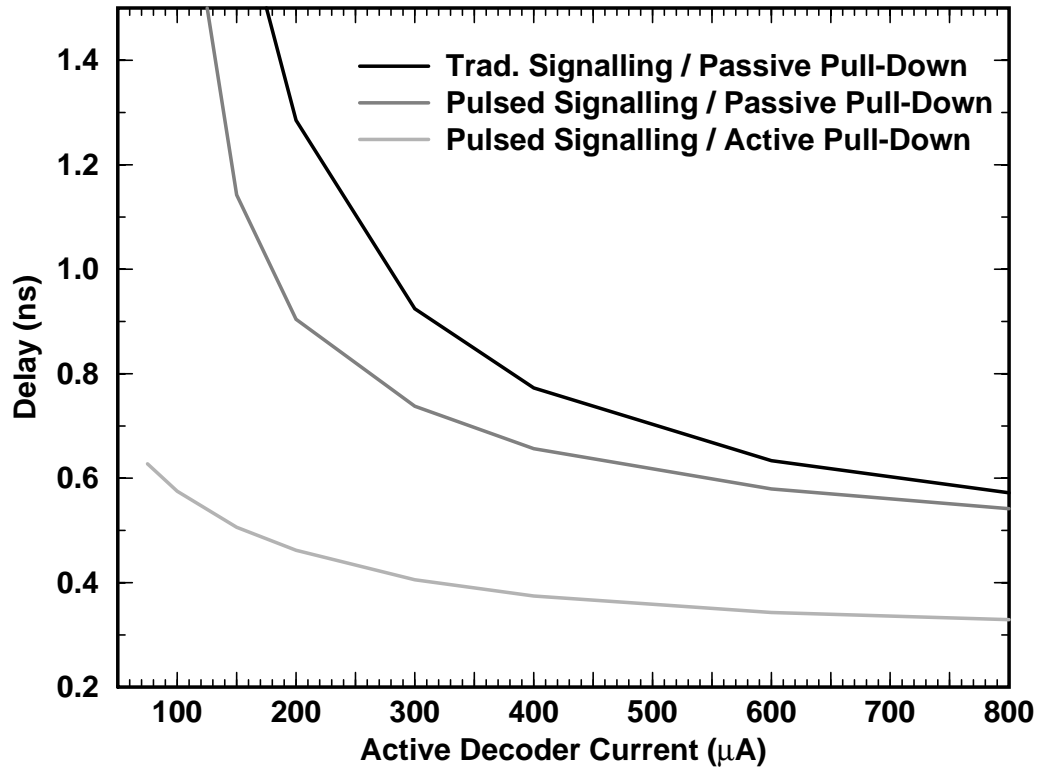


Figure 3-10 Advantages of Pulsed Signalling for Diode Decoders

The data indicate that at an example current of $400\mu\text{A}$, pulsed decoder signalling delivers a rather modest 120-ps (15%) gain by itself, but also enables the use of pulsed word line circuitry that delivers an additional 280-ps gain for an overall selection delay reduction of 50% for these two stages. The figure clearly indicates that reducing the required Darlington base charge can produce fast decoders at much lower decoder current. This might lead one to wonder how little static current would be enough to provide fast access, if some way were found to dynamically dump the base charge into the decoder. The next section investigates adding explicit capacitance to the decoder inputs to supply this charge.

3.4.2 Capacitively-pulsed Diode Decoders

Increasing the parasitic capacitance of the input diodes increases the amount of charge transferred to the decoder and provides fast rise times with lower static decoder current (i.e. higher R_{Dec}). While adding capacitance normally slows switching speed, the circuit of Figure 3-11 is different because the capacitors *feed* the input signals *forward* (i.e. directly) to the decoder without requiring any device switching nor RC delays; on the selected decoder all the inputs rise at the same time so there is $N_{Inputs}C_{In}$ working to charge the decoder together, where N_{Inputs} is the number of decoder inputs. Because the source of the feed-forward charge is a change in the voltage across C_{In} , the address lines must swing more than the internal decoder node. Circuit constraints limit the realizable difference between these swings to be fairly small, so C_{In} must be relatively large in order to deliver the required Darlington base charge. C_{In} is large enough that it requires less area to implement C_{In} as a separate component rather than simply increasing the area of the input diodes.

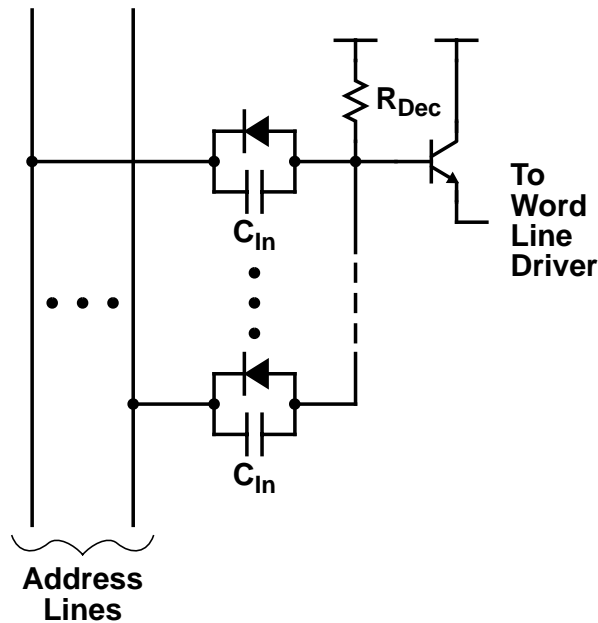


Figure 3-11 A Capacitively-Pulsed Diode Decoder

The chief drawback of increasing C_{In} is the disturbance created on unselected decoders that connect to selected address lines. A decoder connected to only one unselected address line has a large amount of charge dumped onto it as the selected lines rise, since the change in voltage across its capacitors will be nearly the entire address line swing. This undesired charge raises the internal decoder node, which in turn raises the unselected address lines as the voltage across the decoder diodes increases. Pulsing extra current from

unselected address lines while the selected lines are rising fights the undesired charge and prevents the unselected lines from rising. However, since there are so many unselected decoders the undesired charge is large. Using nonlinear C_{In} reduces the charge dumped onto unselected decoders, thus reducing both the rise in barely-unselected decoders and the power spent in keeping the unselected address lines low.

Resetting a capacitively-pulsed diode decoder requires pulling the selected lines low, which restores the charge on the feed-forward capacitors. Quickly restoring this charge requires much more current than the static decoder current, so pulsed reset currents are appropriate. The selected decoder rapidly resets due to the feed-forward input capacitors and the exponential current characteristics of the input diodes.

Raising the decoder output using feed-forward capacitance requires that the address lines rise further than the decoder output so the voltage across C_{In} decreases. For a fixed decoder swing, the extra address line swing is therefore roughly inversely proportional to C_{In} , but neither value can be arbitrarily large without other penalties. Because the decoder high level needs to be essentially V_{CC} (so the high word line level does not degrade) and because the inactive (reset) level on the address lines is simply one V_{BE} below the decoder low level, increasing the address line swing over the decoder swing requires a selected address line to be higher than $V_{CC} - V_{BE}$, which is difficult to accomplish with emitter followers. Some amount of excess swing is available in practice, since driving the high input capacitance of the decoders tends to make the address buffer emitter follower overshoot its static selected level a bit. However, the amount of overshoot is dependent on high frequency characteristics of the BJT and is therefore very sensitive to process variation. The intrinsic difference in the input diode V_{BE} between high current (unselected decoder) and low current (selected decoder) levels readily delivers about 100mV of excess swing; to achieve enough charge with a small voltage change requires relatively large C_{In} .

However, large C_{In} increases the disturbance of unselected decoders that are connected to selected address lines. For a decoder connected to only one unselected address lines, a total charge of almost $(N_{Inputs} - 1)C_{In}\Delta V_{AdLine}$ is dumped into the decoder, where ΔV_{AdLine} is the swing on the address lines; in order to keep the unselected word line from rising, this charge must discharge through the unselected input diode. A better solution is to use a nonlinear capacitor — a device whose capacitance increases with the applied voltage. Such a capacitor could have a relatively large equivalent value for the selected decoder, where the terminal voltage change is small, and a relatively smaller equivalent value for unselected decoders, which have ΔV_{AdLine} terminal changes.

3.4.3 NMOS Capacitor Diode Decoders

An MOS transistor can implement a nonlinear capacitor, since with the source and drain terminals shorted together the device has a small capacitance from gate to (source-drain) when $V_{GS} < V_{Th}$, due to the lack of any conducting channel, whereas once $V_{GS} > V_{Th}$ a channel forms under the gate and the equivalent capacitance rises substantially. In order to utilize this non-linear behavior for a diode decoder, appropriate driving circuitry is required to ensure that the voltage drop across the MOSFET at the reset state is just above the device threshold so that when the terminal voltage decreases, most of the stored charge will dump onto the decoder internal node quickly and then the rest of the voltage change will dump relatively little charge.

A diode decoder using such a capacitor appears as Figure 3-12. The variable level shifters (one per address line) sets the reset V_{GS} on the NMOS capacitors to a few hundred millivolts above their (body-effect altered) V_{Th} ; they must be variable because the NMOS V_{Th} does not track the bipolar V_{BE} nor ECL swings over process and temperature variations.

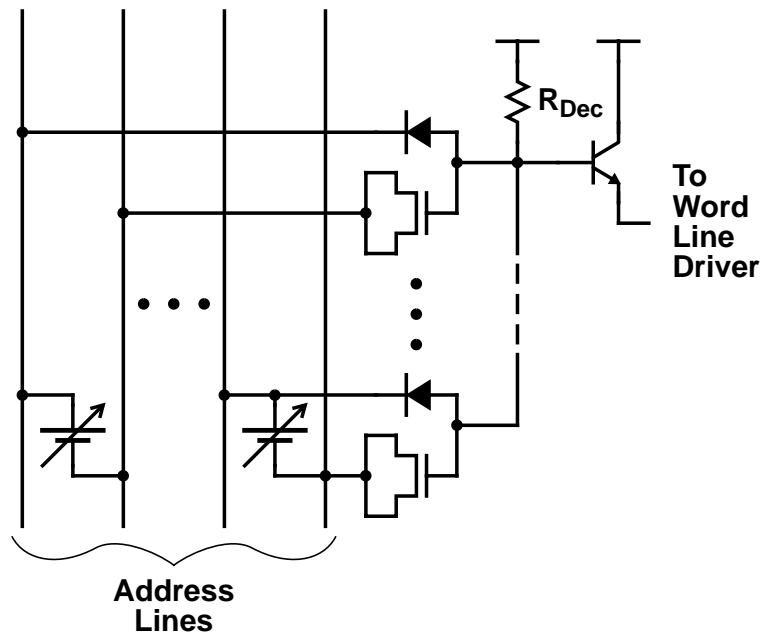


Figure 3-12 A NMOS Capacitor Pulsed Diode Decoder

Circuit simulations indicate that the MOS capacitor reduces the charge dumped into unselected decoders and thus improves decoder performance in two ways. First, for a 6-input decoder with 100- μ A current per decoder and 100-fF capacitance per input the undesirable bump in barely-unselected decoders is reduced relative to linear capacitors from 430mV to 280mV (i.e. by 35%) without any increase in delay at an address line swing of

1.2V. Second, the drop in total injected charge reduces the discharge current requirements on the address lines enough that a 6-bit (64 cell) row decoder constructed from the above gates requires 40% less average address line current than it would with linear capacitors, at a cycle time of 2ns.

The variable level shift required by the NMOS capacitors may be implemented by a modified V_{BE} multiplier circuit. The basic V_{BE} multiplier circuit, as well as a possible modification to give it the desired variable characteristic, appear as Figure 3-13. The traditional V_{BE} multiplier [22] acts as a two terminal device with a programmable diode characteristic (i.e. an adjustable V_{BE}). As the terminal voltage difference V_{Mult} rises from zero, current will flow entirely through the resistors until the voltage drop across R_1 approaches V_{BE} and Q_1 turns on. At this point the base-emitter junction will clamp the R_1 drop to V_{BE} and, as long as the base current of Q_1 remains small compared with V_{BE}/R_1 , the current through R_2 will closely match that of R_1 and hence

$$V_{Mult} = V_{BE} \left(1 + \frac{R_2}{R_1}\right) \quad (3-8)$$

for the range of operation where the terminal current I_{Mult} satisfies

$$\frac{V_{BE}}{R_1} < I_{Mult} \ll \frac{\beta V_{BE}}{R_1} \quad (3-9)$$

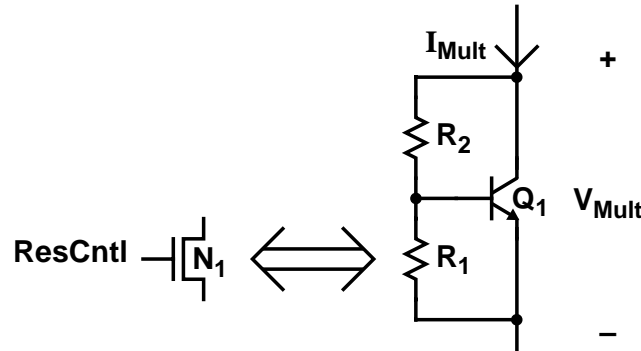


Figure 3-13 An Adjustable V_{BE} Multiplier

Replacing R_1 with a variable resistor (NMOS device N_1 in the Figure) allows the programmable diode voltage to be dynamically adjusted by a control signal $ResCntl$. The equivalent resistance of N_1 , and hence the diode voltage, are determined both by $ResCntl$

3.4.4 Summary

and by the source voltage of N1, since both V_{GS} and the body-effect dependent value of V_{Th} alter N1's current. For a fixed ResCntl, this implies that the NMOS resistance increases as the source voltage increases so thus the programmable diode voltage decreases. This feature is useful for the NMOS capacitor decoder since it makes the variable source voltage decrease as the address lines rise, thereby providing a larger input swing on the capacitors than on the diodes and thus increasing the voltage change across the capacitor. The voltage ResCntl is set by a replica circuit to force N1's resistance in the reset state such that the drop across the NMOS capacitors is a few hundred millivolts above their V_{Th} .

Circuit simulations indicate that the adjustable V_{BE} multiplier performs quite well in rapidly charging the capacitor input lines. However, the limited current range offered by a V_{BE} multiplier creates problems for this application because of the large variation between the standby (reset) and active address line currents. In order to generate the desired diode voltage at the low reset current the resistance values must be relatively large, but large resistance increases the charging delay of the capacitors. Circuit simulations indicate that the extra delays of a V_{BE} multiplier over a simple diode with $R2/R1 = 1/3$ are about (30ps, 45ps, 70ps, 110ps, and 190ps) at active/static current ratios of (1, 2, 4, 8, and 16); since these delays are in addition to the intrinsic base charging delay of a simple diode it is clear that some of the delay performance gained in using capacitively-pulsed decoders is given back in driving them.

3.4.4 Summary

Pulsed circuits show great promise for improving the delay and power performance of diode decoders. While the single greatest delay improvement comes from freeing the rising word line driver from fighting a large static discharge current, the simultaneous rise of the inputs presents an opportunity to use feed-forward capacitance to charge the Darlington base at much lower static decoder current. With nonlinear NMOS capacitors the total injected charge is reduced and thus the total decoder power improves as well. Figure 3-14 compares the decoder plus word line driver delays and average address line current for the decoders discussed in this section. The simulated circuit implements a 1-of-64 diode decoder, with each gate having 6 inputs. The first curve shows the delay of the pulsed decoder of Section 3.5.1 as the static gate current is increased from 75 to 400 μ A per decoder. The other curves show the delay curves for linear and NMOS capacitor decoders as C_{In} varies from 10 to 150fF per input and as the gate current increases from 40 to

200 μ A. The NMOS delays are optimistic because they do not include the delay of the V_{BE} multiplier, which would add about 150ps to the times.

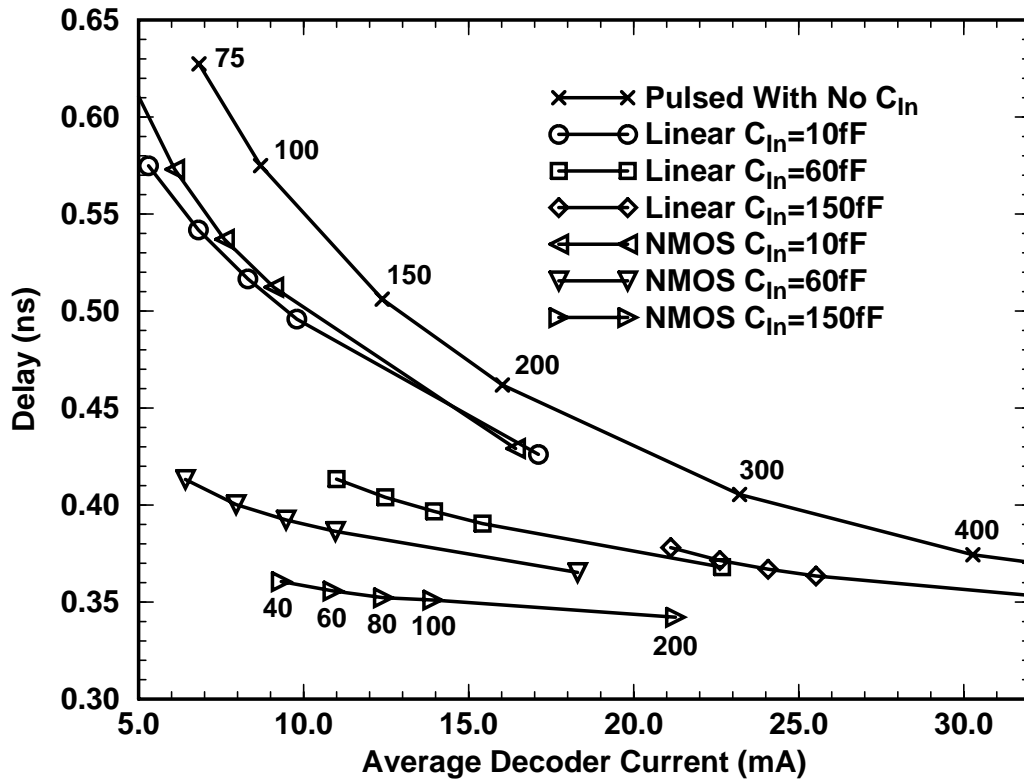


Figure 3-14 Power/Delay Comparison of Pulsed Diode Decoders

The figure shows that NMOS capacitor decoders are able to achieve low delay at much lower static decoder current, and lower average power, than pulsed decoders without capacitors. However, the NMOS decoders have higher delay for a given capacitor size that linear capacitor decoders due to the V_{BE} multiplier delays, albeit at substantially lower power; the lack of a high value per unit area linear capacitor in most digital processes rule out the linear decoder altogether.

The use of bank selection may be combined with these techniques to further reduce power dissipation. A simple pulsed decoder might use a switched PMOS load, as was described in Section 3.3, but the greatly reduced static current of the NMOS capacitor decoder does not require such an approach. Instead, such a decoder dissipates most of its power charging the feed-forward capacitors, preventing unselected address lines from rising, and discharging selected address lines so the goal in using banks is to prevent address lines from switching. Since this approach requires segmenting the address lines so each bank (or each

few banks) has its own set of lines the address buffers become more complex and may require an extra delay stage to accomplish.

The extra complexity in generating the current pulses for unselected but active address lines and the reset currents for selected diode and capacitor decoder inputs, coupled with the extra delay in the address buffers, make the power savings offered by the NMOS decoders difficult to achieve; in practice the speed and power performance of the pulsed static decoders, in combination with switched PMOS loads, is quite adequate and much simpler to achieve. The focus of the pulsed circuit investigation now shifts to *NOR* decoders, where performance improvement impacts not only decoding structures, but also generic ECL logic.

3.5 Pulsed *NOR* Decoders

Many of the fastest reported bipolar and BiCMOS SRAMs utilize *NOR* gate decoders for the following reasons:

- Active-low inputs allow simple wired-or pre-decoding.
- Level-restoring *NOR* gate decouples input and output swings.
- Complementary outputs provide flexibility in building word line drivers.

BiCMOS access times as low as 1.5ns, and bipolar read delays of less than 1 ns have been reported using *NOR* decoders [4 20]. The power of such decoders is not low; a recently reported 256Kb BiCMOS SRAM [5] accesses in 2.4ns (1.5ns on-chip) but requires almost 2A of current for the row circuitry alone. In order to build this type of access performance in a reasonable-power large BiCMOS memory, the *NOR* decoder and word line driver circuit power must be dramatically reduced. One method to accomplish the power reduction is to create a *NOR* gate with a power-down state (like the improved diode decoder of Section 3.3), and then only activate the decoders in the selected bank. Rather than trying to steer the active *NOR* gate current into the selected bank of decoders, a better solution is a current source that may be powered down, so in the reset state no decoder draws full power. Since the address lines of a *NOR* decoder do not share the decoder gate currents, it is also important to reduce the address line power dissipation; a key benefit of pulsed signalling for *NOR* decoders is that it is simple to determine when an address line might transition and to supply the discharge current at only those times.

This section discusses circuit techniques for building pulsed row access paths for BiCMOS memories using *NOR* decoders that minimize power dissipation without sacrificing speed. After describing the basic pulsed *NOR* gate, the discussion focuses on the design of a simple BiCMOS pulsed current source that overcomes many of the limitations of previous designs. In combination with a new voltage regulator, this source delivers a pulsed current that is largely independent of fast changes in the voltage supply levels and that is selected using standard ECL voltage levels. The pulsed current source is used both in the basic *NOR* gate and in the address buffers and line drivers to minimize their power. The pulsed *NOR* banks require a bank selection signal to enable their current sources, but generating this signal in a single gate delay is both required and challenging; a modified diode decoder accomplishes this task nicely.

3.5.1 Basic Operation

A pulsed *NOR* gate for use in a decoder should draw very little current in the inactive state, when its output is guaranteed to be low, and should have a much lower equivalent load resistance in the active state so it can rapidly charge its output. A switched PMOS device provides the desired load characteristics, but the pulsed gate also requires a variable current source that switches between low inactive current and higher active current. Figure 3-15 depicts such a gate, with switched PMOS load P1 and switched current source I_{Dec} . In the reset state, both of the bank selection signals, $\overline{\text{BankSelP}}$ and BankSelQ , are inactive so the standby current source I_{Leak} needs to be large enough to overpower an inactive P1 and thus keep the decoder output at its low level. On a bank selection, both the pulsed current source and P1 become active; on all decoders (except the selected one) I_{Dec} must be large enough to keep the output low. BankSelQ must be active slightly before and after $\overline{\text{BankSelP}}$ to avoid generating glitches on the output.

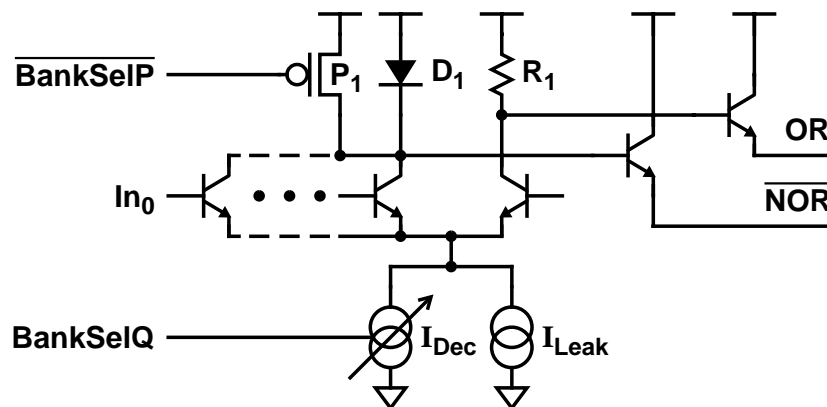


Figure 3-15 A Pulsed NOR Gate

Because the inactive resistance of **P1** is not well-controlled, diode **D1** sets the output low level, which requires some excess I_{Leak} . **D1** also allows the active PMOS load to be saturated, which allows larger decoder output swings with small $\overline{\text{BankSelP}}$ swings. The complementary gate output may be supplied off a normal resistor **R1**, since no decoder save the selected one steers current through this path, the complementary *OR* output is extremely useful for generating control signals for pulsed word line discharge circuits. This decoder can provide delay performance nearly equal to a simple *NOR* decoder at much lower average power consumption, especially for multi-bank designs where only one bank of decoders is ever activated at once. Note that the pulsed *NOR* gate has a longer falling delay due to the switched PMOS load (as mentioned in Section 3.3.2), but this delay is in the reset path, and thus does not increase the critical selection path delay

3.5.2 Pulsed Current Source

The design of a dynamic current source for such a decoder deserves careful consideration. Much work has recently been devoted to active pull-down ECL circuits [40 41 42 43], which reduce the power in their emitter followers by only activating pull-down currents while the output is falling. The existing circuits, as well as the one required for this application, must both handle the same fundamental problem: normal ECL signals are referenced to V_{CC} while current sources are referenced to V_{EE} , so it is difficult to have normal ECL signals turn on current sources due to the allowed variation in $V_{CC} - V_{EE}$. This voltage variation is at least 0.6V in most systems. Many solutions utilize capacitors to provide a variable level shift that allows a V_{CC} -referenced ECL level to control a V_{EE} -referenced current source, as depicted in Figure 3-16. However, capacitor-based solutions suffer from two problems that make them unsuitable for this application. First, while the biasing network that sets the size of the variable level shift can tolerate changes in $V_{CC} - V_{EE}$ that occur slowly with time, they cannot handle rapid changes in the supply voltages; this is bad because pulsed current sources generate rapid changes in the die currents, and these current changes generate rapid changes in $V_{CC} - V_{EE}$ due to the inductance of the package leads. In other words, capacitor-based pulsed current sources have trouble dealing with the supply noise that they generate. Second, the capacitor solutions only output their peak current for a limited time, since the charge stored on the capacitor leaks off while the current source is active; this behavior is often acceptable for simply discharging the output node of an emitter follower, where the logic gate itself keeps the emitter follower off once the pulsed current drops off, but for pulsed logic gates the current needs to remain at the peak level as long as the selection input is active so that the output voltages remain constant.

The pulsed *NOR* decoder therefore requires a new pulsed current source that is not based on level-shifting capacitors.

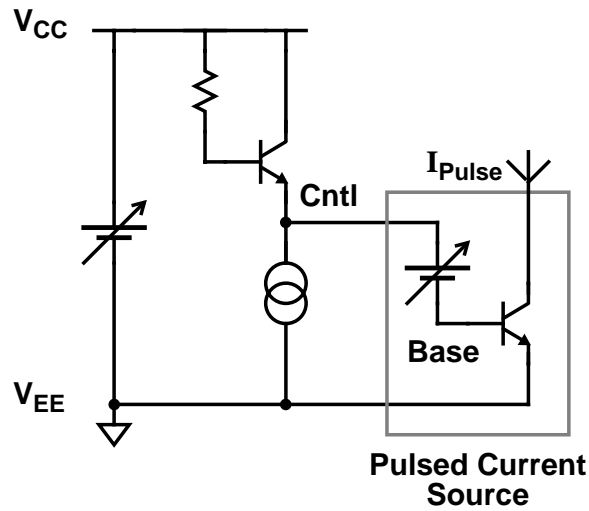


Figure 3-16 Variable Level Shift for Pulsed Current Sources

Recent BiCMOS SRAMs have been constructed with on-chip voltage regulators to permit 3.3-V limited MOS devices to coexist with 5.2-V ECL circuits [38] by generating a V_{SS} for the memory cell array that is $V_{CC} - 3.3$. This thesis proposes that this voltage regulator be set such that building pulsed current sources from this supply be made simple; in other words, the V_{SS} generator should produce a voltage four V_{BE} plus the ECL signal swing below V_{CC} . With such a V_{SS} , a pulsed current source may be simply constructed as in Figure 3-17.

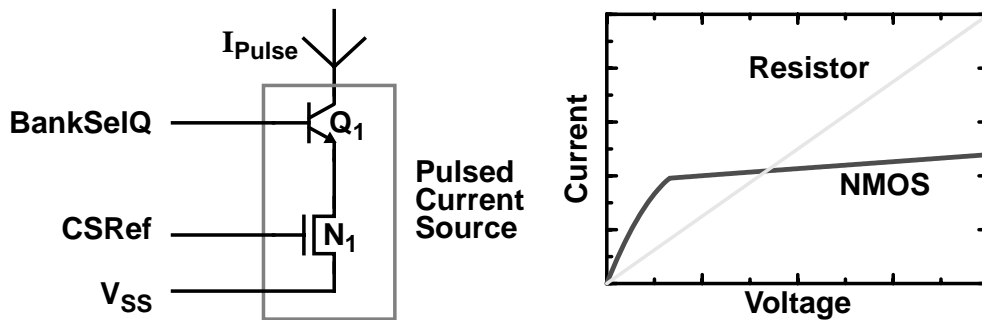


Figure 3-17 A Pulsed Current Source

The operation of this source is simpler to understand with NMOS transistor N_1 replaced by a resistor. Assuming the selection signal is L_3 , it is low at $V_{CC} - 3V_{BE} - V_{Swing}$, and thus Q_1 is on the edge of turning on. As the selection signal rises, V_{Swing} is gradually impressed across the resistor and thus V_{Swing}/R flows through the current source. The

problem with this resistive current source is that the active current is linearly proportional to the input level, so the current does not reach its maximum very quickly. Since the bank selection signals are likely to be in the critical path of the read access, it is essential to make their effects occur as rapidly as possible.

Replacing the resistor with N1, a nonlinear resistor, solves this problem. N1's reference (CSRef) is set such that N1 saturates around the time the selection signal swings midway, so the output current increases rapidly to nearly its maximum value by the time the input gets halfway. The graph in Figure 3-17 shows a comparison of the output current versus selection input voltage for the current source with either a resistor or N1 in the emitter lead. Transistor N1 must be larger than minimum, since it must supply reasonable output currents with a saturation voltage of $V_{Swing}/2$. For instance, in the 0.8- μm reference technology a 0.4-mA pulsed current source would use a 24- μm NMOS transistor.

This current source rapidly delivers a large active/inactive current ratio using a standard ECL selection input, which is useful in many pulsed applications. In order to reduce the component count for the decoder, the leakage current source may be integrated with the pulsed current source by simply adding a resistor in parallel with Q1 of the value $(V_{L2Ref} - V_{SS})/I_{Leak}$. With the parallel resistor, the pulsed current source switches between two fairly well-controlled values with only three components; the resulting NOR gate has only two components more than a traditional ECL NOR, and is thus quite dense.

The CSRef generator is readily constructed using replica techniques as shown in Figure 3-18. The replica pulsed current source (N1 and Q1) are set by the feedback loop such that with a high L3 signal on the base of Q1 the output current matches a reference current I_{Ref} . Emitter follower Q2 provides buffering to reduce loading effects on the sensitive feedback loop. Ensuring that the current source turns on early in the selection swing is a matter of sizing the NMOS devices such that the reference generator produces an output over temperature and process variations that saturates N1. Circuit simulations indicate that the CSRef generator keeps N1 saturated over a wide range of operating conditions.

3.5.3 Pulsed Address Buffers and Address Line Drivers

Since a substantial source of power dissipation in NOR decoders comes from rapidly driving the large capacitance of the pre-decoded address lines, reducing the power in only the NOR gates does not solve the entire problem. This section shows how to pulse the address line circuits to save power and trivially generate the desired input waveforms for pulsed NOR decoders. A good way to minimize the power in logic circuits is to minimize the

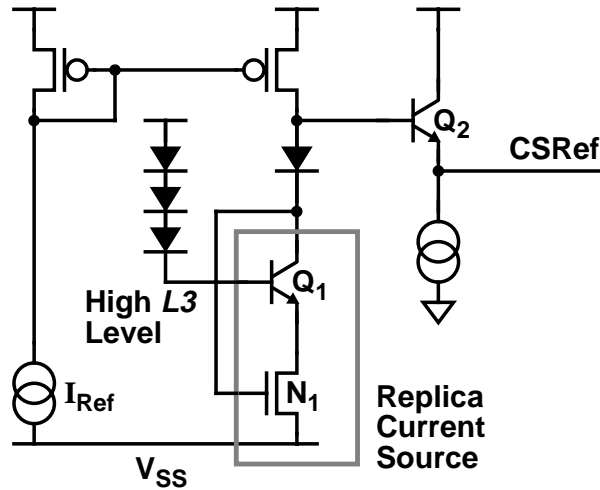


Figure 3-18 Pulsed Current Source Reference

number of transitions they must make; for wired-or pre-decoded address lines, which are active low, only one line in each pre-decoded group goes active, so a high reset level minimizes the number of transitions. This is fortunate because ECL gates require no power to provide high outputs; hence, the pulsed address buffers may have very low reset power.

Besides minimizing the number of address lines that transition, another way to minimize their power is to reduce the capacitive loading on the address lines themselves. For a banked design, using multiple sets of address lines (as in Section 3.3.4) reduces the total capacitance that must transition, since only the set of address lines connected to the selected bank needs to be discharged. Since the pulsed *NOR* gate accepts *L2* address inputs, a good organization is to buffer the address buffer outputs with one level of emitter followers (to isolate the address buffer resistor from the output capacitance) that drive long *L1* global address lines to the banks. At the bank level, the global lines drive the *L2* local (segmented) address lines through a second level of followers. These second followers provide two forms of electrical isolation: they allow different sets of local address lines to be independently discharged (which provides the desired capacitance reduction) and separate the resistance of the long global address lines from the high capacitance of the decoder inputs, which substantially improves the wire *RC* delay.

The preceding discussion ignores the question of where the wired-or pre-decoding should be done. While minimizing the number of global address line transitions would favor pre-decoding at the address buffer, such an arrangement suffers from two problems. Minimizing the transitions only helps if it saves discharge current, and with only one allowed stage of current steering between the *L1* global lines and the *L3* pulsed current source selector,

only two-way current sharing is possible without added delay. Furthermore, building the wired-or at the address buffers adds extra transistors to the address buffer outputs, which lengthens their delay. A better solution is to accomplish the wired-or at the local address line buffers, where the capacitance of the extra devices adds insignificantly to the global address line loading while permitting two-way current steering of the global line discharge current between each address bit and its complement.

At the bank level, the wired-or local address lines reduce the *fan-in* of the *NOR* decoders, which improves their speed. Ensuring that discharge current should only flow into the active set of local address lines is readily accomplished using the bank selection signals already required for the *NOR* decoders themselves; when a group of banks shares address lines then the pulsed discharge current may be selected by the wired-or of the bank select signals for that group. Being more selective about which local address lines to discharge is difficult, since there is almost no voltage headroom between the *L2* local lines and the *L3* bank selection signal. A physical view of the resulting address line routing plan for a sixteen-bank SRAM appears as Figure 3-19; the input addresses are driven to the center of the memory, and from there the address buffers drive the global *L1* address lines to the four quadrants. At the quadrant level, wired-or drivers create the local pre-decoded *L2* address lines, with a shared set for each two banks.

Because the address buffers are the first stage in an access, they are where the clock signal interacts with the address inputs to begin the access. Creating the desired address line waveforms is relatively simple; one way is to add an extra emitter follower to each address line that keeps the line unselected until the clock lets the access begin and that resets the line when the active time has passed. A better solution, due to the availability of pulsed current sources, is to merge this function into the address buffer itself. A pulsed address buffer with both the global and local pulsed address line drivers appears as Figure 3-20. The address buffer is a simple ECL inverter with a pulsed current source that is activated by the clock that starts an access. When the clock is inactive, no current flows in the inverter so the load resistors pull all the address lines high. When the clock rises, one of the inverter outputs falls, and thus the selected *L1* global address line is discharged quickly by another pulsed current source that is steered into the line. The local address line drivers perform both the wired-or pre-decode and the bank selection-pulsed discharge.

Circuit simulations indicate that the reset time nearly equals the required active time for a aggressively-pipelined pulsed *NOR* decoder constructed using these techniques. With the active pulse width half of the cycle time, the use of pulsed signalling saves about half of

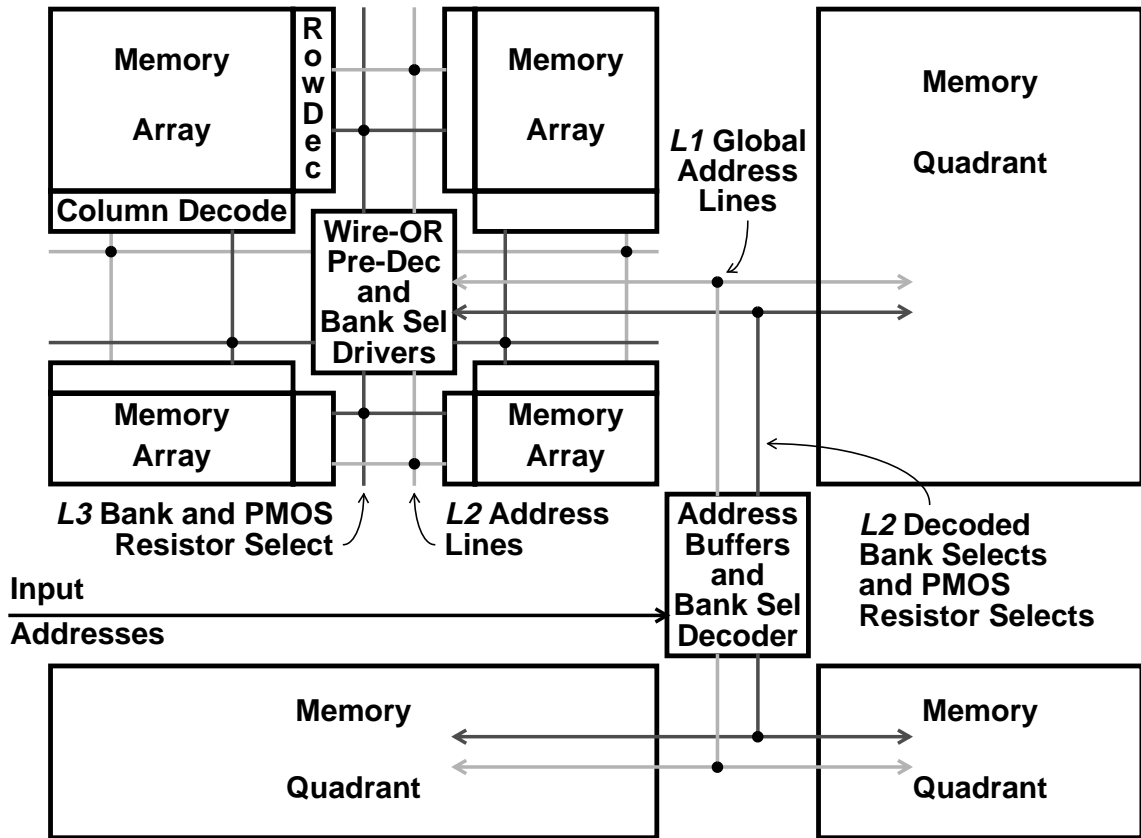


Figure 3-19 Pulsed Address Line Routing

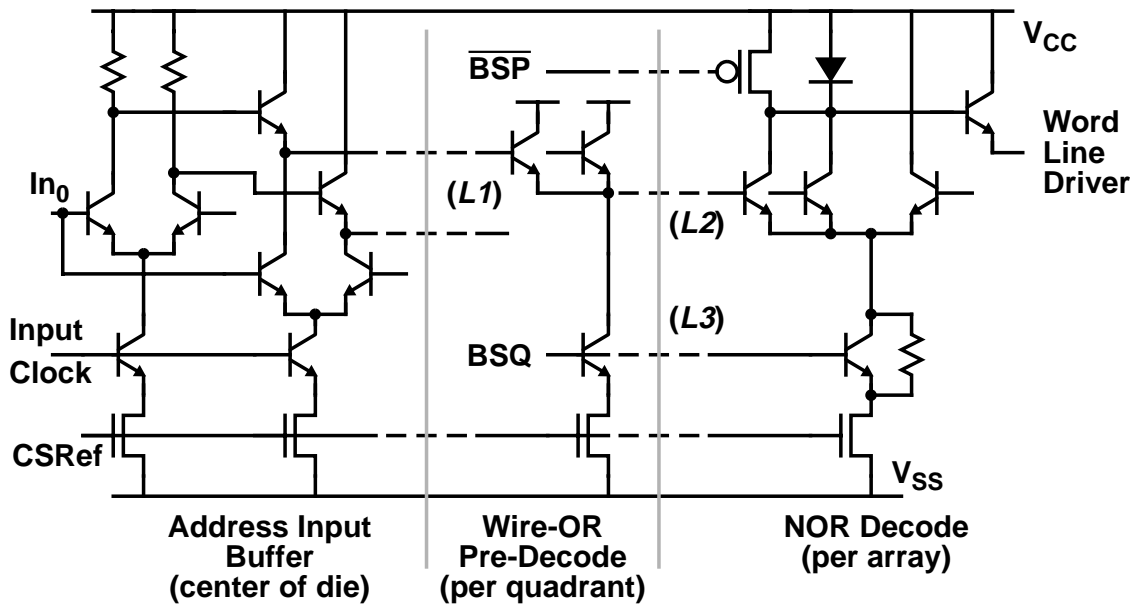


Figure 3-20 A Pulsed Address Buffer with Pulsed Address Lines

the current in all sources Figure 3-20. The global address line current switch reduces the active line current by half, and at the local address lines the current is divided by the number of address line sets. These techniques may therefore reduce the address line power to about 25% of their equivalent static level with very little access penalty. For less aggressive designs, the active time remains the same while the cycle time increases, so the relative power advantage increases.

3.5.4 Bank Selection

The bank selection mechanism must three of requirements. First, it must make sure that only one decoder in the system is selected at once; in other words, it must make certain that decoders in unselected banks are never selected. A simple way to achieve this is to add an extra address input to each decoder and connect it to pre-decoded *L2* bank addresses; unfortunately, by increasing the *fan-in* of the decoder gates their delay rises. A better solution is to add extra *L1* bank address inputs to the wired-or pre-decoding gate that drives the local *L2* address lines, ensuring that unselected address line sets never discharge. When multiple banks share the same set of address lines, this may require that one group of address lines be duplicated for each bank in a group, so the duplicated lines also carry bank selection information.

The second requirement is to provide the **BankSelQ** selection signal for the pulsed current sources in the local address line drivers and *NOR* decoders. This function requires an *AND* decode function with active-high outputs and only the delay of a single inverting gate (since that is how much delay is in the address line paths). The delay requirement rules out both *NOR* gates, which require complementary inputs, and stacked current steering trees, which require an inversion at their output. A diode decoder, on the other hand, can decode in a single gate delay, especially for relatively small numbers of outputs where the address line parasitics are small.

Such a decoder appears as Figure 3-21. This circuit uses a stacked address buffer to implement the reset state; when the input clock is inactive, I_{AdBuf} is steered into each address line and thus all decoder outputs are low; the clock signal is the same *L3* clock that pulses the address buffers of the previous section, so all paths begin simultaneously. When the clock rises, the discharge current is steered away from the selected address lines, which are pulled high by the selected decoder and static PMOS current sources (P1 and P2), which are added to improve the decoder rise time without resorting to a push-pull address buffer; the push-pull buffer is unacceptable because of its added delay. The bank select

decoder is smaller than a row decoder, so relatively small static pull-up currents may rapidly charge the address lines without dissipating too much power.

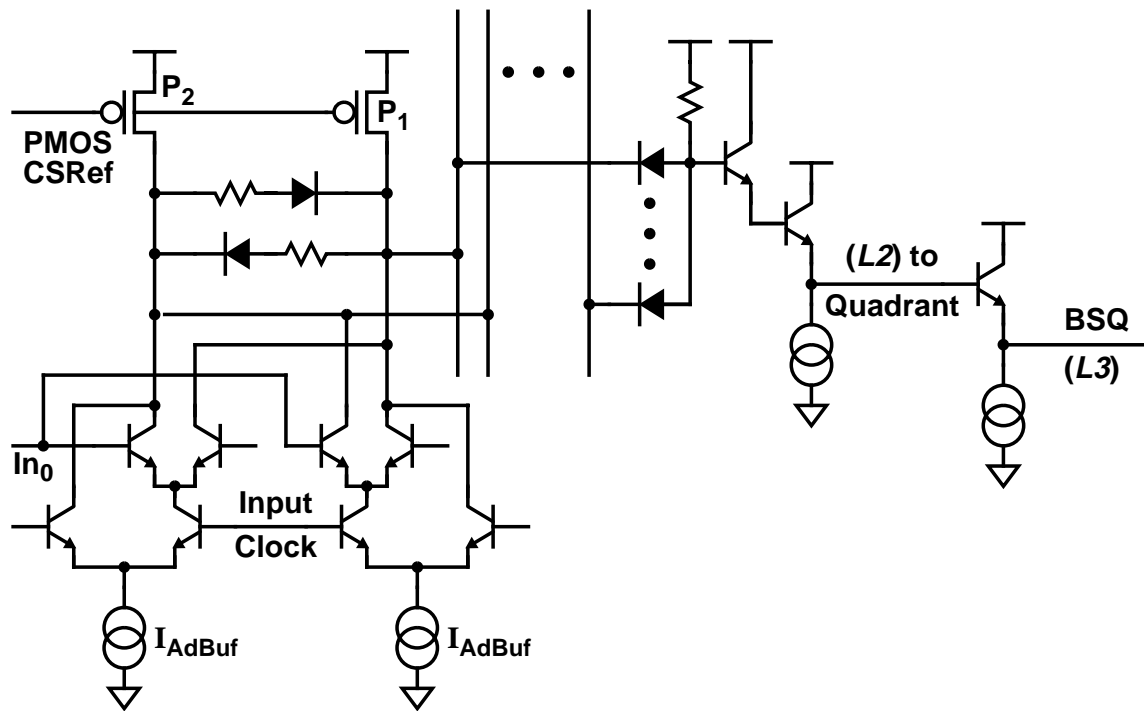


Figure 3-21 A Pulsed Bank Selection Decoder

Meanwhile, $2I_{AdBuf}$ is steered into each unselected address line in order to prevent them from rising; since half the address lines are selected, the others require twice as much current to keep the unselected decoder outputs low. The series diode-resistor combinations prevent the selected address lines from rising further than the decoder swing, and thus reduces the reset delay; the series combination also supports the PMOS current of the selected address line, which reduces the droop in unselected address lines and decoders caused by the differences in address line currents between the active and reset states. The decoder outputs are driven from the center of the die (as depicted in Figure 3-19) at $L2$ to the quadrants. An emitter follower buffer drives the pulsed *NOR* gates and wired-or buffers can generate $L3$ address line set selection signals. The follower discharge currents are interesting candidates for pulsing, but degrading the **BankSelQ** low level (due to V_{BE} differences when the pulsed current turns off) can lead to increased inactive currents in the pulsed currents that it controls.

Finally, the bank selection must activate the appropriate switched PMOS loads, which requires another wired-or with high-capacitance wires that require large currents to rapidly

discharge. The output of the bank selection decoder mentioned above would seem ideal to activate pulsed current in only the selected $\overline{\text{BankSelP}}$; unfortunately, the $L3$ bank selectors have enough delay that the discharge of $\overline{\text{BankSelP}}$ would delay the access. Instead, one level of current steering may be used to steer a pulsed current source (activated off the input clock) between two PMOS selection lines, as in the global address buffers; two-level series gating is impossible because the pulsed current source is activated by an $L3$ signal and the select line drops low enough to saturate a BJT with an $L1$ signal on its base. This solution reduces the PMOS selection power to no more than 25% of the equivalent static power, as in the global address line case. If a shorter pulse was available that rose with the input clock, the power savings would increase since no current is needed to keep these lines low; such a pulse would also be useful for the global address lines, which share this trait.

3.5.5 Reference Generation

The preceding circuits require the generation of a very stable V_{SS} level. On-chip V_{SS} generators have been around for a while, but this one has three unusual characteristics. First, the generated level ($V_{CC} - 4V_{BE} - V_{Swing}$) is large enough that it will not be far from the bottom supply (V_{EE}), so careful design is required to ensure that the circuit discharging this node has enough voltage in which to operate. Second, because much of the SRAM current is dynamically supplied by pulsed current sources, the reference generator must handle large variations in its output current. Finally, this reference is being used to generate stable currents, so the dynamic voltage variation must be relatively small to avoid noise margin problems in gates supplied from this source.

The last two issues put such a severe burden on the reference's transient response to current variations that some form of decoupling capacitance to V_{CC} is required. An extremely large decoupling capacitance is available from the memory array itself; three separate layout regions contribute to this capacitance:

- V_{CC} -connected n-well (which surrounds the PMOS devices) capacitance to the substrate
- n-type drain diffusion capacitance (to the substrate) of the NMOS devices on the high side of the memory cell
- p-type drain diffusion capacitance (to the n-well) of the PMOS device on the low side of the cell

In order to use this capacitance to stabilize V_{SS} , the substrate must be tied to V_{SS} , since the n-well and high side of the memory cell are already at V_{CC} . The implication of this is that no n-type regions that sit in the substrate may drop substantially below V_{SS} or else undesirable substrate current will flow in this forward-biased pn-junction. The source-drain diffusions of NMOS devices and the collectors of BJTs fall into this category.

A V_{SS} generator that meets these requirements appears as Figure 3-22. It is essentially a simple feedback amplifier where Q3 samples the V_{SS} potential, producing a current that reduces that of the Q2-Q1 current mirror, thus allowing V_{SS} to rise until balance is achieved. Because the current through Q2 is wasted, it is desirable to make the current mirror ratio as large as possible, especially since the rest of the SRAM's current flows through Q1. However, the frequency response characteristics of a current mirror degrades with increasing ratio; the additional devices improve the frequency response of the current mirror at large mirror ratios. In particular, the emitter follower and diode combination form a fixed current-gain stage (sometimes referred to as a f_T -doubler [44]) that increases the current available to charge the base of Q1 at high bandwidth; they also ensure that Q2's collector remains at least two V_{BE} 's above V_{EE} and thus safe from substrate-collector forward biasing. R1 provides discharge current for the base of Q1; the traditional current mirror would short Q2's collector to this node to provide this current instead. Diode D1 prevents Q3 from saturating.

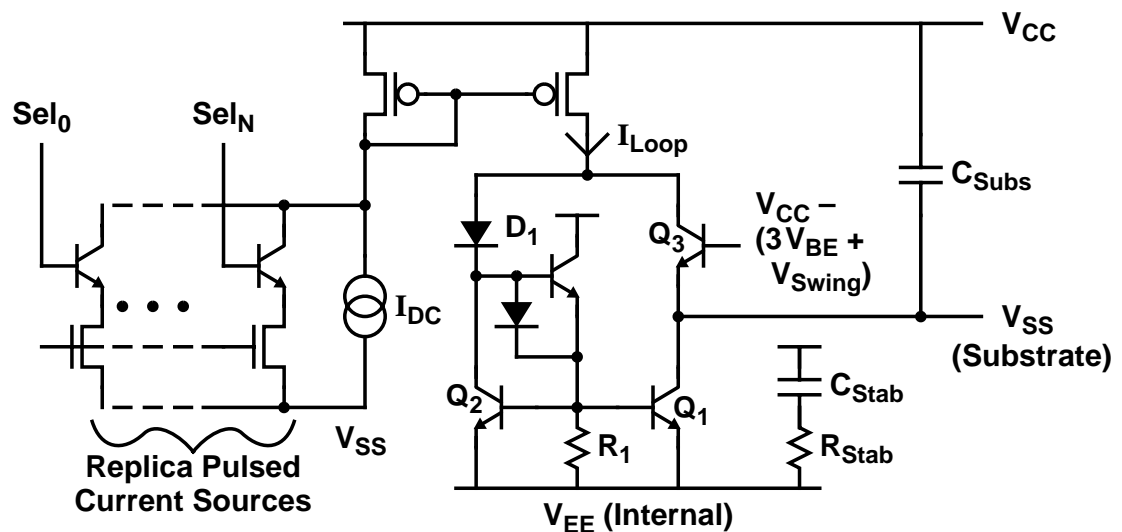


Figure 3-22 A V_{SS} Generator

This basic feedback configuration operates well over a fairly wide range of conditions, but the extreme dynamic output current requirements require a few additional components.

3.5.6 Summary

Making the feedback loop operate over such a wide current range normally would require large gain, which can lead to problems with transient response such as overshoot. Because the dynamic current characteristics of such a design are well known, replica versions of each class of pulsed current source may be constructed to increase the feedback loop current I_{Loop} when each current source is active; this reduces the gain required in the loop to maintain a stable V_{SS} . A more serious concern is the variation in the on-chip V_{EE} supply due to the effects of pulsed current through the inductance of package leads and bond wires. Additional capacitance C_{Stab} , probably formed from PMOS capacitors, in series with a small resistance R_{Stab} stabilizes the on-chip V_{EE} response to current switching.

Circuit simulations predict that this generator will exhibit only a 70-mV peak variation when supplying a 400-mA pulsed current on top of a 200-mA static current, and only 20-mV variation with 300-mV/ns noise on the external V_{EE} lead. The generator exhibits excellent start-up characteristics, tolerating supply ramp rates in excess of 10V/ μ s.

3.5.6 Summary

Pulsed circuit techniques can make a tremendous performance difference for *NOR* decoders in BiCMOS SRAMs. The combination of the switched PMOS load with the pulsed current source permit constructing banks of fast *NOR* decoders with greatly reduced power dissipation. For a sixteen-bank design with an active/reset gate power ratio of ten and with an active time of one half the cycle, the average *NOR* gate power is reduced to only 16% of what a traditional design would require. Pulsing the address buffers and address lines reduce their power dissipation to less than one quarter of the original amount. Finally, the control power overhead for these techniques is modest enough that the overall power of a pulsed design is less than 25% of the equivalent static power, with very little delay penalty. A detailed example of a pulsed *NOR* design appears in Section 5.3.

Furthermore, the V_{SS} and pulsed current source reference generators make the benefits of pulsed currents available to general ECL-style logic designs. While it is non-trivial to generate the required timing relationships between interacting pulsed signals, these circuits can serve as a basis for further exploration.

In comparison with the switched PMOS load diode decoder circuits, the power advantage of the *NOR* decoders is debatable. However, diode decoders have trouble with large numbers of banks, since switching the decoder current among a large number of address line sets requires extra delay. Furthermore, pulsed *NOR* decoders handle large *fan-in* and

fan-out conditions better, due to the quick performance and simplicity of wired-or pre-decoders (with high-current emitter follower drivers). Thus, *NOR* decoders are superior for large memories. Chapter 5 shows that at 256K bits, a pulsed *NOR* design can deliver 25% faster times at nearly the same power level as an optimized diode decoder design.

3.6 Word Line ECL-CMOS Converter

A principal improvement in decoding delay that results from pulsed decoders is due to pulsing the discharge current for the word line driver. In a traditional word line driver (Figure 3-1), a rising word line is loaded both by the memory cells attached to the line and by the shared discharge current, which increases as the word line voltage rises. A pulsed word line driver has the same pull-up circuitry as the traditional driver, namely a Darlington-connected pair of bipolar transistors, but has a dynamic discharge current that does not activate until after the selected word line transitions high. A pulsed decoder and driver have less delay because the Darlington driver requires less base charge to raise a word line that is loaded only by memory cells.

The pulsed word line driver must satisfy several constraints in order to be useful. The most obvious constraint is that the driver should not activate the discharge current until the word line completes its transition. Since the word lines have high capacitance, the discharge current is large so the driver should pull discharge current only from the selected word line or else the power dissipation will be too high. Furthermore, an inactive driver should dissipate very little power, since there are lots of inactive word lines in an SRAM. Finally, the duration of the discharge pulse must be long enough that the word line discharges completely, but not so long that the discharge current fights a word line that rises on consecutive access cycles.

Active discharge circuits for low-swing word lines are not new [45 46 18]. However, their goal is to speed the falling transition of word lines, so most of them activate before the word line is high. An alternative method for generating the desired discharge pulse is to delay the active (rising) input of the decoder until the word line has risen, and then activate the discharge source. If the delay can be controlled well enough, it can be set to discharge the word line as soon as the memory cell characteristics allow, thus minimizing both power dissipation and cycle time. Implementing this delay with ECL bipolar circuitry requires too much power, and using an *RC* network to build the delay does not give good delay matching to the memory cell characteristics. Building the delay from CMOS circuits

improves both the power dissipation and the delay matching, since the required memory cell active time is likely to be dominated by the time needed to write its CMOS latch, this delay is well-matched by the CMOS circuit delays in the pulsed discharge source.

In order to utilize full-swing CMOS circuits to implement the delay, the reduced-swing decoder or word line signals must be converted to larger swings. Many different ECL-CMOS converters have been implemented, but most of them are unsuitable for this task because they dissipate static power. Since the required converter is part of every word line driver, any static power that is dissipated gets multiplied by the number of word lines in the system. A more suitable converter should dissipate no static power, but may take into account the unique characteristic of SRAM word lines: that all of them except one are inactive at any given time [28].

3.6.1 Low-Power Word Line Level Converter

Figure 3-23 depicts a converter suitable for pulsed word line discharge, which is configured to translate a low-swing decoder or word line value into a full-swing signal. The first stage is a signal-amplifying ECL inverter, which may share its current source with all other converters in a bank because no more than one word line is ever high; in *NOR* decoders this stage is unnecessary since the complementary (*OR*) decoder output may be readily utilized, as is discussed in the next section. Transistor P1 is ratioed to easily overpower N1 and hence provide a rapid rising edge; there is static power only in the one converter with P1 turned on. Two stages of CMOS inverters buffer and amplify the output onto the output line, which has high capacitance from the word line discharge circuitry. Transistor N2 is a feedback-driven NMOS device that reduces the delay of both transitions; on the rising edge it is off and hence does not interfere with P1. Once the word line is high N2 turns on to provide more drive for the falling edge.

The reference voltage on the gate of transistor N3 prevents the feedback signal from overpowering P1 until P1 begins to turn off. This signal is readily generated using the reference generator shown in the figure, which mimics the level converter when active, except that the NMOS devices are twice their normal width. This configuration guarantees that the PMOS device, whose saturation current is almost enough to fight the double-width NMOS devices, can overpower the normal-width devices in the actual converter.

Circuit simulations indicate that this level converter can convert an *L2* input to drive a 0.2-pF load in 0.7ns. With a complementary *NOR* gate output the conversion starts as soon as the decoder input, rather than the decoder output, switches. This saves

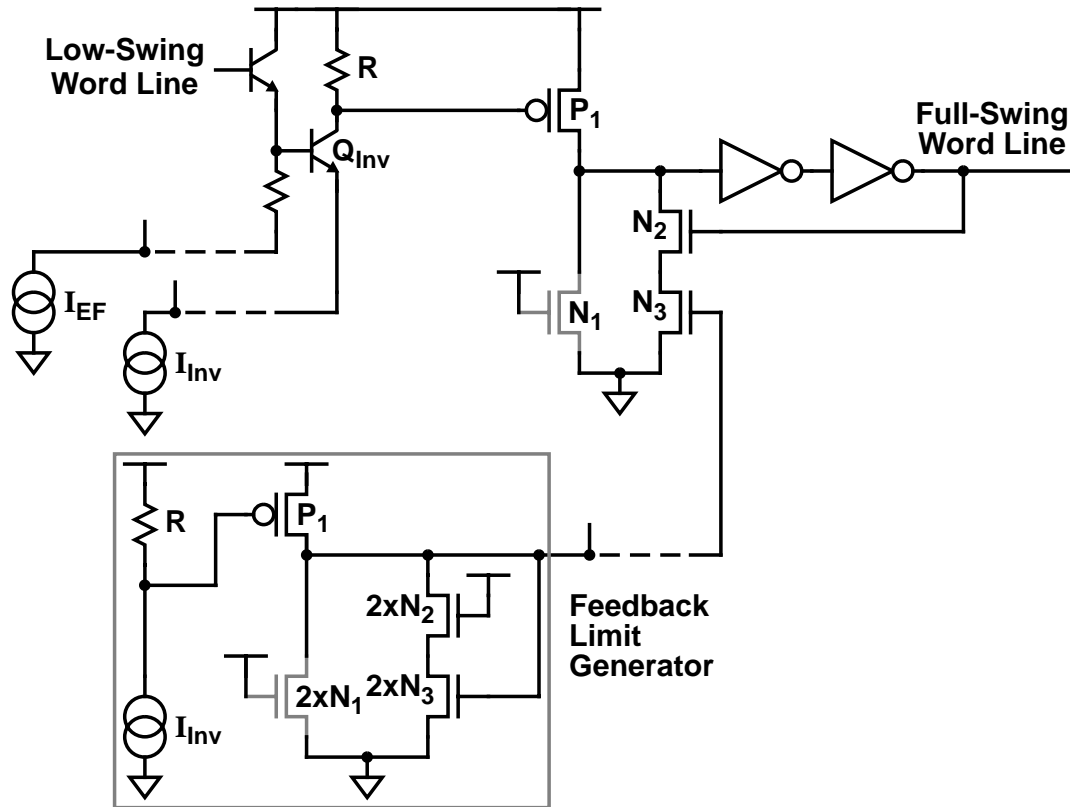


Figure 3-23 A Word Line Level Converter

approximately 0.3 ns. While this circuit is by no means the fastest reported [36], it is excellent for word line discharge applications, since the conversion delay allows the word line to rise, while the reset delay is long enough to let the word line fully discharge. Furthermore, the near-zero static power of this gate allows it to be efficiently implemented on each word line in a memory.

Before moving on to describe the use of this converter in word line discharge, it should be noted that the word line converter has other applications. In particular, Chapter 4 describes its use in generating full-swing write word line signals for the dual-ported CSEA memory cell.

3.6.2 Use in Pulsed Word Line Discharge

A pulsed word line must stay active long enough to write the memory cells. The word line level converter operates directly off decoder or word line levels, and the CMOS inverters in the converter make the delay track the write time of CMOS memory cell latches over process, temperature, and supply variation. Thus, the resulting word line active time is

determined by circuitry that mimics the timing of a memory cell. Figure 3-24 shows the adaptation of the word line converter for use in word line discharge.

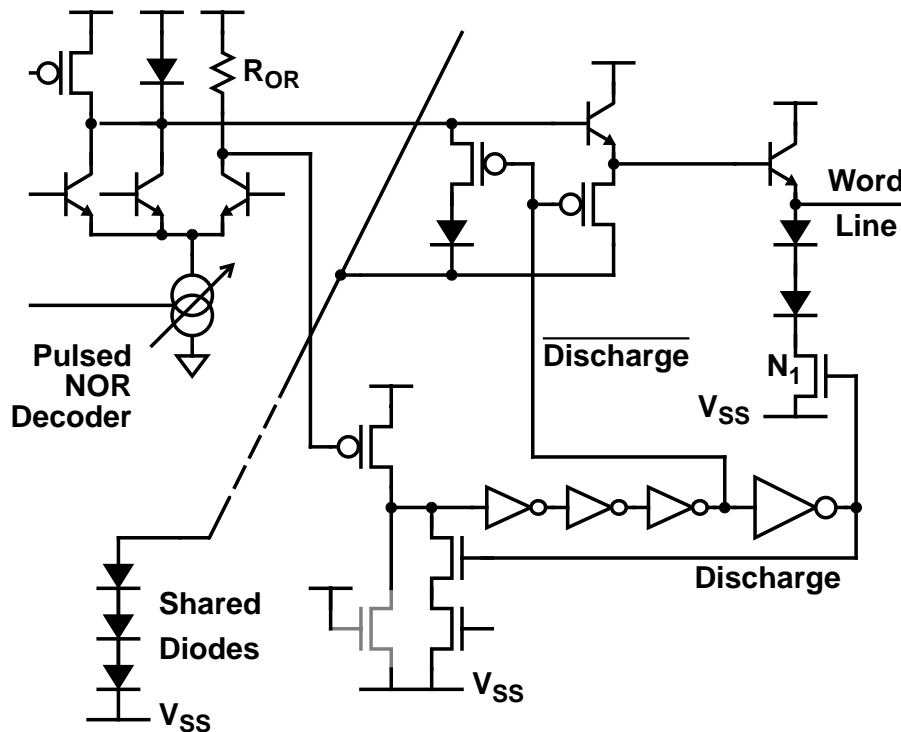


Figure 3-24 A Level Converter-Based Pulsed Word Line Discharge System

This converter shows the interface to the complementary *OR* output of a *NOR* decoder; since the decoder inputs are L_2 , the decoder reference is about $2.5V_{BE}$'s down from V_{CC} so the swing on R_{OR} may be almost three V_{BE} without saturating the reference device. The swing limit is set by high-temperature considerations, where V_{BE} is smallest while signal swings are largest. The basic converter is very similar to the previous section, although the number of CMOS inverters may be increased to provide longer word line pulses (and thus more time to write a memory cell). The converter generates two signals, $\overline{\text{Discharge}}$ and Discharge , which reset the decoder and word line driver. $\overline{\text{Discharge}}$ controls PMOS devices that pull down on the decoder output and the Darlington intermediate node one inverter delay before the word line discharge occurs; this improves the reset characteristic by ensuring that the discharge current does not need to fight an active follower. PMOS devices are best for this stage because the source and drain nodes will stay near V_{CC} , where the NMOS V_{Th} is substantially degraded. Since V_{SS} is a fixed distance from V_{CC} , it is convenient to simply pull the word line driver nodes down until they are the appropriate number of V_{BE} 's above V_{SS} ; diodes perform this function very well, and the stack of three diodes attached to P1 may be shared by all the word lines in a bank.

The NMOS word line discharge device, N1, is controlled by the **Discharge** converter signal and must be relatively large to handle the high active word line discharge currents. Placing the diodes on the drain lead of N1 reduces its size requirement by increasing the available V_{GS} and therefore the current per unit width; however, this configuration will not let the diodes be shared so the area savings may be minimal. Instead, a design could share a larger N1 with a number of adjacent word lines, replacing the inverter that drives N1 with a CMOS *NOR* gate; one diode per word line would still be required in the drain lead to isolate the word lines from one another, but the second diode could be shared. While such a design attempts to pull discharge current from multiple word lines, all of the unselected lines are at $V_{SS} + 2V_{BE}$ and thus do not receive discharge current.

This system has the advantage that it sets the word line active time independently of the address line pulse width, since the discharge circuit affects only one side of the decoder gate and therefore cannot cause itself to reset before the address lines cause the decoder to switch; this removes any worries about a word line becoming selected more than once per access cycle. Once the address line switches the gate current, the non-inverting output rises and the converter then returns to its inactive state. Circuit simulations show that this circuit can generate word line discharge pulses shorter than 1 ns with extremely low static power dissipation. In a real system, small passive current sources would be used on the word line and internal Darlington nodes to ensure that low word lines do not drift high; even considering this current, this technique provides faster access and uses 40% less power than the discharge scheme employed in a previous design (Section 5.1).

3.7 Summary

This section has shown that careful use of MOS transistors can greatly reduce the power, and often increase the speed, of the bipolar circuit blocks often used in SRAM decoders and line drivers. The use of switched PMOS loads, pulsed current sources, and pulsed word line discharge circuits give the designer great flexibility in implementing very fast BiCMOS SRAMs with much lower power dissipation than has previously been possible.

Chapter 4

Sense and Write Techniques for CSEA Memories

Most BiCMOS SRAMs utilize the same memory cell types as their CMOS counterparts. While the resulting memories have very high densities, the NMOS access devices require nearly full-swing word lines to deliver reasonable read current. As Chapter 2 notes, deep sub-micron CMOS devices cannot reliably operate from five-volt power supplies, so a class of BiCMOS memories have been implemented that use internally-reduced supplies for the CMOS devices and standard ECL supplies for bipolar circuitry. Because the “full” CMOS swing is substantially smaller than the ECL supplies, such memories use bipolar circuits to rapidly decode addresses and drive word lines; for example, a recent 4.5-V SRAM uses an internal CMOS supply of 3V, and uses mostly-bipolar circuits to drive its 2.4-V word lines [5]. The low-swing decoders of Chapter 3 are very appropriate for such memories, but the required voltage amplification to convert standard ECL swings into the word line levels slows the access.

The *CMOS-Storage, Emitter-Access* (CSEA) [6] memory cell provides an approach for building BiCMOS SRAMs with word line swings that are much closer to standard ECL levels. CSEA memories deliver read access paths composed entirely of low-swing signals, so their access times more closely match bipolar memories. The CSEA memory cell is superior to bipolar cells because the storage element is composed of a CMOS latch that dissipates no static power. Because it requires full CMOS swings to write the cell, CSEA memories have separate read and write ports. While fully-differential CSEA memory cells have been implemented [47], CSEA SRAMs typically assign a single bit line to each port in order to maximize memory density. The single-ended nature of reads and writes makes CSEA design different from memories using CMOS cells.

This chapter describes the unique characteristics of CSEA memories, and circuit techniques that permit the design of robust, high-density, fast CSEA SRAMs with moderate

power consumption. After opening with additional background on traditional CSEA design, the chapter focuses on the challenges associated with sensing the stored values of CSEA cells. A detailed analysis of the effects of parasitics and supply noise, together with careful circuit design, show that single-ended sensing can be robust. Furthermore, the chapter shows how pulsed circuits can improve the sense speed and reduce the power dissipation of wide-access CSEA memories. Following the sensing discussion, the chapter proposes circuits that deliver the full-swing write path signals that are needed by a CSEA memory. These circuits are fast enough that the cycle time of the memory is not limited by the write access.

4.1 CSEA Basics

A schematic diagram of the CSEA memory cell appears in Figure 4-1. As in a 6T CMOS cell, the data is stored in a static latch formed by cross-coupled CMOS inverters (transistors N1, N2, P1, and P2 in the figure); this configuration provides a robust storage element that dissipates almost no static power. The sources of transistors P1 and P2 are connected to the read word line (rather than the positive supply traditionally used). This signal has ECL-like voltage transitions, always remaining several MOS threshold voltages above the negative supply, V_{EE} , and therefore giving the latch excellent noise immunity. The bipolar transistor Q1 in the CSEA cell, which is connected in an emitter follower configuration, provides high cell read current with small read word line swings, and thus can provide fast access times. The CSEA cell is also nearly as dense as a 6T cell, but has more complex read and write circuits due to the independent, single-ended read and write ports. The read path uses small swings on the read word line and the read bit line for sensing, while the write path uses CMOS-like levels on the write word line and the write bit line for storing a new value into the cell through N3.

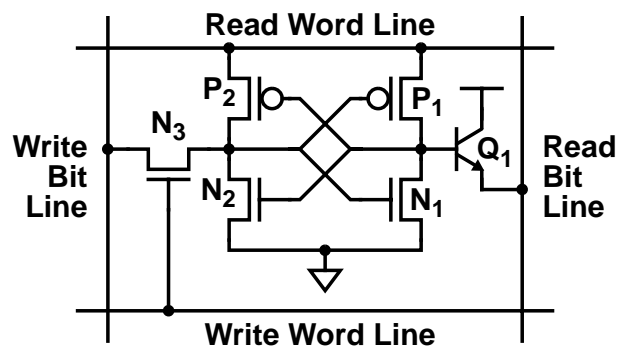


Figure 4-1 CMOS-Storage, Emitter-Access Memory Cell

Figure 4-2 depicts a simplified view of the read access path of a CSEA memory. A row address change causes a switch in the differential outputs of at least one push-pull address buffer, pulling current out of the previously-selected diode decoder while allowing the newly-selected decoder to rise. These decoder changes couple through Darlington-connected pairs to drive the word lines. The previously-selected read word line is discharged by a shared current source while the newly-selected one is pulled up by the Darlington follower. The small swing on the selected read word line couples to the read bit line through bipolar transistor Q1 if PMOS device P1 is conducting (i.e. if the cell stores one). The cell state is detected by switching a shared current to the selected bit line and into the differential pair formed by Q1 in the cell and the bit line reference transistor Q2. The bit line reference is set to be approximately the midpoint of the word line swing, so unselected cells on the selected bit line receive essentially none of the bit line current regardless of their state. The collector of the reference transistor goes into a cascode amplifier that feeds the output buffer. Transistor Q3 pulls unselected bit lines to about one V_{BE} below the selected word line voltage to ensure that these bit lines do not contribute current to the cascode network. This access path uses only small swing signals, and hence is quite fast. Prior work on this type of memory have produced a sub-4-ns 4K SRAM in a $1.5\mu\text{m}$ technology [6].

The cell area penalty for the CSEA memory cell is fairly small. Since transistor Q1 is an emitter follower, its collector is readily shared with collectors in adjacent cells and (in many BiCMOS technologies) with the n-well containing the PMOS devices. The density may often be further improved by merging the source of P1 with the base of Q1. Hence the primary density penalty is the second word line required by the cell. Because the cell is tolerant of large internal collector resistance (the base is at least $2V_{BE}$ down from V_{CC} , so the voltage drop across the collector resistor may be this much without saturating the follower) the V_{CC} wire may be routed on the buried layer of the well/collector and strapped by metal every eight cells or so. For purposes of comparison, a CSEA cell occupying $125\mu\text{m}^2$ [48] supplies twice the read current of a $117\text{-}\mu\text{m}^2$ 6T CMOS cell [25] implemented in the same technology [7].

While the access characteristics and density of the CSEA cell make it an attractive candidate for large, fast, SRAMs, this memory organization is not without its limitations. Its low-swing read port provides fast access, but the traditional bipolar circuits that implement the decoders lead to high power dissipation. Chapter 3 discusses BiCMOS techniques that attack the power issues of low-swing decoders and are ideally suited for CSEA memories. The use of a single bit line for sensing the cell is also troubling, since this cell will not have the common-mode noise cancellation that is found in standard differential bit

line designs. While the use of large bit line currents help mitigate the effects of noise, they also increase the power dissipation, especially for wide access widths. The next section discusses these issues in great detail, and proposes BiCMOS techniques to provide fast, robust reads at reasonable power dissipation. Finally, writing the CSEA memory is a little tricky, because the cell needs CMOS levels on the write word line and the write bit line so that N3 can overpower either N2 or P2 to flip the cell. Section 4.5 discusses techniques that rapidly deliver the required signals, while avoiding problems with disturbing unselected cells on the selected write word line.

4.2 Single-ended Bit Line Sensing

The large transient supply current requirements of a chip produces an environment where the power supplies are not constant voltages. *Electronic supply noise* often affects different internal signals in different ways, depending upon the relative coupling between each signal and noisy supply; when different signals having dissimilar coupling are compared, the result may be different, or at least have different timing, than what is achieved without the noise. Managing the effects of such noise is a key aspect of fast SRAM design, since low voltage swings are used to improve the performance of high-capacitance nodes. Virtually all SRAMs minimize the effects of supply noise by adopting differential signalling for low-swing nodes, where each quantity is represented by two complementary signals. The basic 6T memory cell makes complementary outputs trivial to generate on the bit lines, so the density penalty for differential signalling is typically only the number of bit lines required per cell.

The benefit of differential signalling is simply that connecting and routing two signals in parallel virtually guarantees that the supply noise coupling into each will be similar, and thus the complementary signals should be affected in similar ways. Since basic signal-comparing gates such as ECL inverters or their CMOS equivalents are very tolerant of such *common-mode* noise, differential signalling can greatly reduce the effects of supply noise.

Because of the separate read and write ports of the CSEA memory cell, there is a strong density advantage in making it work with only single read and write bit lines. While the implications of the single write bit line are considered in the next section, this section focuses on the principal concern about the practicality of CSEA memories: obtaining reliable and fast access times in the presence of supply noise with single-ended sensing. This

section shows that the noise immunity is quite good, primarily because of the large read current available from the cell's emitter follower. Section 4.2.1 develops equations to specify static word line and bit line reference voltages that deliver desired differences in the sensed current and hence sense path noise margins. The section then expands these results to include the effects of parasitics and supply noise at the bit line level. Finally, the section describes circuitry to generate the required reference voltage for the bit line reference transistor.

4.2.1 Simplified Sensing

Because the CSEA cell follower (Q1 from Figure 4-3) forms a differential pair with the bit line reference device (Q2), the read operation simply compares the internal voltage of the selected cell to the bit line reference potential *BitLineRef*. When the cell stores one, the right side of the cell latch is high so the base of Q1 follows the read word line value. Conversely, the base of Q1 is at the negative supply when the cell stores zero. In designing the read word line swing and $V_{BitLineRef}$, the quantity of interest is the collector current through Q2, since this current is the input to the sense amplifier. Simple expressions relating these values are readily derived by considering the voltage differences required to achieve desired ratios of the sensed current to the total bit line current, I_{RBL} [49].

The worst-case reading of one occurs when all unselected cells on the bit line store zero, because any current that enters unselected cells subtracts from I_{One} (the current through Q2 when reading one) and thus makes it simpler to read zero. The maximum value of I_{One} is therefore simply determined by considering the differential pair formed by the cell follower and Q2. Neglecting parasitic resistances for a moment, and assuming that the sense device has an emitter W times as large as the cell follower, the required voltage difference between the selected word line and the bit line reference is:

$$V_{RWL(High)} - V_{BitLineRef} = V_T \ln \left(\frac{I_{RBL} - I_{One}}{I_{One}} \cdot W \right) \quad (4-1)$$

where V_T is the "Thermal Voltage" (kT/q) defined in Chapter 2.

When reading zero, any bit line current entering unselected cells decreases I_{Zero} , the current through Q2 in this case. Therefore, the worst-case condition for reading zero occurs when all unselected cells store one. This case is depicted in Figure 4-4. The required

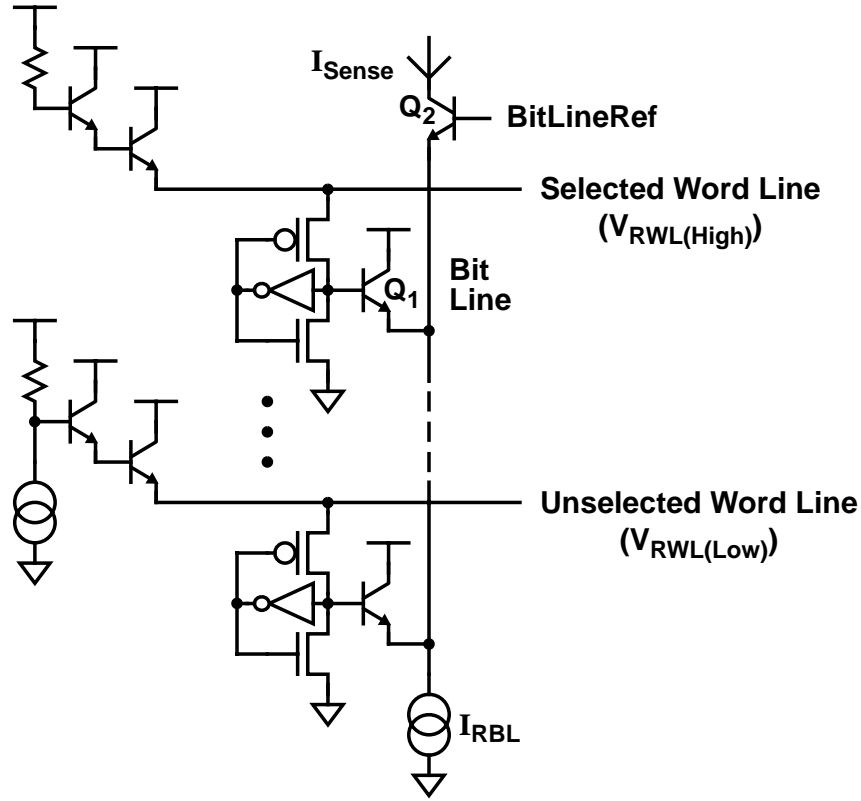


Figure 4-3 CSEA Cell Bit Line Sensing Model

potential difference between the bit line reference and the unselected word line level, given N cells per bit line, neglecting any bit line resistance, is given by:

$$V_{BitLineRef} - V_{RWL(Low)} = V_T \ln \left[\frac{I_{Zero} (N-1)}{(I_{RBL} - I_{Zero}) W} \right] \quad (4-2)$$

For equal current sensing margins between Equation (4-1) and Equation (4-2), the current steering ratios of the two cases should be equal, i.e.

$$\frac{I_{RBL} - I_{One}}{I_{One}} = \frac{I_{Zero}}{I_{RBL} - I_{Zero}} \quad (4-3)$$

Because device matching considerations favor equal device sizes ($W = 1$), the optimal placement for $V_{BitLineRef}$ is closer to $V_{RWL(High)}$ than $V_{RWL(Low)}$. This is due to the combination of unselected cell followers in Figure 4-4, which is modeled by the $(N - 1)$ term in Equation (4-2). For instance, with 64-cell bit lines at room temperature, $V_{BitLineRef}$ should

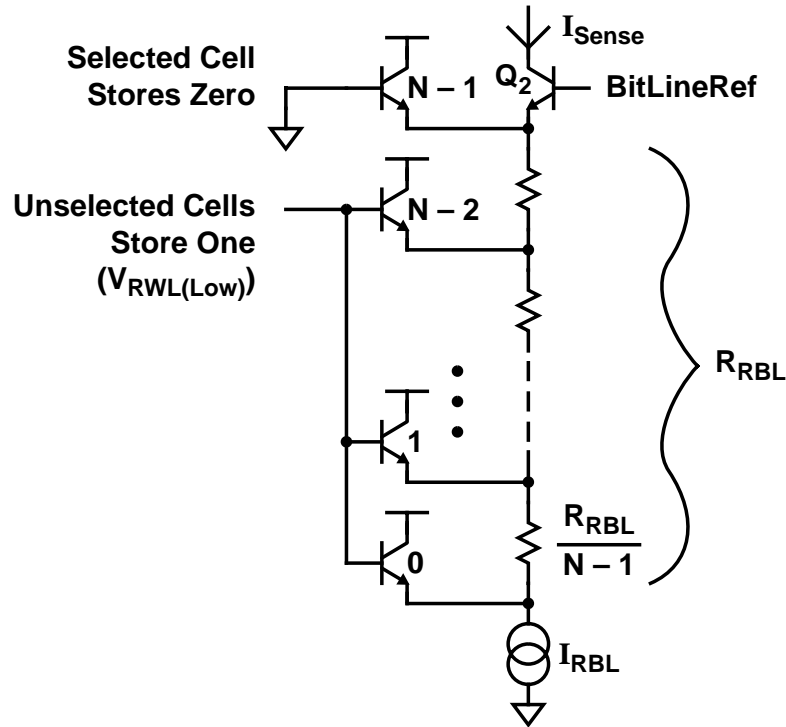


Figure 4-4 Model for Worst-Case Reading Zero

be 107mV closer to $V_{RWL(High)}$. The next sections describe modifications to these basic equations to model circuit non-idealities.

4.2.2 Effects of Emitter and Bit Line Resistance

A major speed advantage of the CSEA memory cell is the high read current densities supported by the bipolar transistor in the cell, but these same currents expose resistive parasitics that may substantially alter the above calculations. Specifically, bit line wire resistance and series emitter resistance both reduce the current ratios, since these resistors appear in the emitter leg of one transistor in the differential pair and therefore add IR terms to the sense equations. The memory designer has little control over either resistance, since density concerns almost invariably constrain bit line widths and emitter sizes to be at or near the minimum (high-resistance end) supported by the technology,

Proper placement of the sense device on the bit line can mitigate the effect of the bit line resistance, R_{RBL} . If the sense device is at the same end of the bit line as the current source, the bit line resistance is in series with the cell follower at the opposite end of the bit line. In this case the voltage difference between the selected word line and the bit line reference must be increased by nearly $I_{RBL}R_{RBL}$ to maintain the desired value of I_{One} . The bit line

resistance actually helps when reading zero, since there will be extra resistance to emitters of cells storing one but on unselected word lines; however, for values of I_{Zero} near I_{RBL} the current not steered into the sense device will be small so the effect of this resistance will be minor.

Alternatively, if the sense device is at the opposite end of the bit line (from the current source) then the bit line resistance does not affect reading one, since in all but the worst case the extra resistance shows up in the emitter of the sense device (and hence actually reduces I_{One}). Therefore the swing only increases by parasitic IR drops associated with the cell follower, so Equation (4-1) becomes:

$$V_{RWL(High)} - V_{BitLineRef} = V_T \ln \left(\frac{I_{RBL} - I_{One}}{I_{One}} W \right) + I_{RBL} \left(R_{Emitter} + \frac{R_{P1}}{\beta} \right) \quad (4-4)$$

where $R_{Emitter}$ is the emitter resistance of the cell follower and R_{P1} is the equivalent on resistance of transistor P1 in the CSEA cell.

When reading zero in the worst case, each of the many unselected cell followers will steal slightly different amounts of bit line current due to the distributed nature of the bit line resistance. Figure 4-4 attempts to make this effect more clear. The bit line resistance can be divided into $N - 1$ equal pieces and therefore the potential difference between the emitters of adjacent cell followers is simply $I_{RBL} R_{RBL} / (N - 1)$, assuming that essentially all of the bit line current flows through Q2 ($I_{Zero} \approx I_{RBL}$). It follows that the current ratio between adjacent devices is

$$e^{\frac{-\rho}{N-1}} \quad \text{where } \rho = \frac{I_{RBL} R_{RBL}}{V_T} \quad (4-5)$$

and thus the total current through unselected devices, I_{Unsel} , is given by:

$$I_{Unsel} = I_0 \sum_{n=0}^{N-2} e^{\frac{-n\rho}{N-1}} \quad (4-6)$$

where I_0 is the current through the bottom unselected cell. By solving the geometric series, and folding the result back into Equation (4-2), while noticing that both R_{RBL} and the

4.2.3 Data-dependent Supply Noise

emitter resistance of the sense device R_{Emitter}/W carry nearly I_{RBL} , the equation for reading zero becomes

$$V_{\text{BitLineRef}} - V_{RWL(\text{Low})} = V_T \ln \left(\left[\frac{I_{\text{Zero}}}{(I_{RBL} - I_{\text{Zero}}) W} \right] \left[\frac{1 - e^{-\rho}}{1 - e^{-\frac{\rho}{N-1}}} \right] \right) + I_{RBL} \left(R_{RBL} + \frac{R_{\text{Emitter}}}{W} \right) \quad (4-7)$$

While it appears that the swing has grown by $I_{RBL} R_{RBL}$, the solution of the geometric series (which appears in square brackets above) is a smaller quantity than the value it replaces ($N - 1$, from Equation (4-2)). This leads to the comparison of required word line swings ($V_{RWL(\text{High})} - V_{RWL(\text{Low})}$) between the two sense device placements that is shown in Figure 4-5. When the sense device is near the bit line current source, the required swing varies linearly with the bit line resistance to maintain I_{One} , as was mentioned above. With the sense device at the opposite end, the increase in swing with resistance is reduced, so this placement is preferred. The figure assumes the 0.8- μm technology of Chapter 1, which delivers 64-cell bit lines that are approximately 1500 μm long, and assumes that I_{One} is 10% and I_{Zero} is 90% of I_{RBL} . With a bit line resistivity of 50 $\text{m}\Omega/\square$, a required word line swing of 400mV is predicted, with the bit line reference 230mV down from $V_{RWL(\text{High})}$. As the following section shows, a 550-mV swing is required in the presence of supply noise.

4.2.3 Data-dependent Supply Noise

Electronic noise coupled onto the bit lines from the power supplies degrades the static sense ratios. Most SRAMs reduce the effects of supply noise by using differential signaling techniques that attempt to make the noise look common mode. A fully-differential CSEA cell does not get much benefit from this technique, since the capacitive power supply coupling of the bit line is primarily through the base-emitter capacitance of the cell followers, whose bases are tightly coupled to either V_{EE} or V_{CC} (through the read word line). Hence the noise coupling is strongly dependent on the data stored in the unselected cells and this coupling does not appear common mode, even with differential bit lines.

It is therefore important to reduce this data-dependent supply noise coupling as much as is feasible. Since the read word line voltage is strongly tied to the V_{CC} voltage (through the

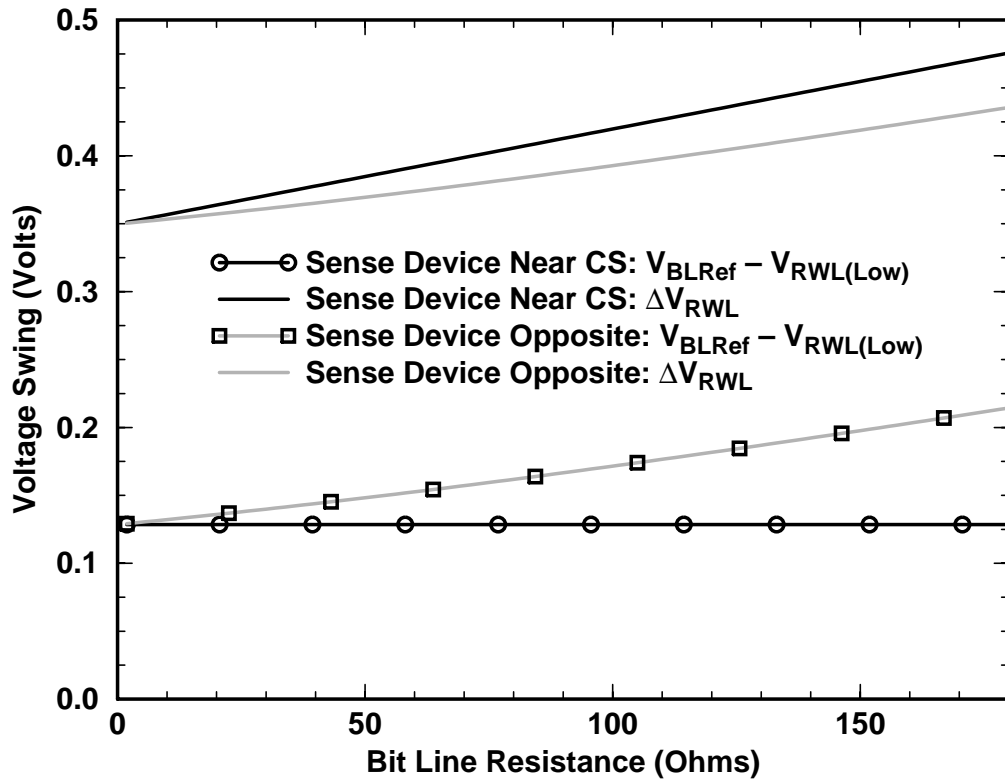


Figure 4-5 Read Word Line Swing Variation

diode decoder and the Darlington driver) and $BitLineRef$ may be constructed to track V_{CC} as well, noise suppression is best obtained by making the bit line voltage as strongly coupled to V_{CC} as possible (and therefore as weakly coupled to V_{EE} as possible). One approach is to add capacitance from the bit line to V_{CC} , thereby increasing the coupling; unfortunately, the amount of capacitance required to have a substantial effect on the coupling is large (because the base-emitter capacitance is such a high fraction of the total bit line capacitance) so this approach will substantially slow the bit lines. An alternative is to decouple the substrate and the negative supply for the memory arrays from V_{EE} ; the on-chip V_{SS} generator of Section 3.5 creates a substrate and negative supply voltage that has stronger coupling to V_{CC} than V_{EE} . While such a technique reduces the magnitude of V_{EE} -related noise pulses, it does not eliminate them, so the effects of supply noise must still be estimated.

Because the only paths to V_{EE} in a traditional ECL circuit are through static current sources, the amount of V_{EE} noise generated on chip in such an ECL system is very small. In order to quantify the amount of externally-generated V_{EE} noise, a model may be readily built for the power supply networks that takes into account package lead inductance,

supply network resistance, and the array capacitance between the supplies. This network low-pass filters incoming noise edges, limiting the edge rate (i.e. the maximum dV/dt) that the internal V_{EE} supply will experience given an external step input. For large CSEA memories (larger than 64K-bits) circuit simulation indicates that the practical maximum edge rates are a few tenths of a volt per nanosecond. A CSEA memory using the V_{SS} generator of Section 3.5 does create its own internal supply noise as the pulsed current sources fire, but Chapter 3 shows that the generator limits the edge rates to roughly 100mV/ns, which is less than the edge rate of externally-generated noise. The rest of this chapter refers to the negative voltage supply, which connects to the substrate, as V_{EE} . The analysis that follows is equally applicable to a system with a V_{SS} generator.

Assuming the bit line reference voltage does not respond substantially to V_{EE} noise, it is reasonable to amend the static sensing equations (Equation (4-4) and Equation (4-7)) to include noise-related terms. As Section 4.2.4 shows, the analysis is accurate as long as the reference responds less than the bit line itself, which is readily accomplished. The supply noise that couples onto the bit lines affects the sensed current. If V_{EE} bounces downward (away from V_{CC}) while the selected cell stores zero, the bit line will follow downward as well, increasing the base-emitter voltage on the sense device and thereby increasing the sensed current; in this case there is no margin degradation whatsoever, provided that the transient response does not substantially overshoot. Similarly, if V_{EE} bounces up while the selected cell stores one the sensed current decreases so the margin is not affected. The two complementary situations cause sensing problems.

When V_{EE} bounces up and the selected cell stores zero, the bit line tries to rise. The injected charge may be simply modeled as a constant current source equal to dV_{EE}/dt times the coupling capacitance. This injected current subtracts directly from the bit line current, and hence decreases the amount of current available to sense; the magnitude of this decrease is independent of the $V_{BitLineRef} - V_{RWL(Low)}$ value, so increasing the word line swing does not help. The simplest option is to insure that the injected current is fairly small compared with the bit line current to minimize the effects on the sensed current. Fortunately, this is not difficult because the cell follower in the CSEA cell can supply much more read current than a 6T CMOS cell of the same size. These high bit line currents are otherwise needed to support the relatively large bit line voltage swings of single-ended sensing. The effects of this injected current are also somewhat mitigated by the fact that the case with the lowest static sense ratios (all unselected cells store one) has the least capacitive coupling to V_{EE} and hence the lowest injected current. Similarly, when unselected cells store zero the static sense ratio is largest while the injected current is largest.

As a result, circuit simulations indicate that the minimum sensed current when reading zero in the presence of noise is, in the end, not very data dependent.

For the 64-cell bit lines of the previous section, the worst-case bit line coupling to V_{EE} is about 700fF, of which approximately 400fF arises from the base-emitter junction capacitance of the unselected cell followers and the rest comes from the bit line wires and access circuits. Thus, no more than 20% of the 750- μ A bit line current is lost as long as the supply noise is slower than 300mV/ns. This current loss is easily mirrored in the sense amplifier reference circuitry (as is shown later), so the major effect of such a loss is simply the increased time required to discharge the bit line capacitance.

When V_{EE} bounces down and the selected cell stores one, the bit line attempts to follow. In this case the injected charge (which may be converted into a current, as above) adds to the bit line current and any of this current that makes it into the sense device will affect the sense ratio. Because the cell follower has a high equivalent base resistance (due to the “on” resistance of P1), the follower cannot instantly supply the extra current needed to keep the bit line from falling. As the bit line falls, it brings the follower’s base with it (coupling through the base-emitter capacitance), increasing the current into the base from the read word line. Eventually this current raises the base back to the level required to statically supply the extra current. In other words, the impedance looking into the emitter of the cell follower (Q1) has an inductive component, so the bit line will temporarily drop more than a static analysis would suggest. The $V_{RWL(High)} - V_{BitLineRef}$ value may be increased by the maximum drop in the bit line to re-establish the sense current ratio from Equation (4-4). Using an equivalent small-signal model for the cell follower, a simple *RLC* circuit may be constructed to compute this drop as:

$$V_{Drop} = \Delta I_{RBL} \left[R_{EQ} + \left(\sqrt{\frac{L_{EQ}}{C_{RBL}}} \right) e^{\frac{\pi - \text{atan}(-\alpha)}{\alpha}} \right] \quad (4-8)$$

where

$$\alpha = \sqrt{\frac{4L_{EQ}}{C_{RBL} R_{EQ}^2} - 1} \quad (4-9)$$

and ΔI_{RBL} is the worst-case injected current (all unselected cells store zero), R_{EQ} is the resistance seen looking into the emitter of the cell follower ($1/g_{m(Q1)} + R_{P1}/\beta$), $g_{m(Q1)}$ is the transconductance of Q1 (I_{RBL}/V_T), L_{EQ} is $\tau_F R_{P1}$, τ_F is the forward transit time of the cell follower, and C_{RBL} is the total bit line capacitance. For the 64-cell bit line design, a read word line swing increase of 120mV is sufficient to maintain the static current sense ratio with 300mV/ns of V_{EE} supply noise.

The size of the drop is strongly dependent on R_{P1} , as shown in Figure 4-6. The figure depicts both the overall drop and the portion of the drop due to $\Delta I_{RBL} R_{EQ}$. The exponential term from Equation (4-8) has a large effect on V_{Drop} only for small values of R_{P1} . Above 5K Ω , V_{Drop} is primarily dependent on the R_{EQ} and square root terms. Minimizing R_{P1} can greatly improve the noise response, but this requires increasing the gate width of P1, which reduces the memory density. Circuit simulation confirms the results of these equations, and indicate robust sensing, given a low-noise bit line reference. Designing this reference is the topic of the next section.

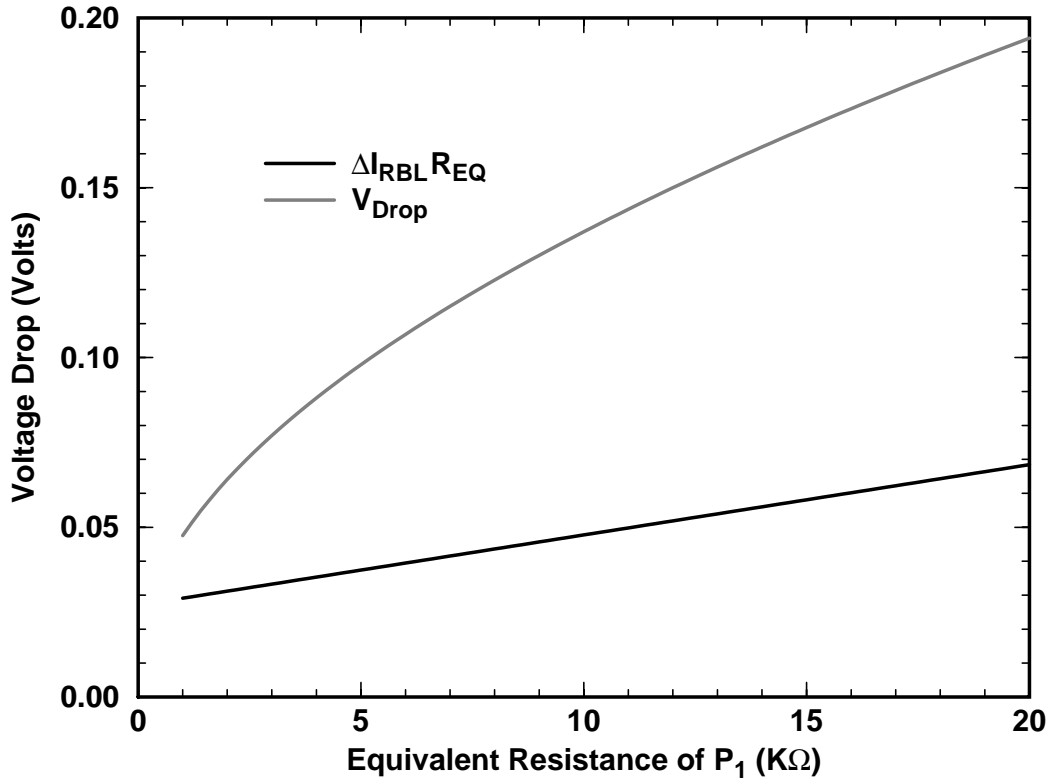


Figure 4-6 V_{Drop} Dependence on R_{P1}

4.2.4 Bit Line Reference Design

The desired bit line reference voltage is specified by Equation (4-4), Equation (4-7), and Equation (4-8). Assuming that the current sources are designed to provide voltage swings that are proportional to absolute temperature (*PTAT*), this bit line reference may be simply generated as a *PTAT* drop from the selected read word line potential (as in [49]) if the components of these equations are roughly *PTAT*. The logarithmic terms (with V_T multipliers) are certainly *PTAT*, and the I_{RBL} terms are nearly *PTAT*, assuming the process resistors do not force I_{RBL} to decrease with increasing temperature.

Section 4.2.3 stipulates that the bit line reference should not respond to V_{EE} noise; this is extremely difficult to accomplish due to the large base-emitter capacitance of this reference to the many unselected and noise-sensitive bit lines. However, as long as the bit line reference moves less than (and in the same direction as) the selected bit line, the sensed current is not adversely affected. Unlike the bit lines, **BitLineRef** should be a static value, so adding coupling capacitance does not delay the access. Greatly increasing the reference's coupling to V_{CC} by adding PMOS capacitance until the worst-case bounce is within the desired range eliminates **BitLineRef** noise problems. In practice this solution is not expensive in terms of area, since PMOS gate capacitances tend to be higher than bipolar base-collector and base-emitter capacitances per unit area. The additional capacitors may be laid out with the sense devices. For the 64-cell bit line design these PMOS devices occupy 6- μm tall patches of otherwise empty area under the bit line reference wire and between the sense devices across the full width of the die.

The resulting bit line circuits provide very robust current input into the rest of the sense network. The next section discusses column multiplexing circuitry that rapidly steers the sense current into a shared sense amplifier, and circuitry to deliver a sense amplifier reference signal that makes the single-ended sense path highly insensitive to supply noise.

4.3 Two-level Cascode Sense Amplifier

The sense amplifier of a CSEA memory must convert the collector current of the bit line sense device into standard ECL voltage levels. Converting the collector current to a voltage could be trivially accomplished by connecting each sense device collector to V_{CC} through a resistor. Since the resulting voltage is not at standard levels, the sensed voltage is compared against a reference using a differential pair to generate the output voltage. While the preceding circuitry rapidly generates the sense output, it is typically too expensive in

terms of area and power to replicate the sense amplifier on a per bit line basis. Furthermore, this circuitry does not address the multiplexing of the sensed data to the outputs.

Because unselected CSEA bit lines have virtually no current in their sense devices, multiple bit lines may share a sense amplifier by simply connecting the sense device collectors to one another. Such an arrangement is very effective at multiplexing among the different bit lines to choose the active one, since it requires no active circuitry. The principal drawback to performing all the required column multiplexing by connecting collectors is that the capacitance on the shared node increases and thus the RC delay on this node becomes prohibitive.

Many bipolar memories insert a cascode device between the sense resistor and the highly capacitive shared collector node to improve the sensing speed by reducing the loading on the resistor while reducing the required voltage swing on the shared node [16], as depicted in Figure 4-2. The cascode device isolates the resistor from the shared capacitance, and the current through the cascode changes exponentially with voltage changes on the shared node. Thus, the swing on the shared node is greatly reduced, so the time required for the sense current to charge the capacitance is reduced and therefore the sensing speed is improved.

Good cascode design for large memories needs to address factors that degrade the performance of real circuits: noise injection and parasitic wire resistance. The next section describes how to design a cascode network that provides excellent noise immunity and is followed by a two-level cascode design that reduces the effect of wire resistance.

4.3.1 Sense Reference Design

The sense amplifier compares the level-shifted sense resistor voltage to the sense amplifier reference, **SenseRef**, to determine the output data. The goal of the reference generator is to keep **SenseRef** halfway between **SenseOut**'s high (i.e. one) and low (zero) levels independent of process, temperature, and supply variations. A traditional way to track such environmental variation is by using a replica of the circuit whose behavior is to be matched in the generator. However, in this case a single replica will not work, because the required output is the average of the one and zero levels; it is extremely difficult to generate a bit line sense current midway between the two levels, due to the grossly different effects of supply noise on bit lines reading one versus those reading zero. A superior solution is to use two replicas that each mimic reading one of the values, and average their outputs. Fortunately, the averaging is simply accomplished, as shown in Figure 4-7, by

summing the replica currents across parallel sense resistors. The resulting **SenseRef** has the desired voltage behavior, and has low area and power overhead.

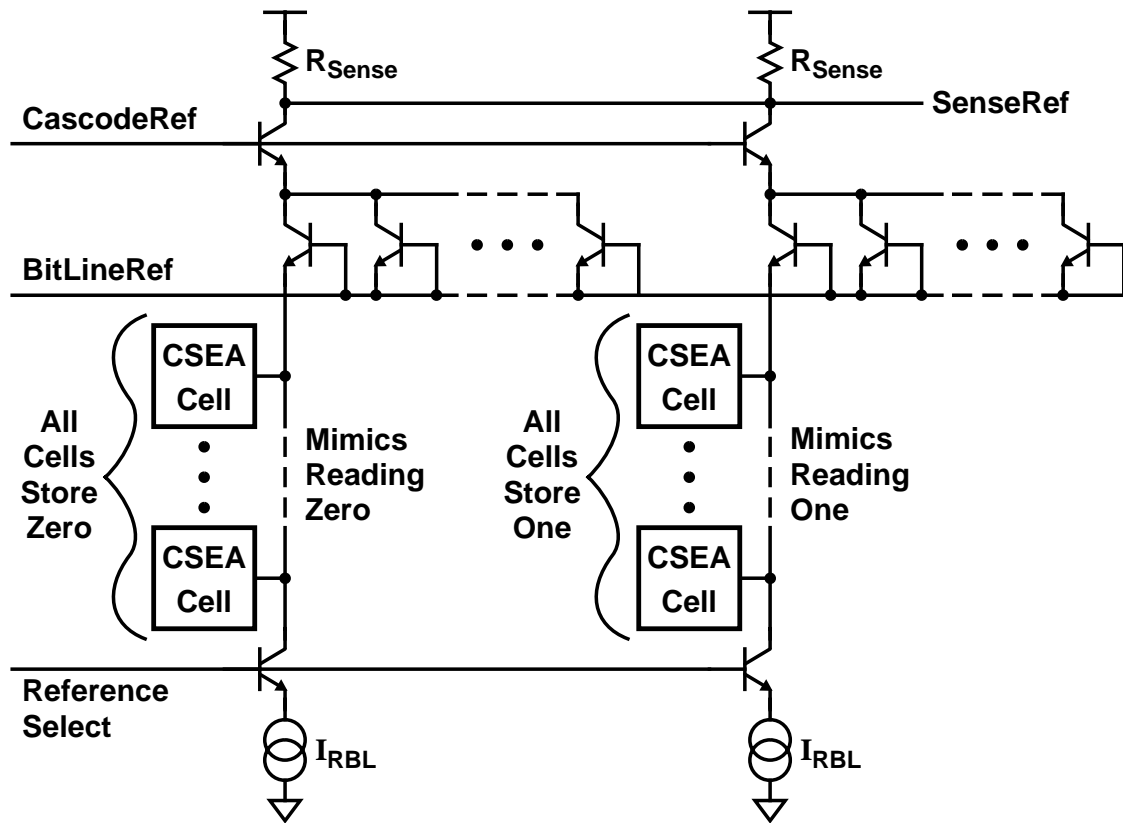


Figure 4-7 Sense Amplifier Reference Circuit

The replica circuits generate the average of reading one and zero for the following reasons. Currents that are the same between the two cases generate the same drop on the reference as on the actual sense resistor, while those that differ (like the bit line current when reading zero) show up as half their normal effect. This circuit helps cancel cascode noise effects, since the reference circuit's cascode networks behave like the read data's network.

Since these reference sense networks should run the full width of the die for accurate tracking, the replica bit lines may be readily reproduced on a per bank basis, with only the selected bank pulling I_{RBL} from its replicas. In this way the reference may also compensate for local supply and $V_{RWL(High)}$ variations. The effects of unselected bit lines on the replica network are mimicked by distributing dummy sense devices along the shared cascode nodes that have their emitters tied to **BitLineRef**. The net result is to produce a well-centered reference that may be simply compared to the associated outputs from the data sense networks using a simple differential pair. The resulting sense data output has noise

margins similar to differential sense schemes while maintaining the memory density advantages of a single read bit line per CSEA cell, since the area penalty of a pair of replica bit lines per bank is only 1% for 256-cell word lines. The power penalty is also small, since it is just the power required to sense two additional bit lines.

4.3.2 Two-level Cascode Network

The simple cascode sense amplifier performs very well with a few tens of bit lines per sense amplifier; for large memories with narrow access widths, substantially more column multiplexing is needed. For instance, a 256-kb memory with 64 cells per bit line has 4096 bit lines, so if the memory has an access (word) width of four bits then each sense path requires a 1024-input multiplexer. As the number of bit lines sharing a sense amplifier increases, the delay at the shared collector node increases as well; not only does the number of collectors (and hence the parasitic capacitance) increase but also parasitic resistance in the wire connecting the collectors increases the voltage swing on the node. Substantial resistance of the connecting wire adds distributed RC delay to the cascode sensing time. For instance, a 256-input sense amplifier whose connecting wire runs the length of a die has about 0.5 ns of RC delay.

A second level of cascoding may be added to reduce this delay. As depicted in Figure 4-8, the bit line sense currents sum in a tree fashion, first locally through one cascode device and then globally through a second. This arrangement greatly reduces the capacitance on the shared global sense wire, which has substantial series resistance (approximately 200Ω for a 256-kb design), while reducing both the capacitance and the resistance of the local sense wires. Hence the overall sensing delay is substantially reduced both because of the reduction in the distributed RC delay and because the total capacitance to charge is reduced by isolating most of the unselected bit line sense devices behind the first-level cascodes.

The weak current source (I_{Leak}) in the figure prevents first-level cascode devices attached to only unselected bit lines from turning off and thereby increasing the voltage swing required to reselect them. As long as the sum of all of these current sources is small compared with the maximum sensed current (approximately I_{RBL}), the required swing across the sense resistor is not substantially increased. These sources and the rest of the two-level cascode network must be implemented in both the data sense paths and the sense reference replica paths in order to guarantee good reference matching. The two-level cascode sense

operate in “soft” saturation (i.e. with their base-collector junctions slightly forward biased), increasing the available swing for the sense resistor. This latter solution requires careful worst-case design to limit the maximum base-collector biases to prevent access time degradation from charge storage in this junction and latch-up from excess current injected into the substrate.

Design of the cascode references must also consider electronic supply noise. With the high current gains provided by cascode sensing, a downward bump in V_{EE} , coupled onto the emitters of the cascodes, could overwhelm the current being sensed. With two-level cascode sensing, the major source of noise currents are the first-level cascodes that have only unselected bit lines, since there are many more unselected cascodes and thus more potential noise current sources. Reducing the percentage coupling to V_{EE} of the sensitive nodes is clearly desirable, but only the wire capacitances (which may be routed over V_{CC} -connected material rather than the V_{EE} -connected substrate) may be coupled to V_{CC} without penalty; this is sufficient for the second-level cascode device, whose emitter capacitance is largely wire. Explicit V_{CC} capacitance may be added to the emitter nodes of the first-level cascodes, but is undesirable because it slows the sensing speed. Simulations indicate that making the first-level cascode’s base (i.e. **Clamp1**) coarsely track the voltage response of an “unselected” first-level cascode’s emitter (via a replica network) greatly improves the noise response.

If **Clamp1** exactly tracked the emitter response of unselected first-level cascode transistors, then their V_{BE} would not change so they would pull no noise current from the second-level cascode device. The reference generator of Figure 4-9 makes **Clamp1** nearly match the behavior of unselected cascode emitters. The circuit employs a replica first-level cascode circuit, with diode-connected BJTs in place of the cascode stack. Although the current through the pull-up resistor changes as the replica emitter node, **CascodeMatch**, responds to supply noise, the current difference is small enough that the response is not greatly altered. Because I_{Leak} is small, it is poorly suited for directly driving the generator output, so emitter follower **Q1** buffers the replica emitter value, which is then level-shifted up to drive the output. Since **Clamp1** is generated by both V_{BE} and IR drops, it is simple to make **Clamp1** track level and swing variations with temperature. This reference generator keeps the two-level cascode sense amplifier largely insensitive to supply noise.

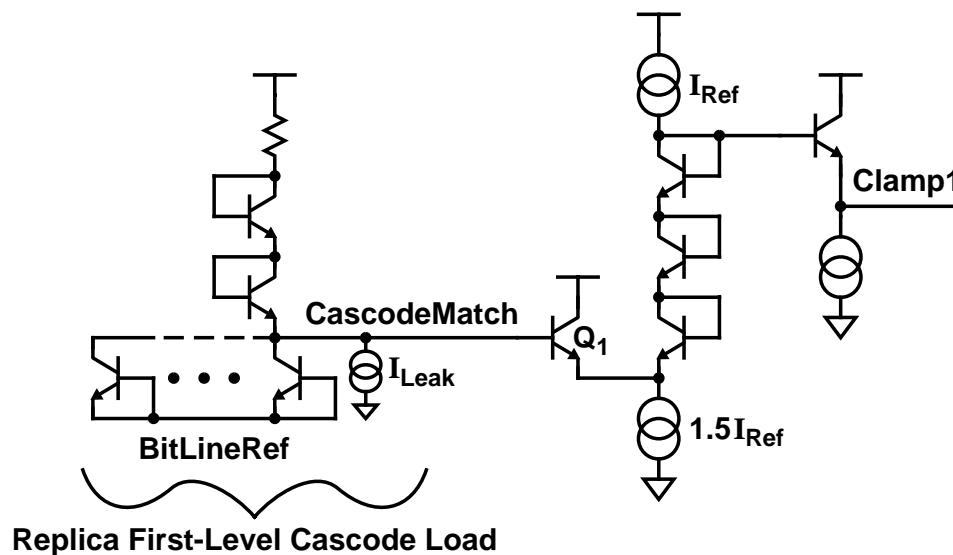


Figure 4-9 Clamp1 Reference Generator

4.3.4 Results

In order to assess the performance offered by the techniques described thus far this chapter, a circuit model for the sense path of a $64\text{K} \times 4$ CSEA memory is simulated to determine its access time under transient supply variation. The stimulus is a diode decoder with switched PMOS load, which drives a Darlington word line driver and delivers a 550-mV read word line swing, as determined in Section 4.2.3. In order to simulate the effects of random supply noise, a $\pm 300\text{-mV/ns}$ V_{EE} voltage pulse is moved in time relative to the stimulus to determine the position in which the noise most delays the access.

Figure 4-10 shows the worst-case access, where a -300-mV/ns V_{EE} noise pulse start 0.1 ns before the word lines cross. The figure depicts a transition from reading a cell storing zero to a cell storing one. From the figure, the effects of the noise pulse are clearly evident in the sensed data value (**SenseOut**) and the sense amplifier reference (**SenseRef**). The access penalty due to the noise source is only 0.25 ns, which is 18% of the total delay from the word line crossing **BitLineRef** to the sense amplifier outputs resolving. With such performance, it is clear one may construct CSEA SRAMs that retain their speed advantages in the face of supply noise.

A principal component of the sense delay for this bit line sense method is the time required to charge and discharge the bit lines. Switching from reading zero to reading one on an active bit line has the longest delay because the cell follower does not turn on until the read word line rises from $V_{RWL(Low)}$ to $V_{BitLineRef}$. The actual delay is lengthened by

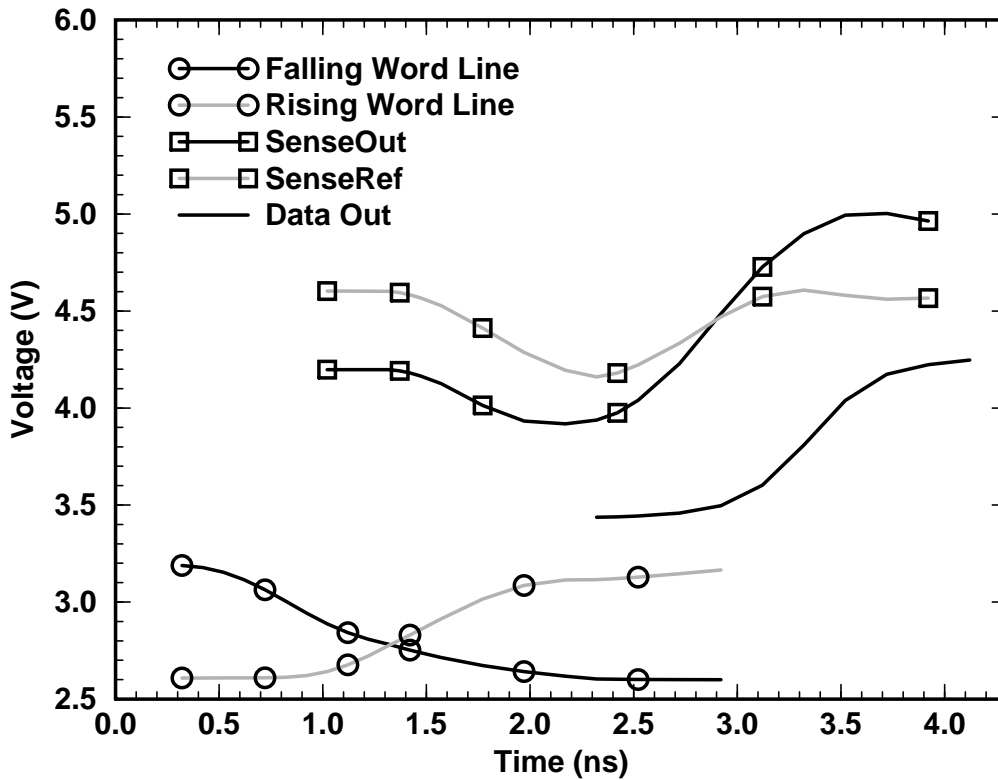


Figure 4-10 Sense Path Performance with Supply Noise

the RC time constant that results from the resistance of P1 and the effective base capacitance of Q1. This path is slower than the one-zero transition by approximately 0.3ns. The next section introduces a new sensing method that reduces this delay by beginning each access with the word line level equal to the bit line reference, which minimizes the bit line voltage change required to resolve the access and thus improves the delay.

4.4 Pulsed Sensing

Chapter 3 describes the use of pulsed circuit techniques to reduce the delay and power dissipation of low-swing decoders. This section applies the pulsed current sources and switched PMOS loads of Chapter 3 to the sense path of a CSEA memory, thereby delivering similar performance gains. As in the decoders, the ability to begin each access in a known state (and thus tailor the selection and reset waveforms on each node) provides the basis for delay reduction. In particular, by resetting the bit line to a lower voltage and then pulsing both the word line and the bit line reference, the sensed current resolves more quickly than in the sensing method of Section 4.3.

Pulsed techniques also save power by only activating current sources when a signal could transition. Such savings are especially important for wide access width memories, which read more bits at once and therefore use more sensing power. While their power dissipation may be higher than narrow width SRAMs, wide-word memories are typically faster because they require less column multiplexing. Because key circuit techniques of the section require per word overhead, the control complexity and power, and the memory density, of such circuits are minimized for wide-word CSEA memories. This section opens with a discussion of the basic pulsed bit line circuits, continues with peripheral and reference circuitry that support the bit lines, and closes with simulation results that quantify the performance advantage of pulsed CSEA sensing.

4.4.1 Theory of Operation

With pulsed signalling the differential pair formed by Q_1 and the sense device can be reset to levels that minimize the sensing delay by reducing the voltage change both on the bit line and on the internal cell node that is required to switch the bit line current. The simplified differential pair of Figure 4-11, switches the fastest if the input is reset to the reference potential, because I_{RBL} is steered to one side or the other as soon as the input begins to transition. The CSEA sense situation is more complicated, due to the extra $(N - 1)$ unselected cell followers on the bit line. If all the word lines are reset to $V_{BitLineRef}$ the rising selected word line will rapidly steer the bit line current away from the sense device if the selected cell stores one. However, when the selected cell stores zero, the unselected cells that store one become important. In order to let the sense device steer the bit line current, the unselected word lines must therefore fall from $V_{BitLineRef}$.

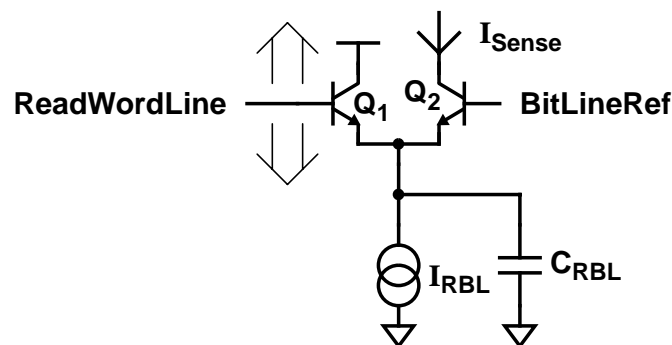


Figure 4-11 Oversimplified Bit Line Sense Model

While this arrangement delivers very fast access, it is completely impractical because it forces all of the read word lines in a bank to transition, which requires too much power. If the access begins with all word lines and $BitLineRef$ reset to $V_{RWL(Low)}$, and the selected

4.4.1 Theory of Operation

word line rises to $V_{RWL(High)}$ while the reference rises to $V_{BitLineRef}$, an equivalent arrangement results. At reset, the “differential pair” is at its trip point, and the difference between the currents quickly resolves as the inputs transition. Figure 4-12 compares idealized switching waveforms for the sense method of Section 4.2 to the new method proposed here. The figure shows that the new pulsed method develops differences between the base voltages as soon as the signals begin to transition, while the original method does not resolve until the word line crosses $V_{BitLineRef}$. All the signals complete their transitions in equivalent places, so both methods deliver equivalent noise margins.

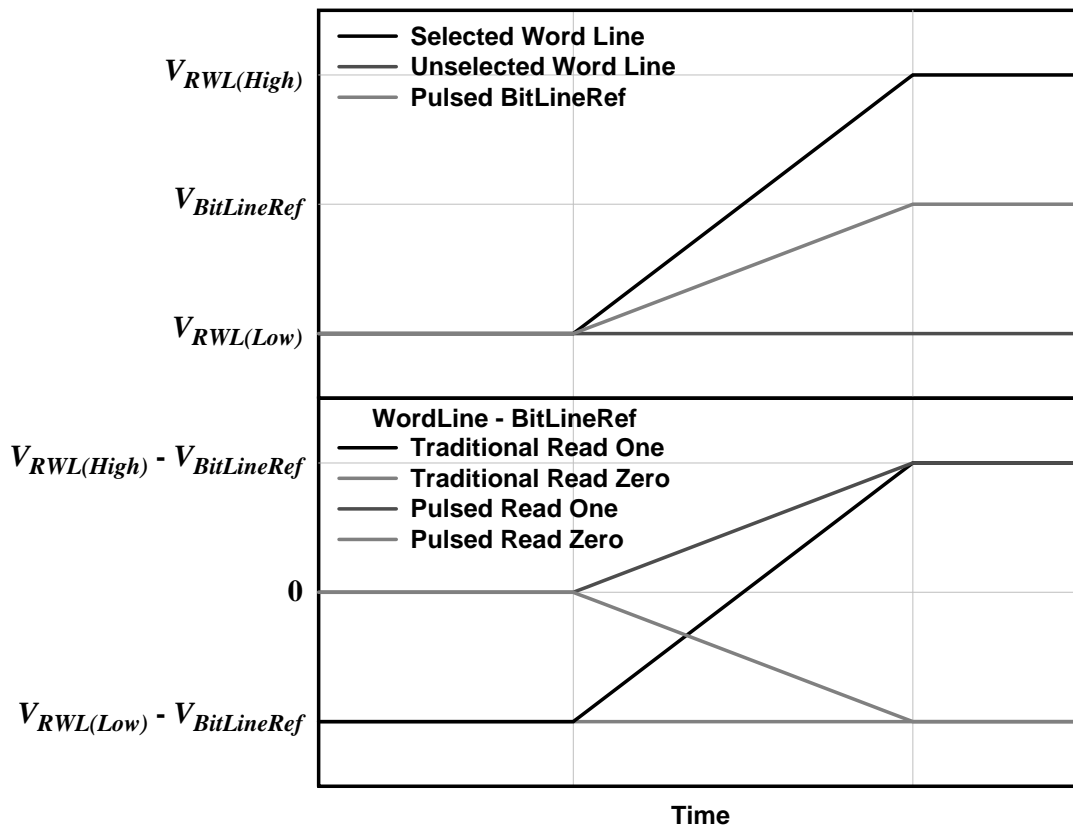


Figure 4-12 Comparison of Switching Waveforms

The preceding discussion ignores the reset level of the bit line and the granularity of the bit line reference. The bit line reset level is determined by speed versus power and noise margin considerations. The access time is improved with lower reset levels, since both the bit line reference device and the cell follower turn on earlier as the reset level decreases. Ideally, the bit line should reset to $V_{RWL(Low)} - V_{BE}$. However, low reset levels imply higher power, because both the selected and unselected bit lines in a bank rise to $V_{RWL(High)} - V_{BE}$ if their cells on the selected word line store one, and discharging these bit lines to the reset level can require more power than is saved by using pulsed signalling.

Furthermore, low reset levels increase the unselected bit line sensitivity to supply noise, since drops in supply levels could cause the bit lines to fall enough to turn on their sense device. Another problem with low reset levels involves variation in the word line rise times due to differences in loading between word lines connected to cells that store mostly one or zero; cells that store one impose a higher load due to the base charge required by the cell follower to charge its bit line. The problem with this variation is the difficulty in building a bit line reference driver that tracks the variation.

With pulsed signalling, a hybrid solution is possible that provides fast access at reasonable power. By resetting the bit lines near the active zero level (i.e. $V_{BitLineRef} - V_{BE}$), the swing on unselected bit lines that store one and the word line loading variation are reduced to manageable levels. Furthermore, the access delay may be reduced by activating a pulsed bit line current source and releasing the reset circuitry at the same time the word line and bit line reference are rising. Because the internal cell voltage lags the word line level due to the current required to charge the cell follower, there is enough time to partially discharge the bit line before the cell follower turns on. In this way selected bit lines effectively have a lower reset level, which improves their speed.

With a reset level at approximately the active zero level, unselected bit lines in the selected bank can couple noise into the sense network if their bit line reference rises enough to turn on the sense device. For this reason, the bit line reference must be driven on a per-word basis, so only selected bit lines ever have a rising bit line reference.

4.4.2 Pulsed Bit Line Circuitry

A circuit diagram of such a pulsed bit line appears as Figure 4-13. The bit line circuitry is somewhat similar to the static case, with a NMOS reset device (N1) replacing the bit line pull up device and with a pulsed current source replacing the steered bit line current. In the reset state, all of the read word lines, the bit line reference, and the pulsed current source control (BitLineCS) are low, while the bit line reset, BitLineReset, is high so N1 sets the bit line to its reset level BitLineResetRef.

As an access begins, N1 must turn off so that it does not interfere with the access. While the row decoder raises the selected word line, the column (i.e. word) decoder in each bank activates the pulsed current sources and the bit line reference for the selected word. The selected bit lines therefore begin to drop until they are met by either the rising word line (if their selected cells store one) or BitLineRef; in either case the bit lines begin rising, and the capacitance of the bit lines provides additional loading, and hence additional sense

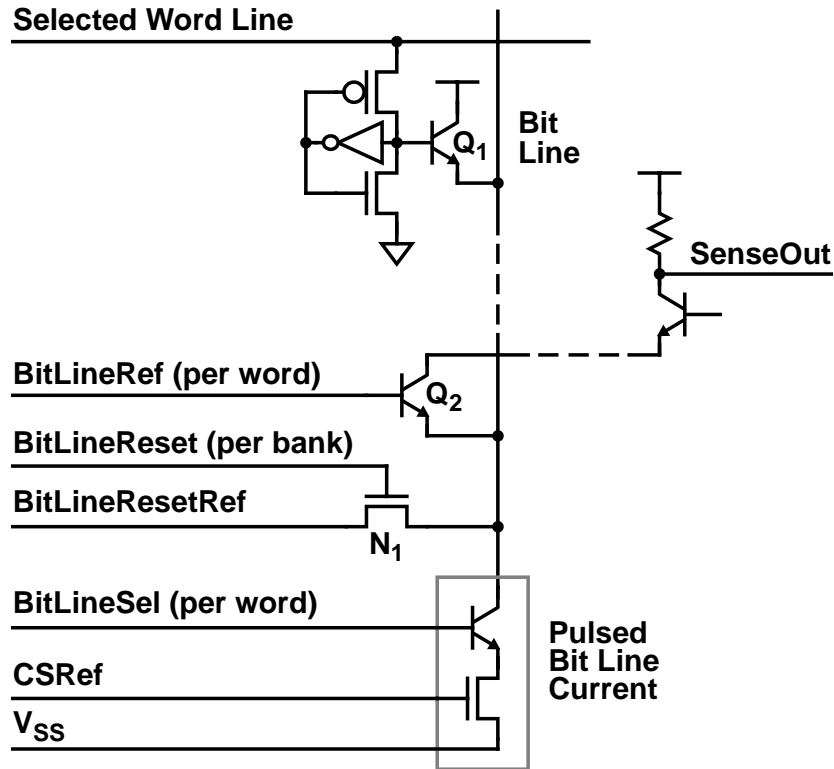


Figure 4-13 A Pulsed CSEA Bit Line

current that is steered through Q1 or Q2. While the bit lines rise this excess current helps the sense network resolve its answer more quickly, and allows the size of the pulsed current source to be reduced. Once the sensed current resolves, the sense amplifier must latch the result before the pulsed bit line current turns off, or else the data will be lost.

At the end of the access all of the control signals return to their reset levels, so BitLineReset turns N1 back on to reset the bit lines. The sense path thus prepares for its next access. Simulated waveforms for a single access appear as Figure 4-14. The waveforms include two bit lines from the selected word: one that stores zero and one that stores one.

The BitLineReset signal deserves special mention. Because the reset level of the bit line is about $V_{CC} - 3.5V_{BE}$, BitLineReset only needs to drop this low to turn off N1 during an access. This lets the BitLineReset driver be implemented from bipolar logic, since the low level does not saturate the current source. A swing of about $2.5V_{BE}$ is enough on N1, which only needs to turn on hard enough to reset the bit lines. As the figure shows, the BitLineReset driver overshoots its DC level, which reduces N1's resistance and thus speeds the bit line reset. A second BitLineReset issue involves the unselected bit lines of

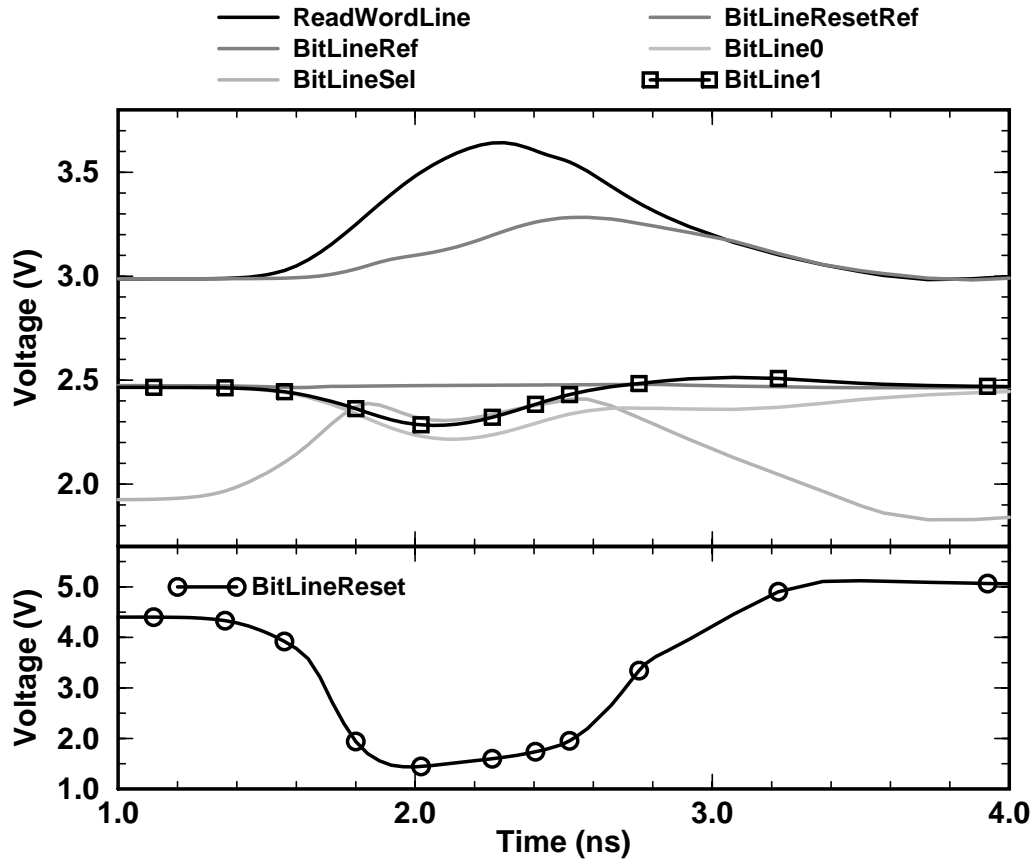


Figure 4-14 Simulated Pulsed Bit Line Waveforms

the selected bank. Since these bit lines will be pulled up by any selected memory cells that store one, the reset circuitry should not fight these transitions. For this reason, `BitLineReset` should be shared by all the words in a bank, so all bit lines in that bank are released when any word is accessed.

The cascode sense amplifier is nearly identical to the static sense amplifier of Section 4.3. In particular, a single-level cascode network is usually sufficient for wide word accesses, which require less column multiplexing. For instance, a memory with a 64-bit word requires sixteen times less column multiplexing than a 4-bit access, so the number of collectors on the cascode node of a wide memory is no more than the number of collectors on the (global) second-level cascode node of the narrow memory.

4.4.3 Peripheral and Reference Circuits

The performance advantages of pulsed sensing are obtained only if peripheral circuits generate well-timed signals at desired potentials. This subsection describes circuits to

generate the **BitLineRef**, **BitLineCS**, and **BitLineReset** signals, as well as the **BitLineResetRef** reference.

In order to achieve fast sensing with adequate noise margins, **BitLineRef** must track the characteristics of a typical word line, albeit at a lower swing. To accomplish this, one could build the reference driver using the same circuitry as a word line, with a resistive voltage divider between the dummy word line level and the low word line level to accomplish the amplitude reduction. Unfortunately, the resistive divider alters the characteristics of the resulting **BitLineRef**: if the resistors are large then there is delay in the rising waveform that delays the access, and if the resistance is reduced then the current through the resistors alters the shape of the dummy word line swing, which ruins its tracking.

Alternatively, the **BitLineRef** driver of Figure 4-15 utilizes a dummy word line (with all cells storing zero) and the same basic *NOR* gate and discharge circuitry as in the word line decoder and driver, with one exception: since not all of the inputs will be needed to select the desired word from the row, the bank current source selection signal **BankSelQ** may be used to dynamically pull a fraction of the decoder current from the gate load even when the gate is selected, thus constraining the high level of the **BitLineRef** signal. Because the switched PMOS load is nonlinear, the output swing ratio of the **BitLineRef** driver to a word line driver is not simply the current ratio. Furthermore, the low current density in unselected (low) word line drivers requires that the gate output rise before the Darlington devices turn on enough to charge their loads; this rise is subtracted from the output swings of both a word line driver and the **BitLineRef** driver. Therefore, detailed circuit simulations must be performed to select the proper fraction of the decoder current to switch in when the **BitLineRef** driver is active; for the 0.8- μm technology describe in this thesis, 40% gives both fast access and good noise margin over process and temperature variations. Since this scheme requires one dummy word line (for loading) for each word in a row, the area penalty is smallest for wide word widths.

The **BitLineCS** driver may be constructed from another pulsed *NOR* gate to ensure its time correlation with the other active signals. As shown in Figure 4-16, the output uses a simple *L3* driver from Section 3.5. The extra output is used to generate a wired-or signal that controls per bank pulsed current sources, such as that on the **BitLineReset** driver and on the sense amplifier latch.

The **BitLineReset** driver is very simple; since it operates on a per bank basis and is high in the reset state all that is required is a simple resistive load and a **BankSelQ**-pulsed

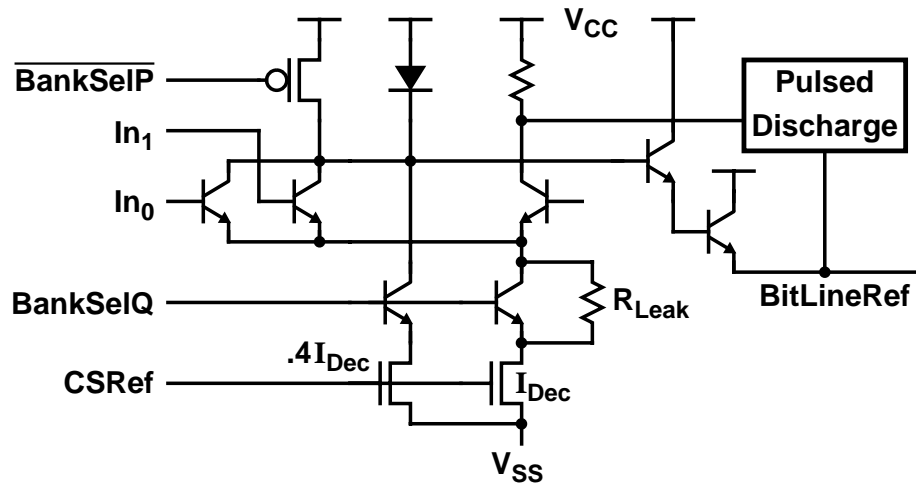


Figure 4-15 Pulsed Bit Line Reference

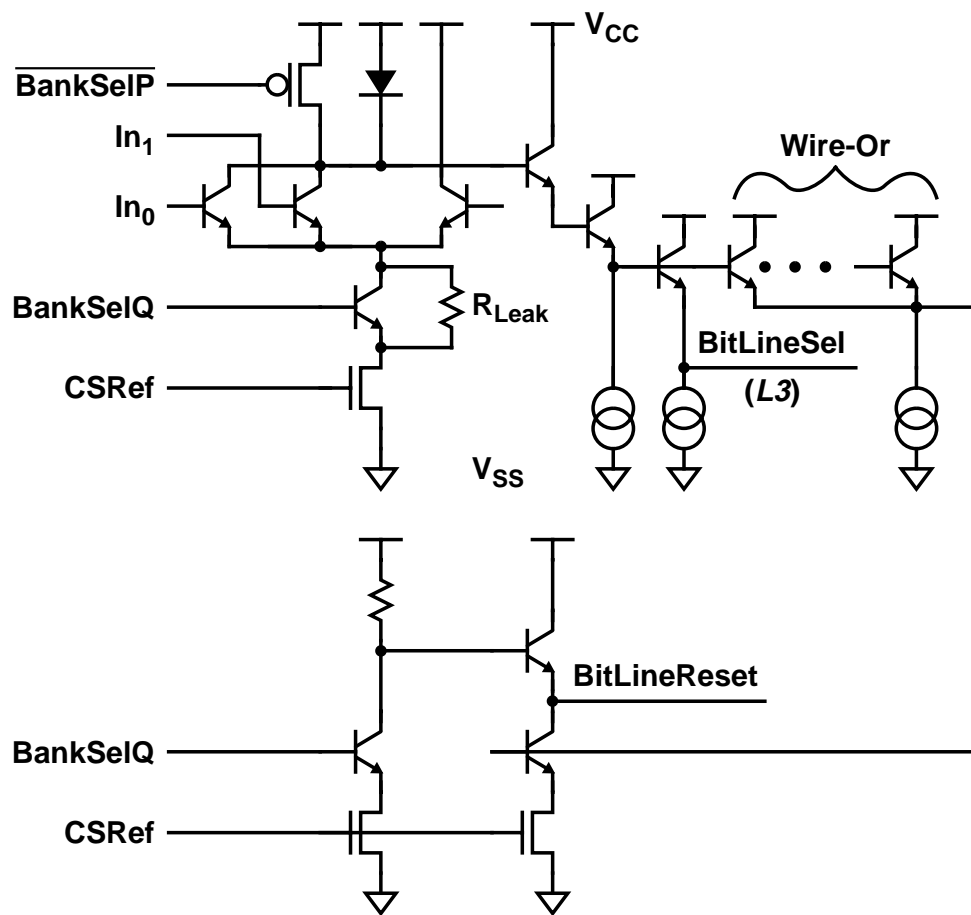


Figure 4-16 Pulsed Bit Line Control Circuits

current source, with a pulsed emitter follower output. The output current is controlled by the *OR* of the **BitLineCS** signals for the bank so that the **BitLineReset** signal has similar timing. With a $2.5\text{-}V_{BE}$ swing on the resistor the **BitLineReset** level is $V_{CC} - 3.5V_{BE}$, which is enough to turn off the reset devices. The delay associated with discharging **BitLineReset** is not critical because the current available from the reset devices is substantially smaller than the pulsed bit line current, so the delay does not increase much if **BitLineReset** is a little late.

The desired bit line reset value is defined relative to V_{CC} , since it involves signals generated from that supply, but with an on-chip V_{SS} generator the difference between the reset value and V_{SS} is well specified, so the reset references may be defined relative to whichever supply makes the design simpler. Because the predominate dynamic current required to reset the bit lines comes from discharging unselected bit lines where the selected cell stores one, **BitLineResetRef** must be able to supply large discharge currents and it is therefore convenient to give **BitLineResetRef** a diode-like characteristic; as Figure 4-17 shows, this is readily accomplished using a V_{BE} multiplier circuit to build a programmable diode of the desire value.

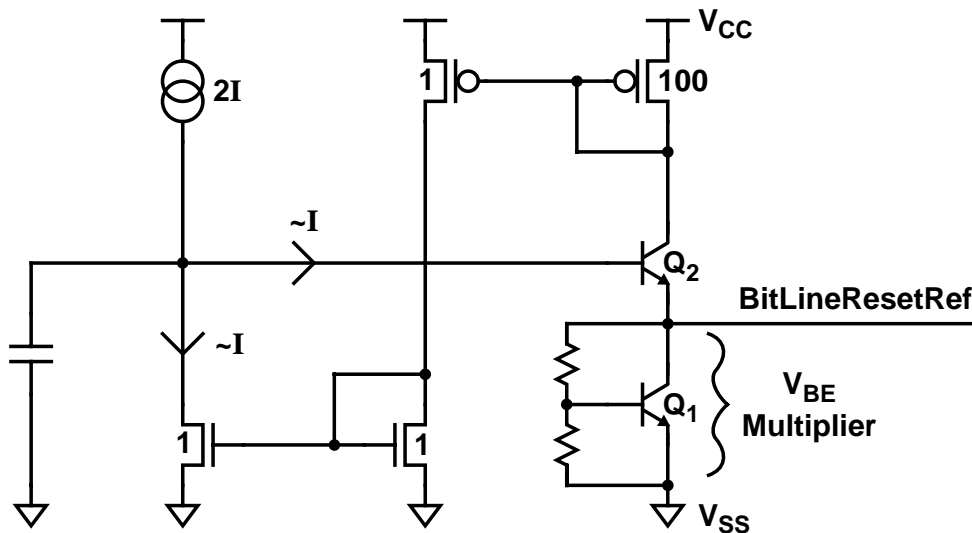


Figure 4-17 Pulsed Bit Line Reset Reference

Q_2 supplies leakage current to prevent inactive bit lines from drooping and the current required to keep the V_{BE} multiplier looking like a diode; it does not need much active current because the operation of the bit line prevents it from ending an access much below **BitLineResetRef**. Since its primary output is a current whose value should be controlled to limit the inactive bit line currents, Q_2 's base is generated using the simple current

mirror-based feedback circuit shown in the figure. To minimize the power dissipation, the reference divides the follower current by 100; the static current source supplies twice this current to compensate for the base current of the follower. The large capacitance slows down the voltage response of the base to current spikes, since the output voltage should be based on long-term average currents. Note that the resulting base potential is determined entirely by the leakage current required by the bit lines and the static current in Q1, so BitLineResetRef is truly determined by the V_{BE} multiplier.

The sense amplifier reference may be constructed as in Section 4.3.1, with two reference columns (one mimicking reading one and the other zero) per word. Simulations indicate that the reference behavior more closely tracks the worst-case bit lines when the data values on the reference lines are interleaved (i.e. each reference line stores half ones and half zeroes, but the two lines always store opposite values on any give word line).

4.4.4 Results

A simulation model of one bank in such a pulsed bit line CSEA SRAM was constructed to estimate its performance. With 64-bit words, 256 cells per word line, and 64 cells per bit line (i.e. the same bank parameters as in the previous section) plus four dummy word lines per bank for the pulse bit line reference circuits, the sensed bit line currents cross their reference values about 1.0ns after the decoder inputs transition. The slowest read access is reading zero from a bit line that stores ones in all other cells (due to increased base-emitter capacitance) on a word line where all other cells store one (since ones require charging the cell follower's base-emitter junction). This access is depicted in Figure 4-14. The current through the bit line sense device crosses that of the replica bit line's reference only 0.35ns after the selected word line reaches midway, which is much less than the 0.85-ns delay for the original static bit line sensing technique.

The pulsed sense path is more robust than the static path with respect to supply noise. While the static bit line current is reduced by roughly half, the pulsed bit line reference and word line signals deliver dynamic sensed currents during the signal transitions that nearly equal the static bit line current of Section 4.3. Since the currents are nearly equal when the signals are most vulnerable to supply noise, the delay caused by a certain amount of supply noise is similar. However, the on-chip V_{SS} generator, which makes effective use of the decoupling capacitance of the memory arrays, limits the maximum V_{SS} edge rates to roughly one quarter of the 300mV/ns rates simulated in the previous section. Thus, the pulsed path has nearly the same sensitivity to supply noise, but less noise to deal with.

Pulsed decoding and sensing are able to substantially reduce the access time of a CSEA SRAM. However, the performance of a CSEA memory can be limited by the delay in its write path. The next section focuses on ensuring that memory writes do not limit the achievable cycle time.

4.5 CSEA Writing Techniques

The read port of the CSEA memory cell permits the construction of very fast SRAMs with only low-swing signals in the read access path. However, the write port requires large swings on its write word line and write bit line in order to successfully overpower the CMOS latch that forms the storage element. Thus, some sort of level conversion is required. A low-power word line level converter suitable for this purpose is discussed in Section 3.6. Similar converters may be readily constructed to provide large-swing bit line signals as well.

The principal other challenge is to rapidly write the CSEA cell through its single access device while not writing unselected cells on the selected write word line. The next section discusses this issue in more detail, while Section 4.5.2 proposes an effective way to deal with the challenge by avoiding partial write selection altogether.

4.5.1 Single-ended Versus Differential Cell Writing Issues

The traditional 6T CMOS memory cell of Section 2.2.1 is written through two NMOS access devices, each of which is connected to one of the differential bit lines. In order to write the cell, the access transistor on the side of the cell that needs to drop overpowers the PMOS pull-up device, discharging the internal cell node until reaching the switching point of the other inverter in the cell. Once the switching point is reached, the positive feedback of the cell storage latch completes the change in state. To accomplish this, the bit line on the discharging side of the cell is driven low to provide the discharge current, while the other bit line is held at a relatively high level to minimize any effects from this opposing bit line. Because the write access width is typically smaller than the number of cells on each word line, there are usually cells on the selected word line that should not be written. Avoiding such *write disturbance* for the 6T cell simply requires keeping both cell bit lines at a high enough value that they cannot supply enough current to flip the cell; because these bit lines are used for both writing and reading the cell, the starting value for reading is chosen to be this “safe” level so that inactive bit lines do not need to transition between read and write accesses.

The CSEA memory cell (see Figure 4-1) has only one write access device N3 and thus its write bit line typically must perform three functions:

- Writing one — Since N3 is connected to the complemented side of the cell, a cell value of one implies a low voltage at the access device so to write one the bit line must be low enough for the access device to overpower the weaker PMOS pull-up transistor P2.
- Writing zero — In a similar way, writing zero requires that the access device overpower the NMOS pull-down device N2, so the bit line must be high.
- Avoiding write disturbance — For unselected cells on the selected word line, the bit line must be high enough not to overpower P2, and low enough not to overpower N2.

The width of N3 should be larger than N2 so that there is adequate noise margin in writing zero, especially since NMOS transistors pull down better than up; this makes it much easier to write one, thus raising the bit line voltages at which ones may be written. Unfortunately, this reduces the voltage range where writes will not occur, increasing concerns about write disturbance. By reducing the switching point of the N1-P1 inverter, the width of N3 may be reduced since writing zero becomes simpler.

In his thesis, Yang [49] discusses these issues in great detail and describes a method to size all of the cell transistors to provide both robust writes and minimal disturbance to unselected cells. However, the resulting transistor sizes are mostly non-minimum, and therefore the CSEA cell area increases. Furthermore, while the resulting static noise margins are large enough to be safe, they are not so large that writes occur very quickly. In other words, N3 is not large enough that its current easily overpowers that of N2, so writing zero takes much longer than on a 6T cell. Finally, driving three-level write bit lines is difficult, so the bit line control circuits tend to require more delay than those for differential writes.

An alternative would be to add an additional NMOS device to the CSEA cell, which would allow differential writing. This solution, however, increases cell area, primarily by requiring an extra write bit line that must contact each cell. Because memory density is a critical component of overall SRAM performance, there is room only for a single write bit line in a high-performance CSEA design.

Since each such gate drives multiple cells (i.e. the access width), the area penalty of the local word line drivers is amortized across the access width; for a 4-bit wide CSEA design the cell array area increased only 16% to accommodate the drivers (see Section 5.1). The area penalty drops substantially for larger widths, since the area penalty for splitting the memory array is much larger than the penalty for increased driver width as the word width grows. The addition of the global write word line does not increase the cell area, since it replaces the metal wire that would run over the higher resistivity polysilicon word line to improve the RC word line delay in a conventional design.

The overall write performance of such a design is quite good. With local word line qualification, write disturbance ceases to be an issue, so the cell may use minimum-sized devices for N1, N2, and P2; P1 is typically larger to reduce the effective base resistance of Q1 and thereby reduce the base-charging delay. N3 should be large enough to easily overpower N2, and thus quickly flip the cell. Thus, word line qualification permits the use of dense CSEA cells that write quickly, at very modest area penalty and without the use of fancy three-level bit line drivers.

Furthermore, the use of the low-power level converter further improves write performance. By adopting similar level converters for the write word line, column select, and write bit line paths, all the signals that accomplish a write have similar delays. With nearly equal delays and active times, the write path can accomplish *wave pipelined* writes, where the current write need not finish before the next read or write cycle may begin. This is possible because of the independent read and write ports of the CSEA memory cell. With this capability, the delay requirements of the write path may be somewhat relaxed, since the overall SRAM may then have a cycle time that is shorter than the actual write path delay. The word line level converter and the local word line qualification circuit thus prevent write delays from limiting the cycle time of CSEA memories.

4.6 Summary

Sensitivity of the single-ended read bit line of the CSEA memory cell to electronic supply noise has been considered a significant barrier to the construction of robust CSEA SRAMs. This chapter shows that electronic supply noise need not limit the performance of such memories. It describes techniques that can robustly sense and amplify the data stored within a CSEA cell with very low delay. Because of the high read current of a CSEA cell, the bit lines are fairly tolerant of capacitive coupling from the power supplies. The

4.6 Summary

two-level cascode sense amplifier and replica bit line circuits of Section 4.3 provide quick access for large CSEA memories while maintaining good noise immunity. Section 4.4 describes the application of pulsed circuit techniques to the sense path, and the performance gains that may be obtained.

This chapter also discusses issues associated with the write path of CSEA memories. The problems with single-ended writing, namely fancy three-level write bit lines, skewed cell device ratios that decrease memory density, and slow write times, which all arise from avoiding write disturbance, are described and then eliminated. Using a simple word line qualification gate borrowed from divided word line memories, only the cells to be written are connected to an active write word line, thus removing concerns about disturbing unselected cells on the selected word line.

In combination with the decoding techniques of Chapter 3, the sense and write techniques of this chapter enable the construction of very high performance CSEA memories. The next chapter explains the results of applying these circuit techniques to high-density, high-speed, and reasonable power CSEA SRAMs.

Chapter 5

Results

This thesis has presented a number of new circuit ideas to improve the performance of various SRAM building blocks. This chapter describes the results of combining these building blocks to construct CSEA-based SRAM subsystems. The three designs of this chapter illustrate the system-level performance advantages of the techniques of this thesis. The designs differ from one another in two important ways. First, the described SRAMs each have a different target. The first one is a research prototype, built to demonstrate the feasibility of some core circuits and verify a memory cell design. The second design is a standard asynchronous SRAM with substantially more design effort invested in process, temperature, and supply variation considerations and is a more appropriate match for the technology in terms of die size, memory capacity, access time, and power dissipation. The third design is a synchronous SRAM subsystem that utilizes the new pulsed ECL circuit ideas of Chapters 3 and 4 to provide greatly-improved access times. The other major difference between the designs is the level of design experience. The designs are presented in chronological order, so the successive designs show an increasing level of design maturity.

All of the designs utilize the 0.8- μm BiCMOS technology discussed in Chapter 1 and used in examples throughout this thesis. Furthermore, all designs share the same basic cell layout and array sizing, which makes comparisons among the designs simpler. The CSEA cell occupies $154\mu\text{m}^2$, although Section 5.1.1 describes how the same cell could be built in only $125\mu\text{m}^2$. The banks each contain 64 rows and 256 columns of memory cells, although some designs add extra cells to generate the sense amplifier reference. The input and output buffers, as well as the row decoder, word line driver, column decoder, sense circuitry, and write circuitry vary between designs.

This chapter begins with a discussion of an experimental $16\text{K}\times 4$ SRAM that was fabricated in 1989. The next section discusses improvements to the basic design required to produce a higher performance and more robust $64\text{K}\times 4$ SRAM. Section 5.3 describes a

prototype on-chip synchronous SRAM subsystem that delivers significantly faster access and cycle times at nearly identical power dissipation.

5.1 An Experimental 64K CSEA SRAM

Some of the early circuit ideas from this thesis were successfully integrated in a 64-Kb CSEA SRAM that was fabricated in 1989. The fabricated die has two significant layout errors that required post-fabrication modification, as described in Section 5.1.3. Furthermore, the limited available die area forced the design away from its performance target. With decoding circuits that deliver greater power savings as the number of banks increases, the power performance of a 64-Kb design with a relatively small number of banks (since the bank design was optimized for a 256-Kb SRAM) is worse than could be achieved. However, this SRAM does deliver impressive performance, and it provides both measured results and extracted design database information that are crucial for the design of the later SRAMs. This section begins with a description of the cell design, discusses the chip architecture, and shows the circuits used in the design. It next describes the test and measurement results, and closes with a description of what key knowledge was gained in the implementation.

5.1.1 Cell Design

The basic CSEA memory cell schematic, reprinted in Figure 5-1, provides the starting point for the cell design, which has two interrelated parts: device sizing and physical layout. The two parts are related by the restrictions that layout design rules place on the device sizes and by the effects of layout parasitics on the cell performance. For ease in generating design rule-correct layout, all physical layout of the chip was constrained to fit on a $0.4\text{-}\mu\text{m}$ grid, so device sizes were limited to multiples of $0.4\text{-}\mu\text{m}$.

The device sizing process began with all minimum devices to minimize total cell area; for MOSFETs the minimum gate W/L was $1.2\text{-}\mu\text{m}/0.8\text{-}\mu\text{m}$, while a minimum bipolar device had a $1.6\text{-}\mu\text{m}\times 0.8\text{-}\mu\text{m}$ emitter area. Device sizes were then increased for three different reasons:

- P1 grew to reduce its on resistance and thereby reduce the base charging delay for Q1, which is an important component of the sensing delay.
- N3 grew to make sure it was strong enough to overpower N2 and thus write zero into the cell. Since the SRAM uses local write qualification, write disturbance is

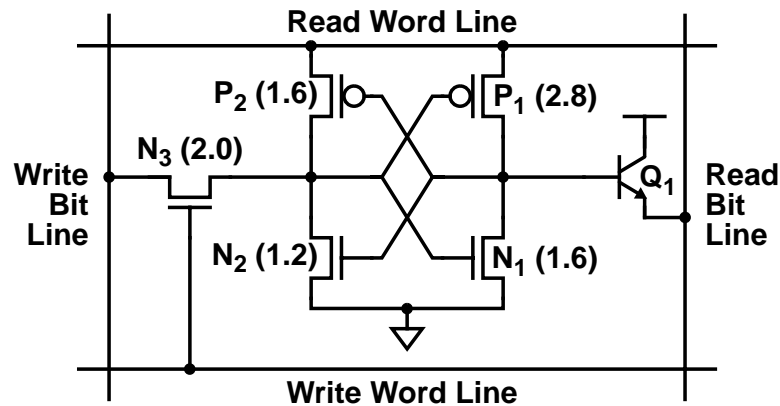


Figure 5-1 Fabricated CSEA Memory Cell

not an issue so there are no constraints other than cell area and bit line capacitance that limit the maximum W of $N3$.

- $N1$ and $P2$ grew to adjust the switching point of the $N1$ - $P1$ and $N2$ - $P2$ inverters to make it easier to write the cell; this requires less area than simply increasing $N3$ further due to the extreme aspect ratio of the cell layout.

Figure 5-1 shows the final device widths in microns.

The resulting cell layout is shown in Figure 5-2. A key feature of the fabrication technology that permits a small cell layout is the TiN “local interconnect”, which provides a contact between the gate polysilicon and the drain diffusion without requiring any contact to the metal layer. The cell area is further reduced by not including a collector contact in each cell, by merging the collector and n-well regions, and by merging the base region of $Q1$ with the source of $P1$, as is discussed in Section 4.1. The cell measures $154\mu\text{m}^2$, but this relatively large area is partly due to the design grid. The same device sizes may be integrated in only $125\mu\text{m}^2$ if the design grid is relaxed to $0.1\mu\text{m}$. This cell size compares quite favorably to the $117\text{-}\mu\text{m}^2$ 256-Kb 6T CMOS cell, built in the same technology, which is reported in [25], especially since the CSEA cell delivers twice the read current of that 6T design.

5.1.2 Organization

The memory is organized as 16K words by 4 bits; internally the SRAM is divided into four ($4\text{K}\times 4$) banks, each with 64 rows and 256 columns. The local write qualification gates and collector contacts occur every eight cells, since two qualification gates share a vertical track and drive opposite local write word lines; with such an arrangement no

5.1.2 Organization

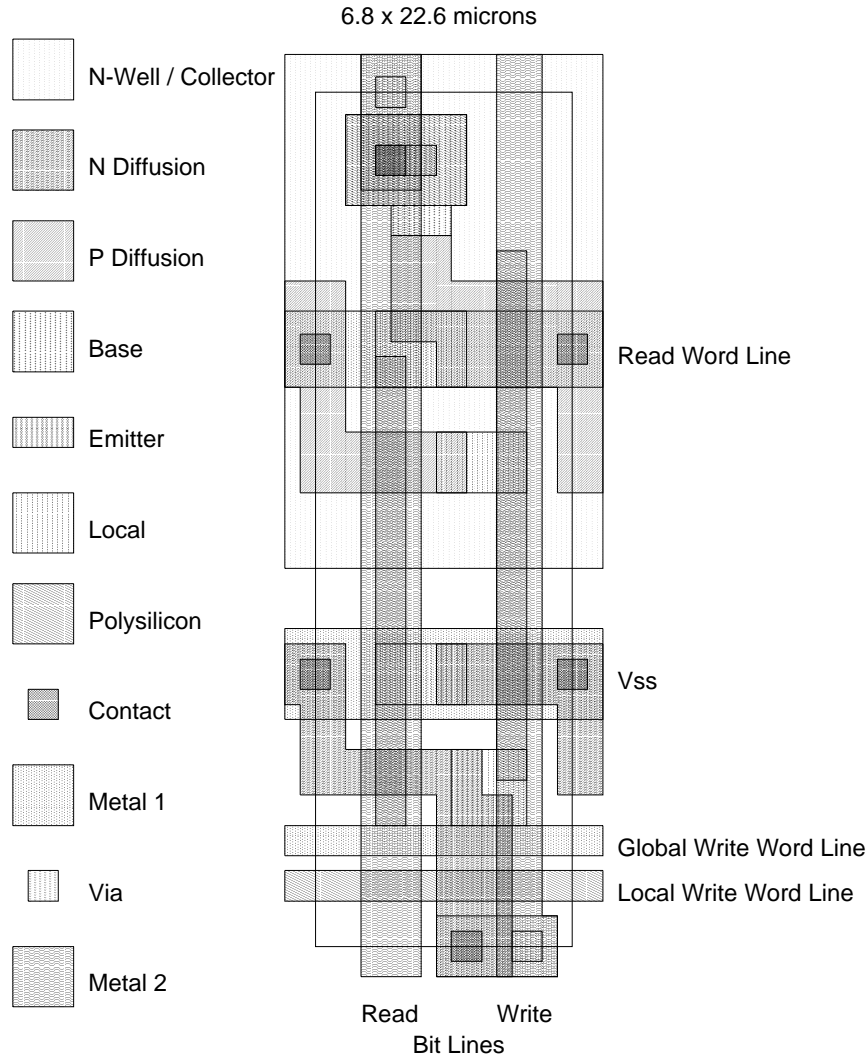


Figure 5-2 CSEA Cell Layout

bipolar transistor is more than four cells (about $30\mu\text{m}$) away from a collector contact, and with the buried layer under the collector and n-well regions the extra series collector resistance is less than 100Ω .

A block diagram of the chip appears as Figure 5-3. The row decoders and word line drivers are placed in the center of each memory bank to reduce the RC delay of the read word line. The chip contains 4 sets of row decoders, but only two sets of column decoders because vertically adjacent banks share the same decoders. While the independent row decoders ensure that only one read word line is selected at any time, the shared column decoders switch currents into four selected read bit lines both above and below the decoder. The bit line reference devices and two-level cascoded sense amplifiers (see Section 4.3) are on the opposite end of the bit line from the decoders, so there are parallel

sensing paths on the top and bottom of the chip, which are multiplexed at the output buffer. The address buffers and switched PMOS resistor selection drivers, as well as the on-chip reference generators, are near the center of the die to minimize the propagation delay of their signals to the decoders. Input write data and write enable signals enter the chip from the left side and are converted to CMOS levels, while the read data output buffers are at the right side; all data and address I/O occur using ECL 10K-style levels.

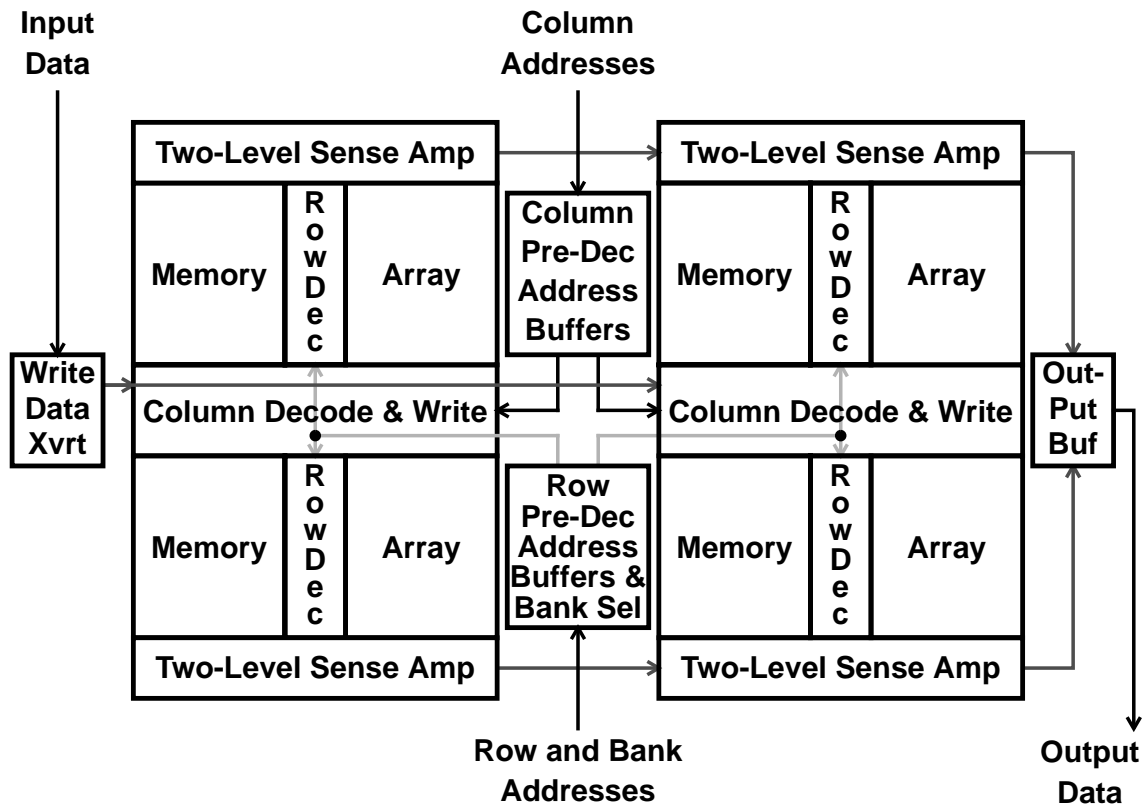


Figure 5-3 16Kx4 SRAM Organization

Both decoding paths utilize the same basic circuitry; pre-decoding address buffers drive diode decoders with switched PMOS load resistors. The pull-down current for both row and column decoders is switched between separate address line sets for the left and right sides; thus, the two banks of row decoders on each side share address lines. The read word line drivers are simple Darlington pairs with resistively-coupled shared static current discharge, while the write word line driver uses the read word line value to convert to CMOS swings and drive an active-low global write word line across the array to the local word line qualification gates. The bit line drivers steer shared currents into eight read bit lines, while releasing the reference devices that hold those bit lines high enough to prevent inactive bit lines from injecting current into the sense network. On writes the bit drivers also

send the converted input data onto the write bit lines while raising the column select input to the write qualification gates.

The *critical* (i.e. slowest) access path through the read circuitry begins with a transition of the most significant address bit, which selects between the left and right half of the memory. As shown in Figure 5-4, this address pin drives an ECL inverter that controls the discharge current for the switched resistor selection signal ($\overline{\text{BankSelP}}$). This path has the largest delay because no other path needs two current switching stages to get to the decoders. Furthermore, the critical path passes through the row decoders because the word lines have more delay than the bit lines. Another path from the same address input drives a pre-decoding address buffer to generate the BankSelQ signal; this path is faster because it requires only a single current switch delay.

5.1.3 Measured Results

A chip photomicrograph of the fabricated $16\text{K}\times 4$ memory appears as Figure 5-5; the figure is rotated 90° relative to Figure 5-3 to better fit the page. The die measures $6.0\times 4.4\text{mm}$, although the active die including all routing occupies less than $5.4\times 4.0\text{mm}$. Of this 21.6-mm^2 active area, 54% is covered by the memory cells and write qualification gates; the qualification gates add 16% to the array areas, including the area of the shared collector contacts that would be required even without the gates. The chip is packaged in a 48-pin ceramic DIP. While this is certainly not a high-speed package, it simplifies test board construction and provides access to internal reference signals for monitoring and overpowering.

The fabricated chip contains two design flaws that required both laser and focused ion beam repair. The first flaw, which results in the current source reference generator regulating at substantially higher current than desired is repaired by laser cutting a first metal wire that links two devices in the generator; once this link is cut, the desired voltage can be supplied from off-chip. The second flaw involves the selection signal for the output buffer multiplexers. The chip incorrectly selects for output the data from the top sense amplifiers when the selected word line is in a bottom array, and vice-versa. This error is repaired by cutting the differential selection signal and re-routing it using both the sputtering and deposition features of a focused-ion beam machine.

Due to problems with the write enable circuitry, the memory functions most reliably with $V_{CC} - V_{EE} = 5.5\text{V}$; at this supply voltage the chip draws 320mA for a total power dissipation of 1.75W. At a case temperature of 70°C , the measured access time for a worst-case

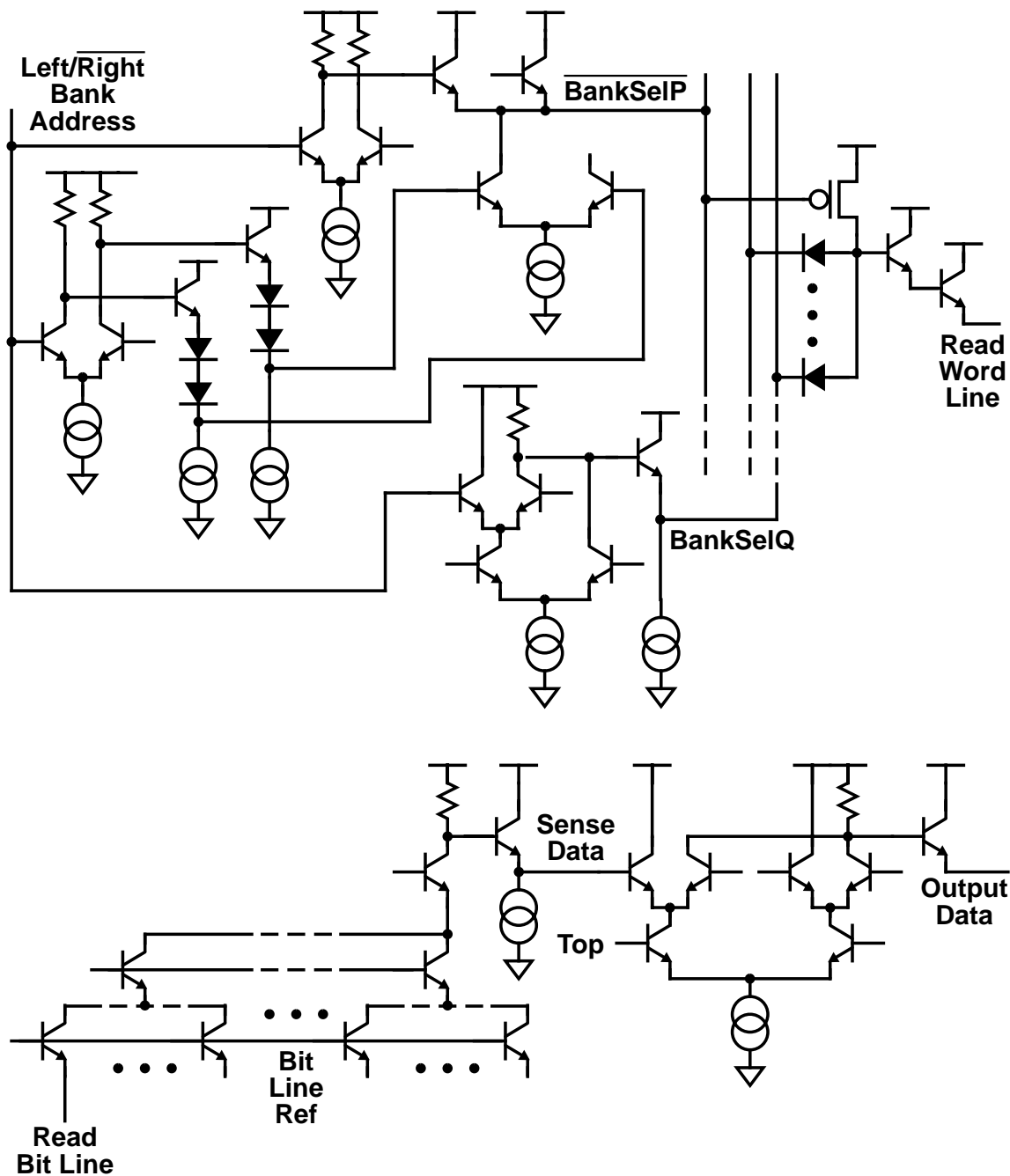


Figure 5-4 Critical Access Path for 16Kx4 SRAM

address transition, which switches between left and right banks, is 3.7 ns. An oscillograph of such a transition appears as Figure 5-6, with the output pin driving a 50-Ω termination to $V_{CC} - 2V$. Limitations in test equipment prevent accurate measurement of the write pulse width and cycle times, but the memory writes reliably with pulses shorter than 4 ns.

Figure 5-5 Chip Photomicrograph of 16K×4 CSEA SRAM

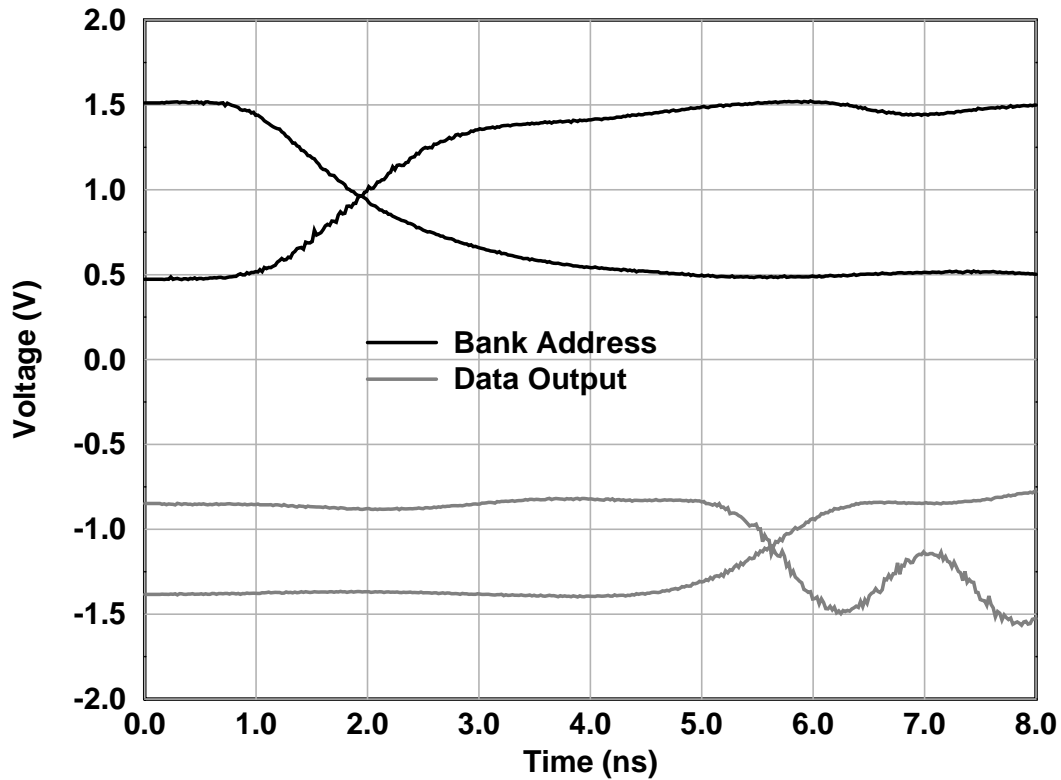


Figure 5-6 Oscillograph of Bank-switching Read Access

The measured results agree quite well with circuit simulation of the extracted chip layout plus measured package parasitics. Simulated transient waveforms for critical nodes during a worst-case access appear as Figure 5-7. The fabricated design provided invaluable feedback by proving the operation of the switched PMOS load decoders, the two-level cascode sense amplifier, and the word line level converter. The design database from the 16K \times 4 memory is also the starting point for the other designs, which use the same basic memory array but change the peripheral circuits to achieve higher performance.

5.2 Proposed 256K CSEA SRAM

This section describes a 256K CSEA memory that extends the 64K design in straightforward ways. Except as noted below, the decoders and arrays are identical to the fabricated design. A principal improvement is superior supply noise rejection provided by the sense and cascode reference circuits of Section 4.3. The original 16K \times 4 memory uses reference generators that do not track the supply sensitivities of the circuits that they control. The access time is reduced by several means. First, the critical path is shortened by controlling the BankSelP discharge current switch with an emitter follower-buffered version of the

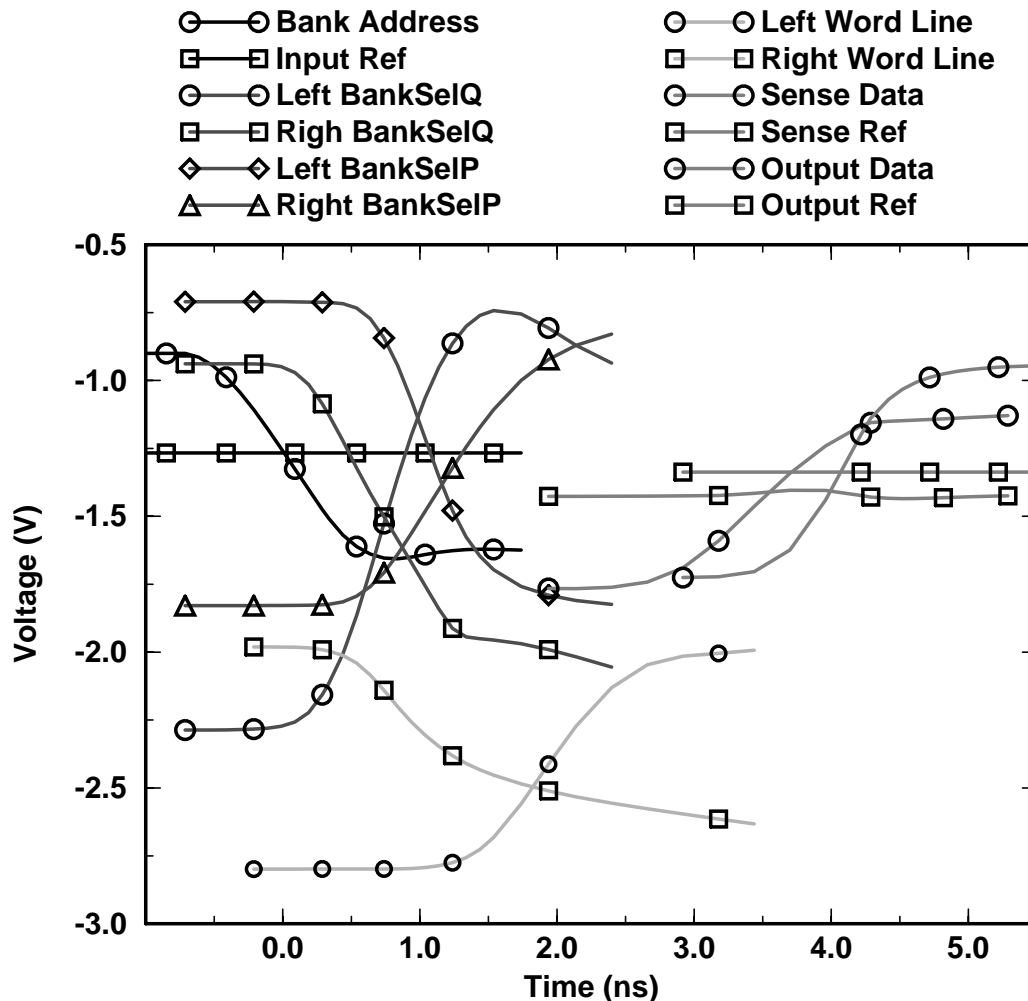


Figure 5-7 Simulated Switching Waveforms for 16K \times 4 SRAM

input address, rather than the inverter-buffered version used above; circuit simulations indicate an access time improvement of about 300ps. Because of increased design maturity, the 256K memory has improved power partitioning to speed accesses. It also specifies a two-level metal version of the process technology, which improves the parasitic bit line wire resistance because the second metal layer in a two-level process is typically thicker than second metal in a three-level process. Finally, the design specifies a more appropriate package, so less time is lost in the package traces.

However, larger memories require longer wires, so it is important to ensure that the wires do not slow the access. To achieve this goal, the 64K \times 4 SRAM uses four sets of address lines, so each set of lines goes to four row (or two column) decoders. In order to further minimize the address line loading, the row decoders are moved to the area between arrays. As shown in Figure 5-8, this allows a decoder to share its address wires with the decoder in the adjacent bank. While it improves the address line switching, this organization

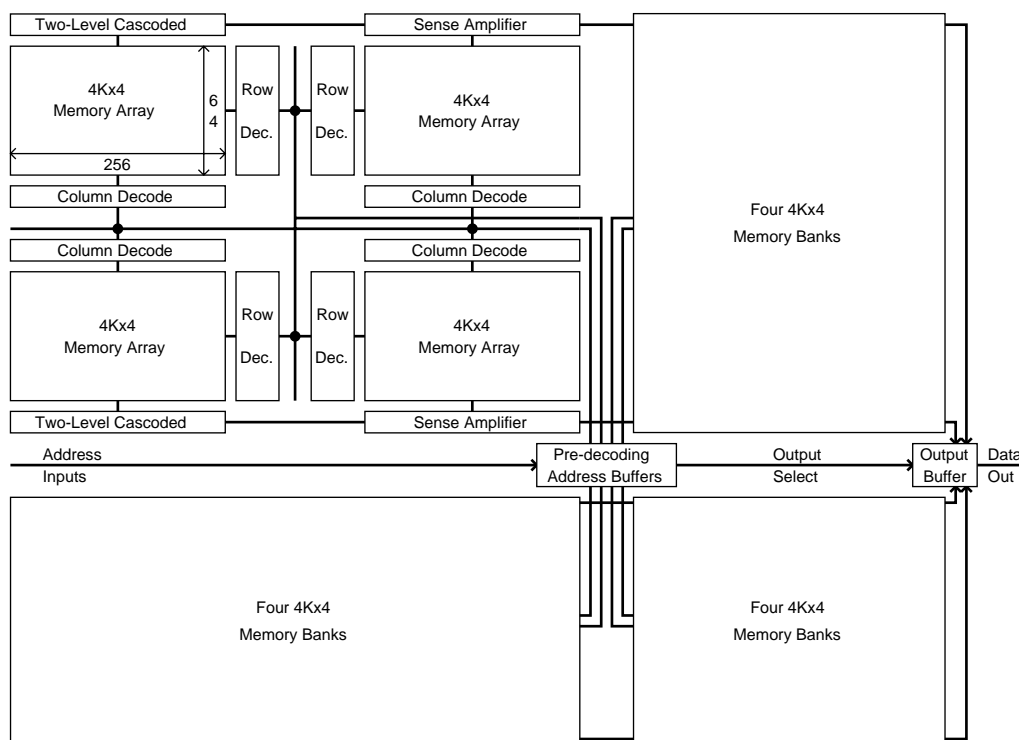


Figure 5-8 64K×4 SRAM Organization

increases the delay of the read word line, since the Darlington driver sees the entire word line resistance, rather than two half branches in parallel. To avoid this four times increase in RC delay, the proposed design splits the Darlington pair such that the final emitter follower is still in the center of each array. Because the cell layout of Figure 5-1 has room for extra first metal tracks, the connection to complete the Darlington pair is simple.

Another place where long wires cause problems is in the two-level cascode sense network: the RC delay in the second-level wire, which runs the length of the die, threatens to increase the access time. This problem is reduced by splitting the wire in the middle and replacing the second-level cascode device with a two-emitter transistor that connects to each wire. While placing the top cascode device in the middle of the wire increases the distance to the output pads versus the original arrangement, this path is lightly loaded and driven by an emitter follower, so it remains quick.

5.2.1 Results

Figure 5-9 shows a circuit simulation of a worst-case bank-switching read access for the 64K×4 CSEA design; a -300-mV/ns V_{EE} noise pulse is placed 1.35ns after the input

transition so as to maximize the access penalty (note the similar drops in **SenseOut** and **SenseRef**). This access requires 0.2ns for input pad, level shifting, and buffering, 0.65ns for selecting and driving the gates of the PMOS resistors, 0.6ns for pulling up the decoder, the Darlington pair, and the read word line (to the bit line reference potential), 0.85ns for accessing the CSEA cell and reducing the reference device's current to 50% of the bit line current, 0.6ns for the two-level cascoded senseamp, and 0.5ns for the output buffer and 50-Ω output pad drive. This simulated design has a read access time of 3.4ns at a junction temperature of 70°C, using 550-mV read word line swings and 2.3W of power. Thus, this memory is four times larger than the 64K-bit memory and has a faster access time at a very modest increase in power dissipation. The use of switched PMOS load diode decoders limits the power increase, because adding decoder banks does not add much extra power.

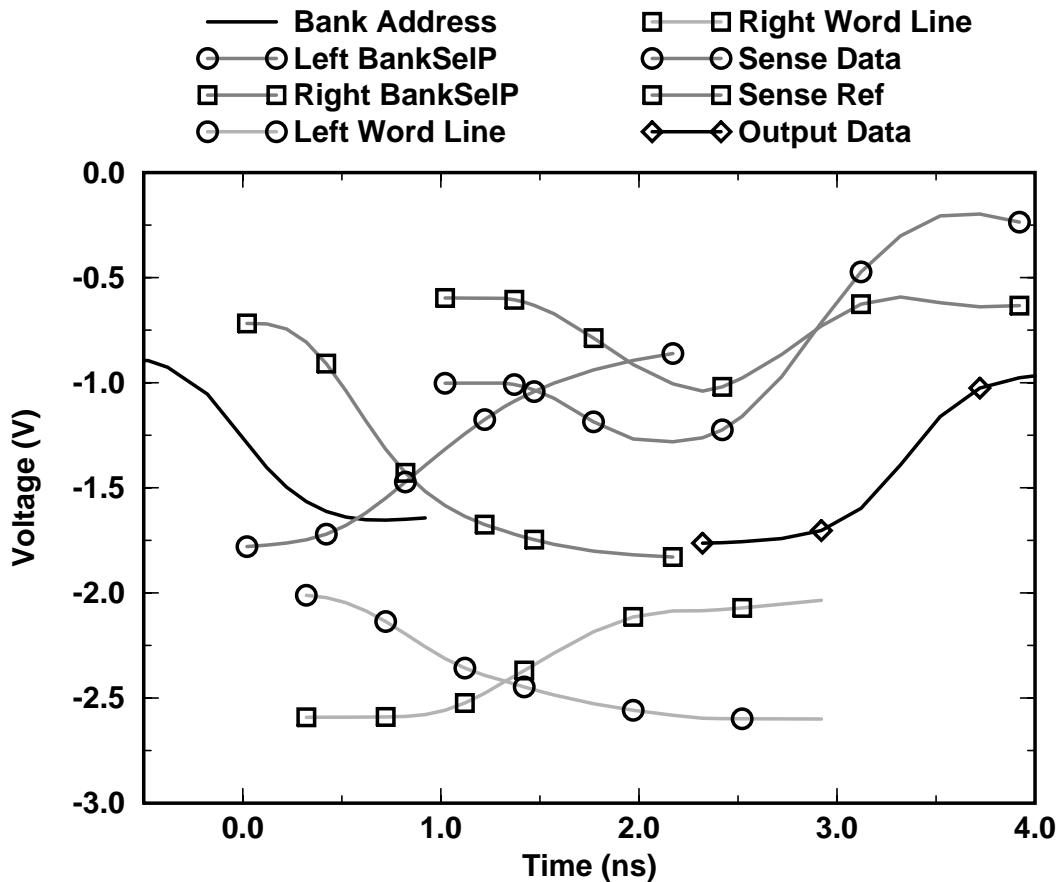


Figure 5-9 Simulated Switching Waveforms for 64K×4 SRAM

5.3 A Synchronous 256K CSEA SRAM

This section investigates the use of the pulsed decoding and sensing techniques of Chapters 3 and 4 to build faster CSEA memories. Limiting when signals may change allows the circuits to begin each access in a reset state so that only active-going transitions are in the critical path. Synchronous SRAMs are faster because these active transitions may be tuned for high-speed operation without concern for the resetting (de-activating) transitions, which are accomplished after the access by separate circuits. Since the resetting circuits require power in addition to the active-path circuits, it is crucial to reduce this power consumption to make ECL-style synchronous memories practical. The pulsed circuits of this thesis provide the required power savings.

The $4K \times 64$ memory uses the basic organization depicted in Figure 5-10. The emitter follower input buffers drive the input addresses to the center of the die, where the pulsed address buffers of Section 3.5.3 generate true and complemented global address lines. Separate bank select decoders (Section 3.5.4) simultaneously generate the per-bank $\overline{\text{BankSelP}}$ and $\overline{\text{BankSelQ}}$ signals. At the quadrant level, wired-or gates with $\overline{\text{BankSelQ}}$ -pulsed current sources drive the pre-decoded local address lines to the row and column *NOR* decoders. The pulsed row decoder raises the selected read word line while the pulsed column decoder activates the read bit line current and raises the selected $\overline{\text{BitLineRef}}$. Finally, the sensed bit line current is multiplexed via a single-level cascode network to a shared sense amplifier, where the sensed voltage is compared to a reference generated via replica bit lines on the selected word line (as in Section 4.3.1).

This synchronous access path delivers impressive performance. The delay from the *Go* signal, which activates the pulsed address buffers, to the crossing of the sensed data and reference signals is only 1.7 ns. This compares very favorably with the 2.7-ns delay for the same stages of the asynchronous $64K \times 4$ design above. Including the input and output buffering, simulations indicate that the synchronous design requires less than 2.5 ns, which is an improvement of about 25% over the 3.4-ns asynchronous one.

The power dissipation of the pulsed ECL circuits of this memory increases with both the pulse width and the frequency of the current source selection signals. Circuit simulations indicate that a conservative pulse width for this design is 1 ns. The pulsed discharge signals for the active-low global and local address lines and the $\overline{\text{BankSelP}}$ lines do not need current to keep the signals low, so they could use shorter pulses. With approximately 1-ns selection pulses, the current for the major blocks of the synchronous SRAM varies as

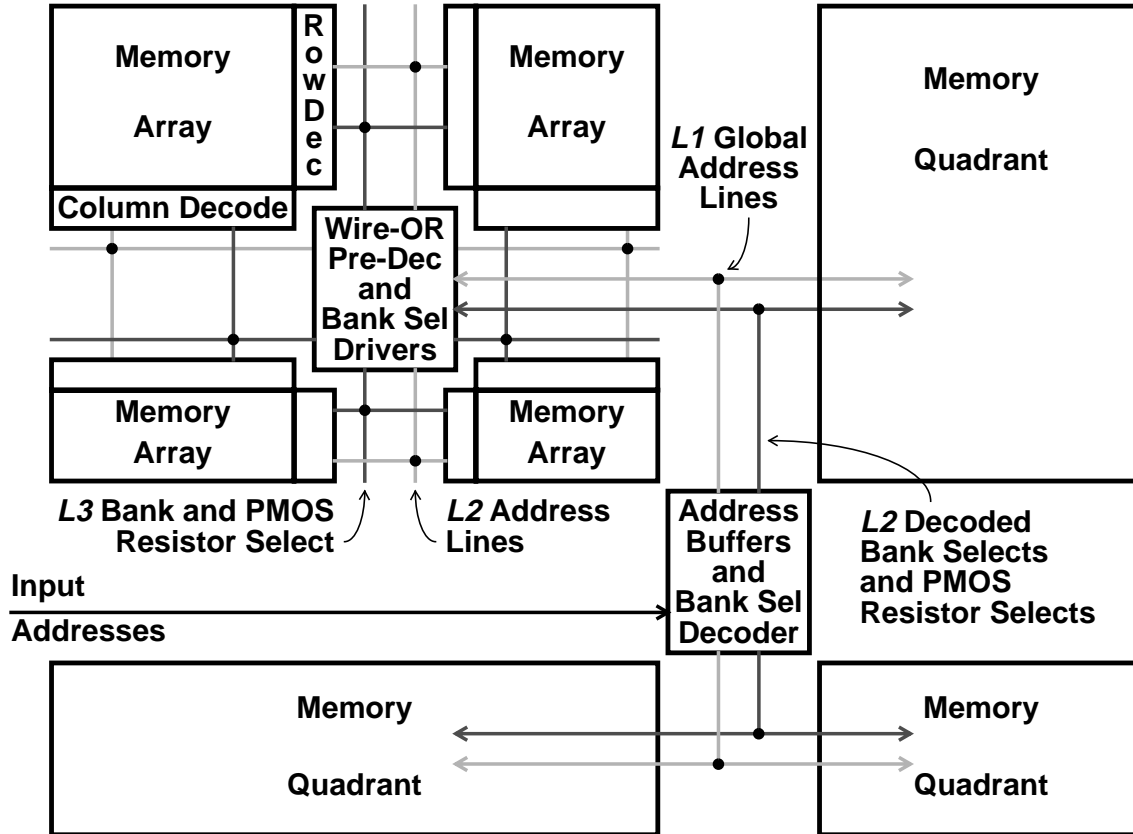


Figure 5-10 Pulsed Address Line Routing

shown in Table 5-1. The static current of the chip is estimated at around 400mA. This current is used both by traditional static current sources and the leakage currents of the pulsed current sources. If all functional blocks were simultaneously active, the pulsed current sources would use almost 300mA more current. However, the access path uses selection signals that are delayed relative to one another such that not all blocks are active at once. The average current at cycle times of 2.5 and 5ns is also displayed in the table. At 5-ns cycles, the synchronous memory dissipates about the same amount as the asynchronous one, while delivering significantly faster access.

Table 5-1 4K×64 SRAM Power Variation

Functional Block	Currents (mA)		Average at Cycle Time	
	Static	Peak	2.5 ns	5 ns
References	20	0	20	20
Input Buffers	25	0	25	25
Address Buffers	10	60	34	22
Bank Select Decoder	45	0	45	45
Switched Resistor Decoder	7	55	29	18
Quadrant Drivers	110	25	120	115
Row & Column Decoders	55	45	73	64
Word Line Discharge	60	20	68	64
Bit Line Currents	40	30	52	46
Sense Amplifiers	40	50	60	50
Totals	412	285	526	469
Power (Watts @ 5.2V)	2.1	1.5	2.7	2.4

The preceding analysis does not include the power required to drive the data signals off the memory chip, since SRAMs that are 64-bits wide are most useful for applications desiring very high-bandwidth on-chip memories. The SRAM described here achieves 3.2GBytes/s memory bandwidth at a cycle time of 2.5ns while dissipating 2.7W. This performance compares very well even with memories designed in more advanced CMOS and BiCMOS process technologies. The power dissipation is much lower than the 15-W 256K 0.5- μ m BiCMOS design of [5] that has an access time, neglecting the input and output drivers, of 1.5ns. Our 0.8- μ m pulsed memory (without its *IO* drivers) is only about 0.5ns slower. Both the access time and power dissipation are superior to the 3.5-W 3.8-ns 512K pipelined CMOS memory of [13].

5.4 Summary

This chapter has shown some of the potential offered by the techniques of this thesis to produce very fast BiCMOS SRAMs that have large capacity and reasonable power dissipation. The increasing sophistication and design maturity of the techniques is illustrated

by Table 5-2, which compares the three memory designs of this chapter. The table demonstrates how the overall memory performance may be substantially improved by paying careful attention to the peripheral circuits, which occupy little area but consume most of the delay and power of an SRAM.

Table 5-2 SRAM Performance Comparison

Capacity	64K	256K	256K
Organization	16K x 4	64K x 4	4K x 64
Access Type	Static Asynchronous	Static Asynchronous	Pulsed Synchronous
Access Time	3.8ns Measured	3.4ns Simulated	2.5ns Simulated
Power	1.75W	2.3W	2.4W (200MHz)
Technology	0.8- μ m BiCMOS	0.8- μ m BiCMOS	0.8- μ m BiCMOS
Cell Type	CSEA	CSEA	CSEA
Array Organization	64 Rows x 256 Columns	64 Rows x 256 Columns	64 Rows x 256 Columns

Chapter 6

Conclusion

This thesis examines the question, “How can one effectively use BiCMOS fabrication technologies to construct extremely-fast SRAMs that deliver high memory capacity and reasonable power dissipation?” The simplest answer to this question is to use each transistor type for the tasks they are best suited: low-swing bipolar peripheral circuits for fast switching and full-swing CMOS memory cells for low power. However, such an answer ignores the significant gains that can be achieved by a more integrated approach — one that mixes transistor types within individual circuits to obtain superior performance.

Chapter 3 applies this hybrid approach to the problem of fast address decoding. While low-swing bipolar circuits have traditionally provided the required speed, their power dissipation is too high for many high-capacity memories. Replacing the resistive load element in such circuits with a variable-resistance load built from a switched PMOS transistor allows the circuit to go into a reduced-power standby mode without affecting the output voltage. The chapter showed how the switched PMOS load improves the power dissipation of decoders based on diode *AND* gates. For *NOR* decoders, the PMOS load was combined with a new BiCMOS pulsed current source to produce an ECL gate that has a low-power mode. Because both the PMOS load and the pulsed current source are controlled by low-swing signals, the gates can be selectively powered up without added delay. The pulsed gates therefore save power both by only powering up for a limited fraction of the access cycle and by only requiring activation of one bank of decoders at once. The pulsed current source relies on a special negative supply voltage, which is supplied by a new V_{SS} generator that uses the memory array capacitance to supply the varying current requirements of the pulsed sources.

Achieving fast and robust sensing and writing of the hybrid CSEA memory cell was the topic of Chapter 4. The low-swing read word line of the CSEA cell eases the amplification requirements of the row decoder, but the single-ended read and write ports cause problems

for rapid sensing and writing. Here also a mix of MOS and bipolar transistors provides a high-performance solution. New pulsed sensing circuits dramatically reduce the sense delay by effectively beginning the access with the bit line midway between its zero and one levels. Furthermore, replica bit lines allow pseudo-differential sensing and careful attention to noise coupling in the design of cascode references improve the sense margins. In order to achieve rapid writes through a single NMOS access transistor, this thesis advocates a local write qualification gate, based on the local word line driver from CMOS SRAMs, which guarantees that only cells that are to be written have a selected write word line. Without the constraint that the access device not write selected cells on unselected bit lines, the cell transistor ratios can be relaxed to both minimize the cell area and the write time. The large-swing write signals are generated by a new level converter that dissipates no power when converting zero, so it may be efficiently integrated with the read word line driver to avoid a dedicated write decoder while maintaining low power dissipation. This same converter is very useful for rapidly discharging the pulsed word lines of Chapter 3.

Finally, Chapter 5 describes three CSEA SRAM designs that incorporate the concepts of this thesis. A fabricated 3.8-ns 16K×4 CSEA memory is compared to two more-advanced 256Kb SRAMs in the same 0.8- μ m technology. One, a 64K×4 extension of the fabricated prototype, is estimated to access in 3.4ns. The other design is a pulsed synchronous 4K×64 memory that should achieve 2.5-ns access while dissipating about the same power (2.4W) as the 64K×4 memory. While these results are impressive, we believe that there is significantly more performance waiting to be discovered.

6.1 Future Work

Several significant avenues exist for continuing this work. One need is a concrete physical validation of the pulsed decoder and sensing structures, as well as their support circuits. An excellent option would be the fabrication of the 4K×64 design, for building and testing the “real thing” would answer many questions about these techniques in undisputable ways.

A substantial opportunity for research exists in trying to effectively apply the pulsed circuits to general-purpose logic challenges such as microprocessor datapath design. The potential for significant power savings is very high, since such datapaths tend to have parallel functional units of which only one is active at once; thus fast low-swing circuits could be readily used at reasonable power if the active units can be selectively powered

up. A key challenge here is to handle the complex interactions between pulsed signals in datapaths, which tend not to have as nicely matched delays between signal paths as memories. Good solutions to this problem will require careful considerations of the interactions between microarchitectural and circuit issues to maximize the resulting system-level performance.

Finally, the impact of continued device scaling on the feasibility of BiCMOS technology should be addressed. While ECL-style BiCMOS circuits have survived the transition to 3.3-V power supplies, it is difficult to imagine useful bipolar-intensive circuits on chips whose power supplies differ by less than two V_{BE} . Since it seems clear that the increasing emphasis on very low-power systems for portable applications will force supply voltages down more quickly than would normal device scaling considerations, it is likely that special low-voltage process technologies will be required. BiCMOS does not have a future at supplies below one volt. However, there will still be systems that plug into the wall and that require higher switching speeds than the low-voltage technologies can provide. BiCMOS technology may prove useful for these applications, due to the faster switching speed of low-swing bipolar circuitry. Constructing new circuit families that can continue to provide this advantage as the power supplies continue to shrink will be very challenging.

Bibliography

- [1] Shimada, H., Kawashima, S., Matsumiya, M., Suzuki, N., et al. "A 10-ns 4-Mb BiCMOS TTL SRAM." In *IEEE International Solid-State Circuits Conference*, pages 52–3, February 1991.
- [2] Nakamura, K., Oguri, T., Atsumo, T., Takada, M., Ikemoto, A., Suzuki, H., Nishigori, T., and Yamazaki, T. "A 6ns 4Mb ECL I/O BiCMOS SRAM with LV-TTL mask option." In *IEEE International Solid-State Circuits Conference*, pages 212–13, February 1992.
- [3] Kato, H., Suzuki, A., Hamano, T., Kobayashi, T., Sato, K., Nakayama, T., Gojohbori, H., Maeda, T., and Ochii, K. "A 9ns 4Mb BiCMOS SRAM with 3.3V operation." In *IEEE International Solid-State Circuits Conference*, pages 210–11, February 1992.
- [4] Yamaguchi, K., Nambu, H., Kanetani, K., Idei, Y., Homma, N., Hiramoto, T., Tamba, N., Watanabe, K., Odaka, M., Ikeda, T., Ohhata, K., and Sakurai, Y. "A 1.5-ns access time, 78- μm^2 memory-cell size, 64-kb ECL-CMOS SRAM." *IEEE Journal of Solid-State Circuits*, 27(2):167–74, February 1992.
- [5] Tamba, N., Akimoto, K., Ohhayashi, M., Hiramoto, T., Kokubu, T., Ohmori, S., Muraya, T., Kishimoto, A., Tsuji, S., Hayashi, H., Handa, H., Igarashi, T., et al. "A 1.5ns 256kb BiCMOS SRAM with 11k 60ps logic gates." In *IEEE International Solid-State Circuits Conference*, pages 246–7, February 1993.
- [6] Yang, T.-S., Horowitz, M.A., and Wooley, B.A. "A 4-ns 4K*1-bit two-port BiCMOS SRAM." *IEEE Journal of Solid-State Circuits*, 23(5):1030–40, October 1988.
- [7] Havemann, R.H., Eklund, R.E., Haken, R.A., Scott, D.B., Tran, H.V., Fung, P.K., Ham, T.E., Favreau, D.P., and Virkus, R.L. "An 0.8 μm 256K BiCMOS SRAM technology." In *International Electron Devices Meeting*, pages 841–3, December 1987.
- [8] Abu-Nofal, F., Avra, R., Bhabuthmal, K., Bhamidipaty, R., Blanck, G., Charnas, A., DelVecchio, P., Grass, J., Grinberg, J., Hayes, N., Haber, G., and Hunt, J. "A three-million-transistor microprocessor." In *IEEE International Solid-State Circuits Conference*, pages 108–9, February 1992.
- [9] Lin, H.C. "An optimized output stage for MOS integrated circuits." *IEEE Journal of Solid-State Circuits*, 10(2):106–9, April 1975.

- [10] Wendell, D., DeMaris, J., and Chritz, J. "A 3.5ns, 2K*9 self timed SRAM." In *VLSI Circuits Symposium*, pages 49–50, June 1990.
- [11] Heald, R.A. and Holst, J.C. "6ns cycle 256kb cache memory and memory management unit." In *IEEE International Solid-State Circuits Conference*, pages 88–9, February 1993.
- [12] Towler, F., Chu, J., Houghton, R., Lane, P., Chappell, B.A., Chappell, T.I., and Schuster, S.E. "A 128k 6.5ns access/5ns cycle CMOS ECL static RAM." In *IEEE International Solid-State Circuits Conference*, pages 30–1, February 1989.
- [13] Chappell, T.I., Chappell, B.A., Schuster, S.E., Allan, J.W., Klepner, S.P., Joshi, R.V., and Franch, R.L. "A 2-ns cycle, 3.8-ns access 512-kb CMOS ECL SRAM with a fully pipelined architecture." *IEEE Journal of Solid-State Circuits*, 26(11):1577–85, November 1991.
- [14] Yashimoto, M., Anami, K., Shinohara, H., et al. "A 64K Full CMOS RAM with Divided Word-line Structure." In *IEEE International Solid-State Circuits Conference*, pages 58–9, February 1983.
- [15] Sasaki, K., Ishibashi, K., Ueda, K., Komiyaji, K., Yamanaka, T., Hashimoto, N., Toyoshima, H., Kojima, F., and Shimizu, A. "A 7-ns 140-mW 1-Mb CMOS SRAM with current sense amplifier." *IEEE Journal of Solid-State Circuits*, 27(11):1511–18, November 1992.
- [16] Kawarada, K., Suzuki, M., Mukai, H., Toyoda, K., and Kondo, Y. "A fast 7.5ns access 1K-bit RAM for cache-memory systems." *IEEE Journal of Solid-State Circuits*, 13(5):656–63, October 1978.
- [17] Toyoda, K., Tanaka, M., Isogai, H., Ono, C., Kawabe, Y., and Goto, H. "A high speed 16kbit ECL RAM." *IEEE Journal of Solid-State Circuits*, 18(5):509–14, October 1983.
- [18] Homma, N., Yamaguchi, K., Nanbu, H., Kanetani, K., Nishioka, Y., Uchida, A., and Ogiue, K. "A 3.5-ns 2-W 20-mm² 16-kbit ECL bipolar RAM." *IEEE Journal of Solid-State Circuits*, 21(5):675–80, October 1986.
- [19] Chuang, C.-T., Tang, D.D., Li, G.P., Franch, R.L., Ketchen, M.B., Ning, T.H., Brown, K.H., and Hu, C.-C. "A subnanosecond 5-kbit bipolar ECL RAM." *IEEE Journal of Solid-State Circuits*, 23(5):1265–7, October 1988.
- [20] Shin, H.J., Lu, P.F., Chin, K., Chuang, C.-T., Warnock, J.D., and Franch, R.L. "A 1.2ns/1ns 1K*16 ECL dual-port cache RAM." In *IEEE International Solid-State Circuits Conference*, pages 244–5, February 1993.
- [21] Ayling, J. K. and Moore, R. D. "Main monolithic memory." *IEEE Journal of Solid-State Circuits*, 6(5):276–9, October 1971.
- [22] Gray, P. and Meyer, T. *Analysis and Design of Analog Integrated Circuits*. Wiley, New York, NY, 1984.

- [23] Miyamoto, J., Saitoh, S., Momose, H., Shibata, H., Kanzaki, K., and Iizuka, T. "A 28-ns 64K CMOS SRAM with bipolar sense amplifiers." In *IEEE International Solid-State Circuits Conference*, pages 226–7, February 1984.
- [24] Ogiue, K., Odaka, M., Miyaoka, S., Masuda, M., Ikeda, T., and Tonomura, K. "13-ns 500-mW 64-kbit ECL RAM using HI-BiCMOS technology." *IEEE Journal of Solid-State Circuits*, 21(5):681–85, October 1986.
- [25] Tran, H.V., Scott, D.B., Fung, P.K., Havemann, R.H., Eklund, R.H., Ham, T.E., Haken, R.A., and Shah, A.H. "An 8-ns 256K ECL SRAM with CMOS memory array and battery backup capability." *IEEE Journal of Solid-State Circuits*, 23(5):1041–7, October 1988.
- [26] Kertis, R.A., Smith, D.D., and Bowman, T.L. "A 12-ns ECL I/O 256K*1bit SRAM using a 1- μ m BiCMOS technology." *IEEE Journal of Solid-State Circuits*, 23(5):1048–53, October 1988.
- [27] Tamba, N., Miyaoka, S., Odaka, M., Ogiue, K., Tamada, K., and Ikeda, T. "An 8ns 256K BiCMOS RAM." In *IEEE International Solid-State Circuits Conference*, pages 184–5, February 1988.
- [28] Suzuki, M., Tachibana, S., Watanabe, A., Shukuri, S., Higuchi, H., Nagano, T., and Shimohigashi, K. "A 3.5-ns, 500-mW, 16-kbit BiCMOS ECL RAM." *IEEE Journal of Solid-State Circuits*, 24(5):1233–7, October 1989.
- [29] Matsui, M., Momose, H., Urakawa, Y., Maeda, T., Suzuki, A., Urakawa, N., Sato, K., Matsunaga, J., and Ochii, K. "An 8-ns 1-Mbit ECL BiCMOS SRAM with double-latch ECL-to-CMOS-level converters." *IEEE Journal of Solid-State Circuits*, 24(5):1226–32, October 1989.
- [30] Tran, H., Fung, K., Bell, D., Chapman, R., Harward, M., Suzuki, T., Havemann, R., Eklund, R., Fleck, R., Le, D., Wei, C., Iyengar, N., Rodder, M., Haken, R., et al. "An 8ns BiCMOS 1Mb ECL SRAM with a configurable memory array size." In *IEEE International Solid-State Circuits Conference*, pages 36–7, February 1989.
- [31] Heimsch, W., Krebs, R., Pfaffel, B., and Ziemann, K. "A 3.8-ns 16K BiCMOS SRAM." *IEEE Journal of Solid-State Circuits*, 25(1):48–54, February 1990.
- [32] Fung, K., Suzuki, T., Terazawa, J., Khayami, A., Martindell, S., Blanton, C., Tran, H., Eklund, R., Madan, S., Holloway, T., Rodder, M., Graham, J., Chapman, R., Haken, R., and Scott, D. "An experimental 5ns BiCMOS SRAM with a high-speed architecture." In *VLSI Circuits Symposium*, pages 43–4, June 1990.
- [33] Takada, M., Nakamura, K., Takeshima, T., Furuta, K., Yamazaki, T., Imai, K., Ohi, S., Sekine, Y., Minato, Y., and Kimuto, H. "A 5-ns 1-Mb ECL BiCMOS SRAM." *IEEE Journal of Solid-State Circuits*, 25(5):1057–62, October 1990.

- [34] Maki, Y., Kamata, S., Okajima, Y., Yamauchi, T., and Fukuma, H. "A 6.5 ns 1Mb BiCMOS ECL SRAM." In *IEEE International Solid-State Circuits Conference*, pages 136–7, February 1990.
- [35] Ohba, A., Ohbayashi, S., Shiomi, T., Takano, S., Anami, K., Honda, H., Ishigaki, Y., Hatanaka, M., Nagao, S., and Kayano, S. "A 7ns 1Mb BiCMOS ECL SRAM with shift redundancy." *IEEE Journal of Solid-State Circuits*, 26(4):507–12, April 1991.
- [36] Nakamura, K., Oguri, T., Atsumo, T., Takada, M., Ikemoto, A., Suzuki, H., Nishigori, T., and Yamazaki, T. "A 6-ns ECL 100K I/O and 8-ns 3.3-V TTL I/O 4-Mb BiCMOS SRAM." *IEEE Journal of Solid-State Circuits*, 27(11):1504–10, November 1992.
- [37] Masuda, M., Nishio, Y., and Ikeda, T. "High-speed logic circuits combining bipolar and CMOS technology." *IEICE Transactions*, J67-C(12):999–1005, December 1984.
- [38] Douseki, T., Ohmori, Y., Yoshino, H., and Yamada, J. "Fast-access BiCMOS SRAM architecture with a V_{SS} generator." *IEEE Journal of Solid-State Circuits*, 26(4):513–17, April 1991.
- [39] Muller, R. and Kamins, T. *Device Electronics for Integrated Circuits*. Wiley, New York, NY, 1986.
- [40] Toh, K.-Y., Chuang, C.-T., Chen, T.-C., Warnock, J., Li, G.-P., Chin, K., and Ning, T. "A 23ps/2.1mW ECL gate." In *IEEE International Solid-State Circuits Conference*, pages 224–5, February 1989.
- [41] Shin, H.J., Lu, P.-F., and Chuang, C.-T. "A high-speed low-power JFET pull-down ECL circuit." *IEEE Journal of Solid-State Circuits*, 26(4):679–83, April 1991.
- [42] Chuang, C.T., Chin, K., Shin, H.J., and Lu, P.F. "High-speed low-power ECL circuit with AC-coupled self-biased dynamic current source and active-pull-down emitter-follower stage." *IEEE Journal of Solid-State Circuits*, 27(8):1207–10, August 1992.
- [43] Chuang, C.T., Chin, K., Lu, P.F., and Shin, H.J. "High-speed low-power Darlington ECL circuit." *IEEE Journal of Solid-State Circuits*, 28(12):1374–6, December 1993.
- [44] Feucht. *Handbook of Analog Circuit Design*. Academic Press, 1990.
- [45] Inadachi, M., Homma, N., Yamaguchi, K., Ikeda, T., and Higuchi, H. "A 6ns 4Kb bipolar RAM using switched load resistor memory cell." In *IEEE International Solid-State Circuits Conference*, pages 108–9, February 1979.
- [46] Nokubo, K. et al. "A 4.5 ns access time 1K×4 bit ECL RAM." *IEEE Journal of Solid-State Circuits*, 18(5):515–20, October 1983.

- [47] Tamura, L.R., Yang, T.-S., Wingard, D.E., Horowitz, M.A., and Wooley, B.A. "A 4-ns BiCMOS translation-lookaside buffer." *IEEE Journal of Solid-State Circuits*, 25(5):1093–101, October 1990.
- [48] Wingard, D.E., Stark, D.C., and Horowitz, M.A. "Circuit techniques for large CSEA SRAMs." *IEEE Journal of Solid-State Circuits*, 27(6):908–19, June 1992.
- [49] T.-S. Yang. *High Speed Memory Circuit Design and System Integration*. PhD thesis, Stanford University, February 1989.